AN ABSTRACT OF THE THESIS OF

Ken Soderstrom for the degree of Doctor of Philosophy in Pharmacy presented on August 13, 1998. Title: Characterization of an Amphibian Cannabinoid Receptor.

Abstract approved: _____

Thomas F. Murray

Cannabinoids are drugs with activities like the primary constituents of marijuana. These drugs have been used for centuries but despite this long history significant progress in understanding the pharmacology of this class has only been made over the last decade. Progress has been primarily limited to study of mammalian species. Investigation of cannabinoid pharmacology in an animal with simpler neurophysiology may allow better understanding of the significance of cannabinoid neurochemical systems. *Taricha granulosa*, the roughskin newt, was used to characterize an amphibian cannabinoid receptor.

Behavioral experiments demonstrated that the cannabinoid agonist levonantradol inhibits both spontaneous locomotor activity and courtship clasping behavior. Inhibition of clasping was dose-dependent and potent ($IC_{50} = 0.09$ mcg/animal). Radioligand binding studies using [^{3}H]CP-55940 (a high-affinity cannabinoid agonist) and newt neuronal membranes allowed identification of a specific cannabinoid binding site ($K_d = 6.5$ nM, $B_{max} = 1853$ fmol/mg protein). Rank order of affinity of various cannabinoids determined through competition binding

experiments was consistent with that reported for mammalian species: (K_d, nM): CP-55940 (3.8) > levonantradol (13.0) > WIN55212-2 (25.7) >> anandamide (1665) $\approx$ anandamide + 100 mcM PMSF (2398).

Complementary DNA libraries were constructed and screened for sequences encoding the newt cannabinoid receptor. Overlapping cDNA clones were used to construct a complete sequence consisting of 644 5' untranslated bases, 1422 coding bases, and 242 3' untranslated bases. Northern blotting demonstrated this cDNA is encoded by a single transcript of ~ 5.9 Kb. RT-PCR demonstrated this transcript is highly-expressed in brain. Newt CB1 cDNA was stably-expressed in CHO cells. Use of this cell line allowed measurement of cannabinoid-mediated inhibition of adenylate cyclase activity. This inhibition was dose-dependent and occurred with an affinity consistent with that determined through radioligand binding experiments. Phylogenetic analysis revealed that CB1 cannabinoid receptors have been highly conserved over the course of vertebrate evolution. This high-degree of conservation implies that cannabinoid-mediated signaling is of significant functional importance.

Overall, the experiments described represent the most complete characterization of a non-mammalian CB1 cannabinoid receptor to-date. Further studies of cannabinoid signaling in lower vertebrates may be allow better understanding of the functional importance of this neurochemical system.

Characterization of An Amphibian Cannabinoid Receptor

by

Ken Soderstrom

A THESIS

submitted to

Oregon State University

in partial fulfillment of
the requirements for the
degree of

Doctor of Philosophy

Presented August 13, 1998
Commencement June 1999

Doctor of Philosophy thesis of Ken Soderstrom presented on August 13, 1998

APPROVED:

_____

Major Professor, representing Pharmacy

_____

Dean of the College of Pharmacy

Redacted for privacy

_____

Dean of Graduate School

I understand that my thesis will become part of the permanent collection of Oregon State University libraries. My signature below authorizes release of my thesis to any reader upon request.

Redacted for privacy

_____

Ken Soderstrom, Author

ACKNOWLEDGEMENTS

Pharmacology, like most modern scientific disciplines, is a field that encompasses a wide-range of knowledge and techniques. This range is so broad that it may be impossible for one person to possess expertise in all areas. For this reason, significant progress in the study of pharmacology is usually dependent upon a cooperative effort. The work described here is no exception. I have received assistance and support from many people to whom I would like to express my sincere gratitude and acknowledge their essential contributions.

First, I would like to express my sincere appreciation to my major professor, Dr. Tom Murray. To Dr. Murray I am indebted for the opportunity to pursue this education. Over the course of my studies I've learned from him an enormous amount perhaps most notably the value of persistence in problem solving. Also, I have been instilled with a respect for maintaining high standards in technique and interpretation of results. I've learned the value of experimental results, especially those that are unexpected, and know that good experiments are ones which provide new information, whether anticipated or not. Due to Dr. Murray's involvement I have received thorough training. This training will serve me well and I am sure that my appreciation will only grow over the course of my career.

I would also like to express my most sincere gratitude and thanks to Dr. Mark Leid who has patiently and generously allowed me to finish my studies in his laboratory. Without Dr. Leid's generous provision of equipment and supplies I would

surgical techniques and the design and execution of behavioral studies and their statistical analysis.

Dr. Bill Gerwick and members of his lab including Mary Roberts, Mitch Wise and Ken Milligan have been extremely helpful. I have enjoyed our productive collaboration on cannabinoid-related projects.

The behavioral experiments presented here would not have been possible without the assistance of Mr. Dave Wilson. Dave's role in the conduct of these long and difficult experiments can only be described as ultra-competent. In addition to relying on Dave's technical competence, I am also very proud to have been able to rely on his friendship. The value of this friendship to me over the years is immeasurable.

I would like to thank Frank Johnson for his perspective, friendship and support. Without these I would not have developed an interest in science, or a sense of responsibility to try to contribute to a better understanding of our universe.

Finally I would like to express my heart-felt gratitude to my wife, Amy. Amy has sacrificed and endured without complaint to allow me to pursue this work. Successful completion of this project was dependent on her unflagging support. For all of this and an infinite amount more I cannot be grateful or deserving enough.

CONTRIBUTION OF AUTHORS

Dr. Thomas F. Murray was involved in the design of experiments described in each of the chapters presented in this thesis. Dr. Frank Moore was involved in design of the behavioral experiments described in the second chapter. Dr. Mark Leid was involved in the design of cloning experiments presented in the fourth chapter. All experiments were preformed by the author except for the *in vitro* translation experiment (presented in the fourth chapter) which was performed by Marc Johnson and Simon Evans.

TABLE OF CONTENTS

TABLE OF CONTENTS (Continued)

LIST OF FIGURES

LIST OF FIGURES (Continued)

LIST OF TABLES

CHARACTERIZATION OF AN AMPHIBIAN CANNABINOID RECEPTOR

CHAPTER I. INTRODUCTION AND LITERATURE REVIEW

History of Cannabinoid Pharmacology

Cannabinoids are bioactive molecules representing the principal active constituents of the marijuana plant, *Cannabis sativa*. Preparations of *Cannabis* including those derived from leaves and stems (marijuana) and resin (hashish) have been used medicinally and for their psychoactivity for centuries [1], [2].

Of several cannabinoid molecules present in Cannabis the one primarily responsible for the plant's psychoactivity is Δ^9-THC. This molecule was first isolated and identified by Gaoni and Mechoulam in 1964 [3]. From this time through the 1980's the mechanism of action of Δ^9-THC was unknown and widely thought to be similar to that of ethanol and the general anesthetics: the high lipophilicity of Δ^9-THC is consistent with an ability to alter the fluidity of neuronal membranes. In the mid-1980's evidence began to accumulate that a specific receptor may be responsible for cannabinoid effects. First, stereo-selective activity of Δ^9-THC isomers was demonstrated [4]. Second, cannabinoid inhibition of adenylate cyclase activity was detected [5].

The presence of a specific cannabinoid receptor was unequivocally determined in 1988 [6]. Using tritium-labeled CP-55940 (a high-affinity synthetic cannabinoid with water solubility more favorable than that of Δ^9-THC) Devane, et al were able to

label specific cannabinoid binding sites in rat neuronal membranes [7]. The molecular identity of this binding site as a member of the seven-transmembrane domain-containing super-family of G-protein-coupled receptors was determined soon after discovery of the receptor [8]. Cannabinoid receptor expression was seen primarily in the central nervous system, although limited expression was detected in testes [9], [10]. An additional receptor related to the central nervous system-expressed cannabinoid receptor that is present in macrophages and other cells and tissues of the immune system was identified in 1993 [11].

Since the cloning of the CNS-associated (termed CB1) and peripheral (termed CB2) cannabinoid receptors, additional progress has been made including identification of endogenous cannabinoid ligands, discovery of an antagonist, and elucidation of cell-signaling mechanisms. These recent advances will be discussed more thoroughly in the following sections. Despite this significant progress in understanding cannabinoid pharmacology, an understanding of physiological roles of CB1 and CB2 systems remains elusive.

<u>Cannabinoids</u>

Naturally-occurring Cannabinoids

Several molecules related to Δ^9-THC have been isolated from Cannabis [12]. Of these only a few have been shown to retain psychoactivity, and of these few Δ^9-THC has been shown to be most abundant and potent [13]. Structures of some

naturally-occurring cannabinoids are presented in Figure 1. Δ^8-THC, while less

abundant in marijuana than Δ^9-THC, still retains significant psychoactivity, cannabinol

is marginally psychoactive and cannabidiol is non-psychoactive.
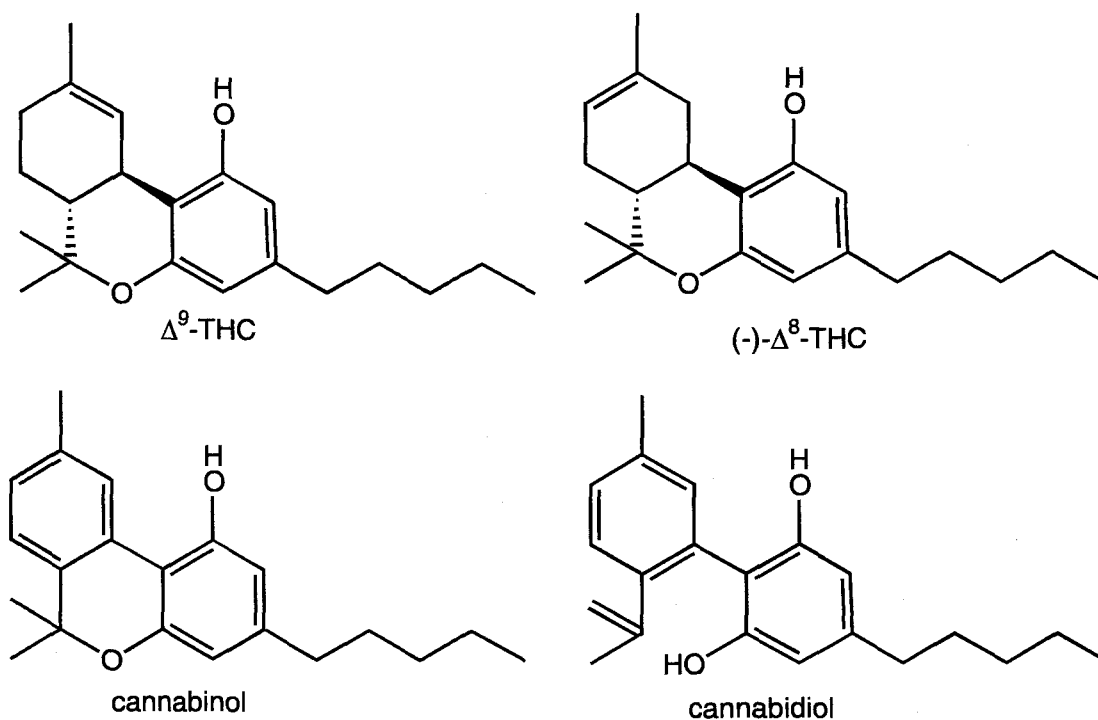
Figure 1. Structures of four naturally-occurring cannabinoids isolated from Cannabis
sativa.

Synthetic Cannabinoids

Tricyclic Synthetic Cannabinoids

In an effort to develop novel analgesics, Pfizer, Inc. conducted extensive

structure-activity experiments on molecules developed based on the tricyclic structure

of Δ^9-THC [14], [15]. These studies resulted in the synthesis of many novel synthetic cannabinoids (Figure 2) some of which (e.g. levonantradol, desacetyllevonantradol [DALN], CP-55940) have higher affinities for the cannabinoid receptor than Δ^9-THC and more favorable water solubility. Improved affinity and water solubility rendered these synthetic cannabinoids important pharmacologic tools. The high-affinity and reasonable water solubility of tritium-labeled CP-55940 were important to the initial identification of specific cannabinoid binding sites in neuronal membranes [7].

Structure-activity experiments using these synthetic cannabinoids were also important for determination of portions of Δ^9-THC that are important for biological activity. A three-point attachment model of cannabinoid-receptor interaction was proposed [15]. The three portions of Δ^9-THC involved in receptor interaction according this model include: 1) the angle of the bond between C9 and C11, 2) the phenolic hydroxyl group, and 3) the presence and length of the hydrophobic side-chain associated with C3. The Pfizer compound CP-47497 is a minimal configuration containing the 3 portions outlined above (Figure 3). CP-47497 is a high-affinity cannabinoid receptor ligand that retains all the biological effectiveness of Δ^9-THC as determined by the Martin multi-parameter mouse model of cannabamimetic activity [13] which includes measures of hypothermia, locomotor activity, catalepsy and analgesia.
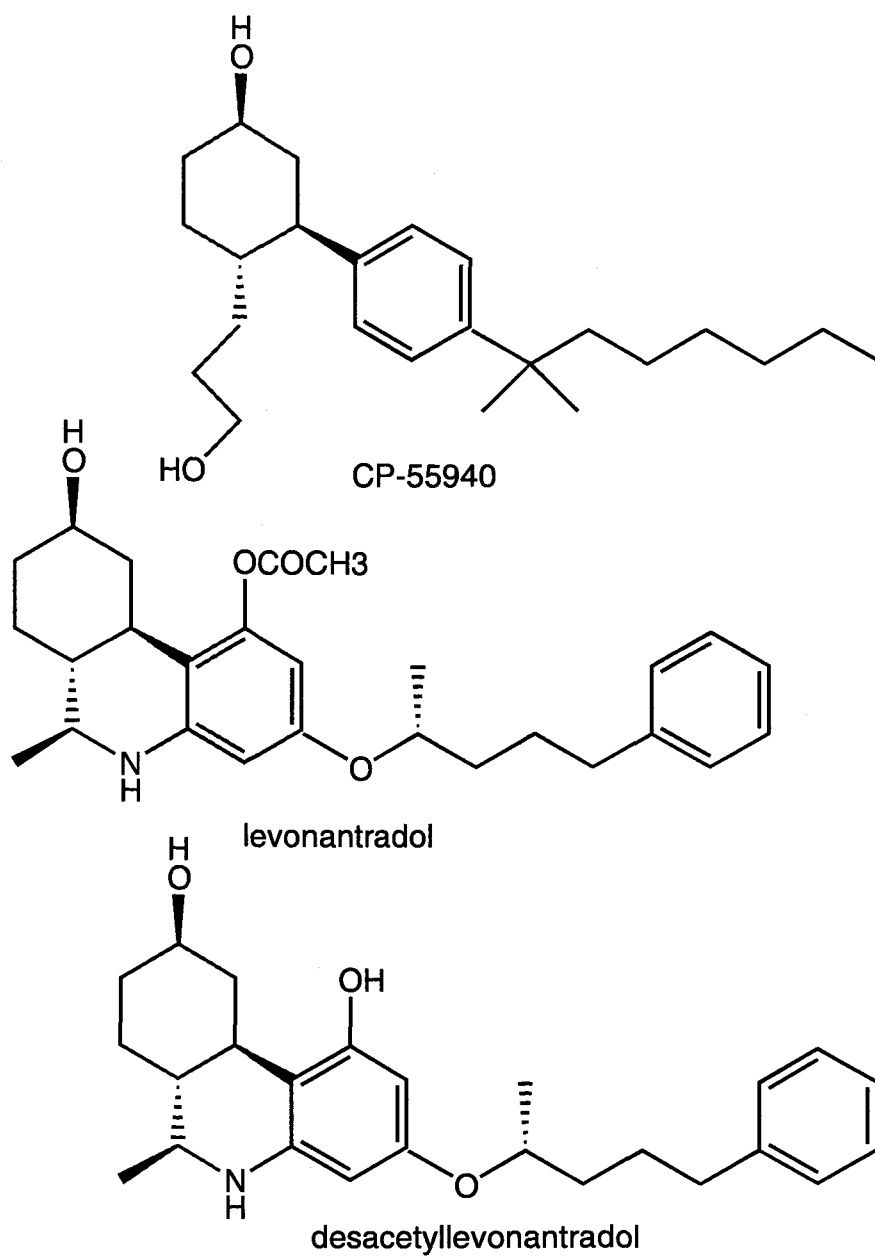
Figure 2. Structures of some tricyclic synthetic cannabinoids.

C9 - C11 bond

phenolic hydroxyl

hydrophobic side-chain associated with C3

Δ^9-THC
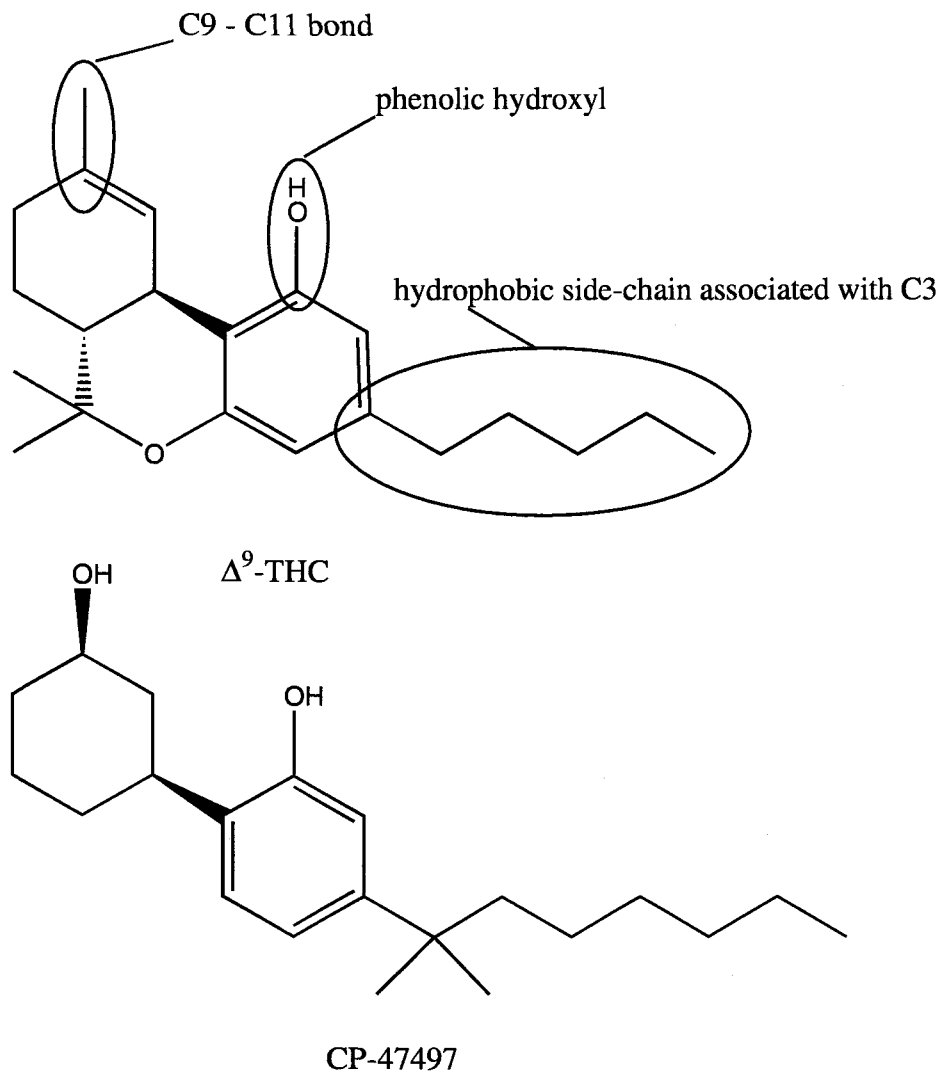
CP-47497

Figure 3. Portions of Δ^9-THC important for cannabinoid activity and the structure of CP-47497, a minimal configuration containing these portions.

A second series of tricyclic synthetic cannabinoids based on the structure Δ^9-THC were synthesized by a group at Hebrew University led by Rapheal Mechoulam (Figure 4). Two particularly-interesting members of this second group of synthetic cannabinoids include the (+) and (-) enantiomers 7-hydroxy-delta-6-tetra-hydrocannabinol-dimethylheptyl [(-)-7-OH-delta-6-THC-DMH (HU- 210) and (+)-7-

OH-delta-6-THC-DMH (HU-211)] [16]. HU-210, is a potent cannabamimetic with anti-inflammatory, and analgesic effects produced at low concentrations relative to Δ^9-THC [17]. In contrast to HU-210, the (+) enantiomer HU-211 interacts specifically with N-methyl-D-aspartate (NMDA) receptors where it acts as an antagonist [18]. The NMDA receptor antagonism produced by HU-211 has been associated with neuroprotective effects [19], [20] and protection from excitatory amino acid-mediated toxicity [21].

A third notable synthetic cannabinoid produced by the Hebrew University group is (-)-11-hydroxyhexahydrocannabinol-dimethylheptyl (HU-243) [22]. In competition binding studies of [^{3}H]CP-55940 binding to rat brain membranes, HU-243 exhibited a remarkably high affinity for cannabinoid receptors (K_i = 45 pM) relative to that of the prototypical high-affinity cannabinoid CP-55940 (K_i = 2 nM) [23]. This high-affinity interaction has rendered the tritiated form of HU-243 a sensitive probe for labeling cannabinoid receptors.

Aminoalkylindole Cannabinoids

A second class of synthetic cannabinoid ligands that are structurally dissimilar from Δ^9-THC were synthesized by a group from Sterling Winthrop, Inc. in an effort to produce novel non-steriodal antiinflammatory drugs based on the structure of the aminoalkylindole cyclooxygenase-inhibitor pravidilone [24]. The most notable member of this series of synthetic cannabinoids is WIN-55212-2 (Figure 5) which has an affinity for CB1 (K_d = 2.0 nM) similar to that of the prototypic agonist CP-55940

[25]. The high-affinity of WIN-55212-2 combined with good solubility has made its
tritiated form an effective tool for labeling cannabinoid binding sites.

HU-210

HU-243
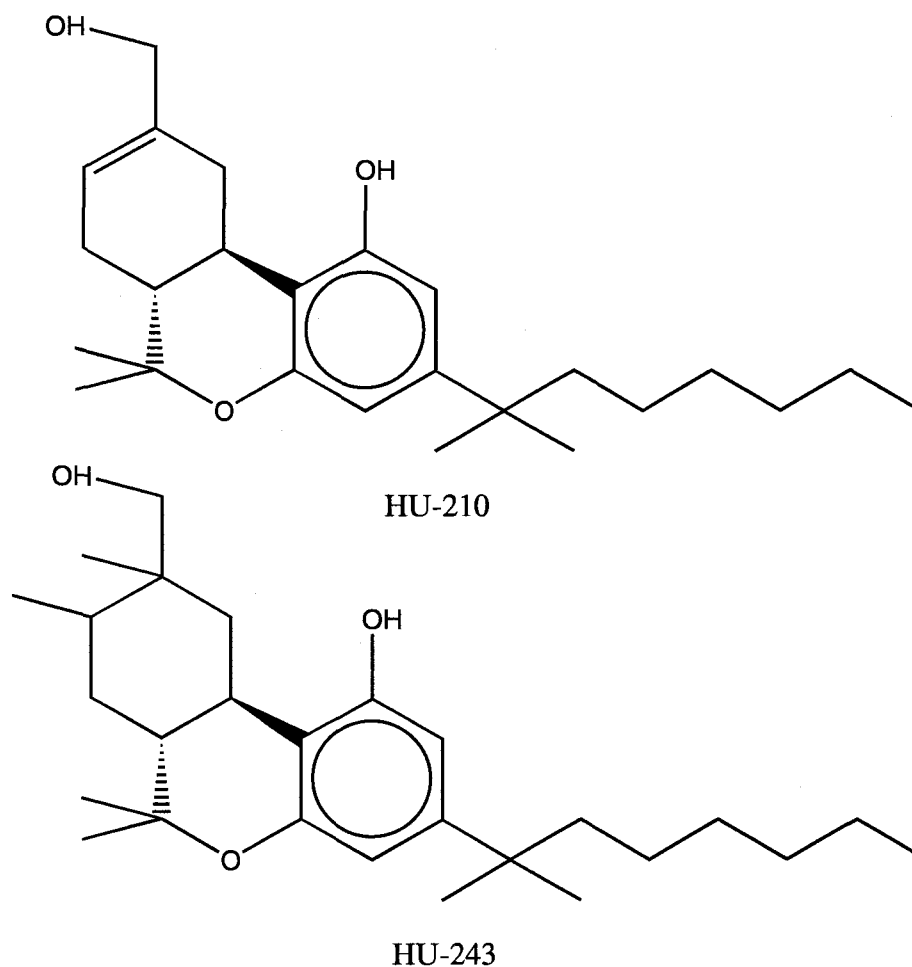
Figure 4. Structures of two potent synthetic tricyclic cannabinoids produced at Hebrew
University.

In contrast to WIN 55212-2 which is a potent agonist in mouse vas deferens
preparations and in mouse antinociceptive and rotorod assays [26], two members of
this series of Sterling Winthrop compounds have been reported to have antagonist

properties. The first antagonist reported, WIN 56098, demonstrated only weak CB1 affinity (K_d > 1 mcM) [27] limiting its usefulness. The second, WIN 54461, has been demonstrated to have a higher CB1 affinity (K_d = 50 nM) but has only been evaluated for antagonism in the in mouse vas deferens preparation [28].

Additional cannabimimetic indole derivatives that share structural similarity with the Sterling-Winthrop series were synthesized by Huffman, *et.al* [29]. The most notable of the Huffman series is JWH-015 (Figure 5) which demonstrates CB2 selectivity with 30-fold higher affinity relative to its specific binding to CB1.

Pyrazole Cannabinoids

A third class of synthetic cannabinoids include two antagonist molecules, both developed by a group at Sanofi Recherche. The first, SR141716A (Figure 6) [30], binds CB1 receptors with high affinity (K_i = 2 nM) and with 1000-fold selectivity over the CB2 receptor subtype [31]. Tritiated-SR141716A has been a useful probe for CB1 receptors [32]. Recent evidence suggests that SR141716A may have inverse activity relative to effects produced by Δ^9-THC, CP-55940, WIN 55212-2 and other CB1 agonists [33]. If these results are confirmed SR141716A may be more properly classified as a CB1 inverse agonist.
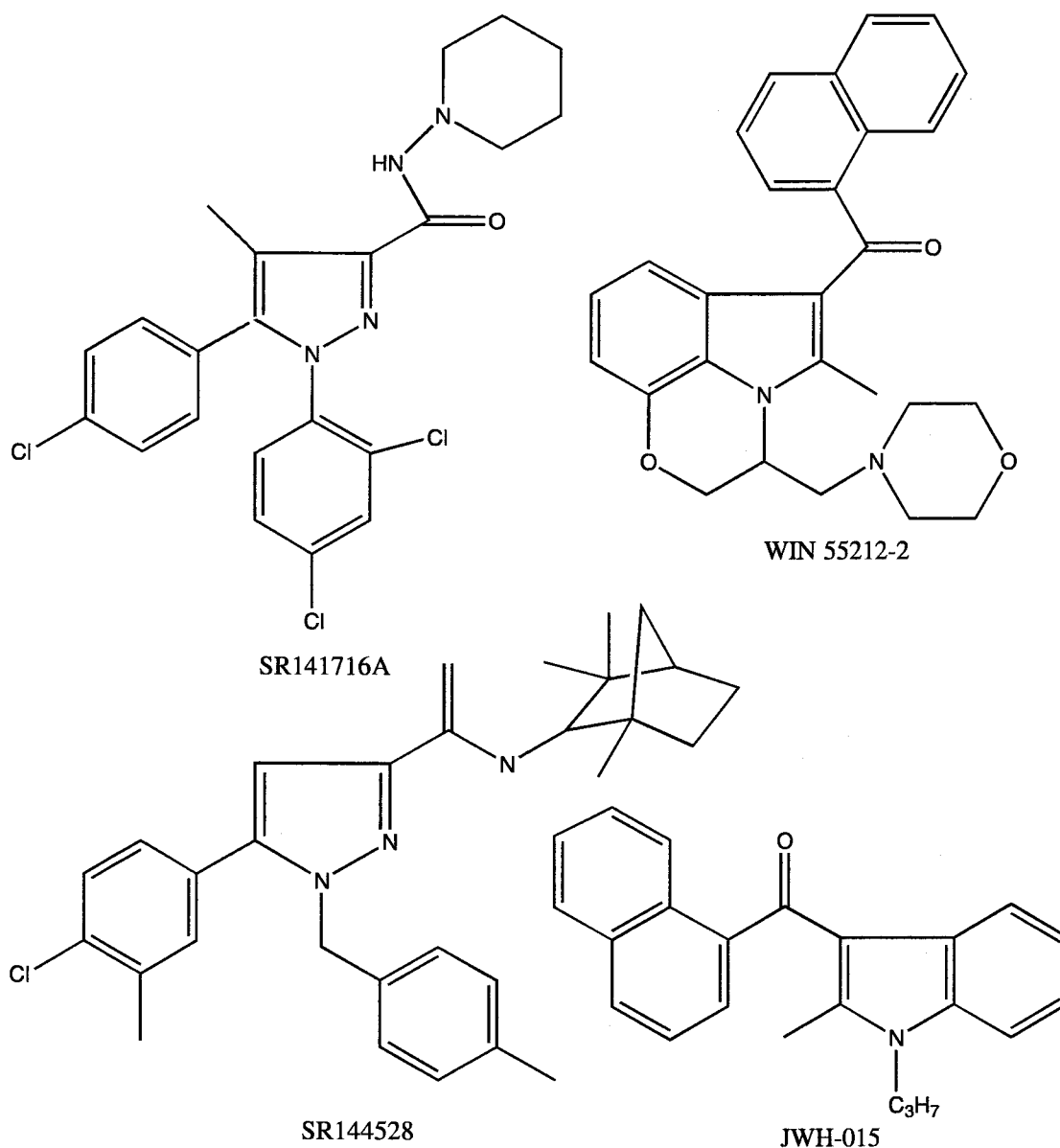
Figure 5. Structures of the aminoalkylindole cannabinoid WIN 55212-2, pyrazole antagonists SR-141716A and SR-144528 and the CB2-selective cannabimimetic indole JWH-015.

A second Sanofi antagonist, SR 144528, was only recently developed. Current information about this pyrazole cannabinoid is limited to a single source [34]. Based on this report, the compound is a highly selective CB2 receptor antagonist ($K_i = 0.6$

nM vs. K_i = 400 nM for CB1) and therefore completes the collection of pharmacological tools necessary to evaluate the known cannabinoid receptor subtypes.

Endogenous Cannabinoids

Discovery of specific cannabinoid receptors implied the presence of endogenous ligands capable of regulating them. Such ligands have been identified and include a group of related fatty acids: arachidonylethanolamide (termed anandamide) isolated from pig brain [35], 2-arachadonyl glycerol [36], [37] found in dog intestine, and mead ethanolamide [38] a compound produced in rats as a result of fatty acid-deficiency.

Anandamide is the most-extensively studied of these fatty acid endogenous cannabinoids and most of the criteria to establish this molecule as a true neuromodulator have been met: Anandamide specifically interacts with CB1 receptors and alters cell-signaling [39]; synthetic, degradative, and signal-terminating enzymes have been demonstrated [40], [41], [42].

Anandamide has been demonstrated to exist as a component of N-arachidonoyl-phosphatidylethanolamine within neuronal membranes as a minor constituent of the phospholipid bilayer. Anandamide formation occurs through phosphodiesterase-mediated cleavage of this membrane phospholipid upon activation of a phosphodiesterase. Activation of this type of phosphodiesterase activity has been correlated to increases in intracellular calcium concentrations [41]. After cleavage, anandamide is able to diffuse to its site of action. After release and diffusion out of

the neuron, anandamide is rapidly and specifically transported back into the cell where it is either metabolized by an amidase that is inhibited by the general serine protease inhibitor phenylmethylsulfonyl fluoride (PMSF) [43], or available for reincorporation to the membrane [41].

An additional endogenously-available fatty acid that is reported to be a CB2-selective agonist is palmitoylethanolamide [44]. Palmitoylethanolamide is one of several related naturally-occurring molecules that are proposed to participate in an autocoid local inflammation antagonism (ALIA). This group of molecules have been evaluated in cultured cerebellar granule cells [45].

In addition to these fatty acid endogenous cannabinoids, evidence for a peptide endogenous cannabinoid has been suggested but not confirmed [46], [47]. Structures of compounds identified as endogenous cannabinoids are presented in Figure 6.
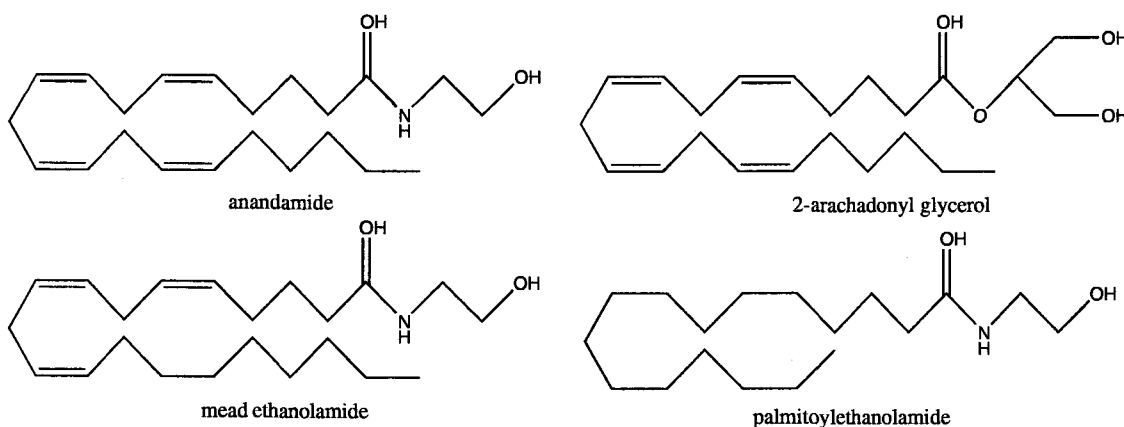
Figure 6. Structures of endogenous cannabinoids.

Cannabinoid Receptors

At least two subtypes of cannabinoid receptors exist: CB1 receptors which are associated primarily with the central nervous system (CNS), and CB2 receptors expressed primarily in tissues of the immune system including macrophages associated with the marginal zone of the spleen. The properties of these two cannabinoid receptors are elaborated below.

CB1

A cDNA encoding the CB1 cannabinoid receptor was inadvertently isolated during the screening of a rat brain library for sequences with similarity to the bovine substance-K receptor [8]. This CB1 clone, termed SKR6, encodes a 473 amino acid protein with seven hydrophobic domains characteristic of the super-family of G-protein-coupled receptors. When expressed in CHO cells, activation of this receptor with cannabinoid agonists effects a reduction in adenylate cyclase activity [48] This effect is consistent with the CB1 activation of Gi that has been demonstrated in primary cultures of neurons [49].

Shortly after isolation of the rat CB1 sequence, the human homologue was cloned [50]. This human receptor is expressed as two isoforms produced from a single gene. These isoforms result from alternate splicing of a 167 base-pair intron present in the sequence encoding the amino-terminal portion of the receptor [51]. The longer messenger RNA corresponds to the original human CB1 cDNA clone. The shorter

isoform, termed CB1A, is truncated by 61 amino acids relative to CB1. The first 28

amino acids of this truncated receptor are unique to CB1A whereas the remaining

protein sequence is identical to CB1. Patterns of CB1 and CB1A expression appear to

be identical although CB1A mRNA is present at lower levels corresponding to about

20% of CB1. Pharmacologic characterization of the two isoforms stably expressed in

CHO cells revealed no significant differences in affinity for various cannabinoid

ligands or functional coupling to adenylate cyclase [52].

Similar CB1 splice variants have not been identified in other species, although

sequences corresponding to two independent genes encoding CB1-like receptors have

been isolated from a pufferfish genomic library [53]. These genomic clones,

designated FCB1A and FCB1B encode amino acid sequences that are 66% identical.

FCB1A and FCB1B share 72% and 59% homology to human CB1 respectively. These

lower vertebrate cannabinoid receptors have not been heterologously expressed and

pharmacology of the CB1-like receptors encoded by the puffer fish clones has not been

investigated.

Other than the puffer fish clones discussed above, the only additional non-

mammalian cannabinoid receptor sequence reported to date has come from an

invertebrate. Using total RNA isolated from leech ganglia as a template, a 480 base

pair CB1-like sequence has been amplified by reverse transcription coupled to PCR

(RT-PCR) [54]. The deduced amino acid sequence encoded by this PCR fragment is

49 % homologous to human CB1. Specific binding of [^{3}H]anandamide to membranes

prepared from leech ganglia has been reported, but identification of a complete leech

cannabinoid receptor coding sequence and more thorough investigation of its pharmacology has not yet been made.

In addition to the sequences described above, cDNAs encoding CB1 receptors have been isolated from the following mammals: cow (partial 205 base pair clone), cat, and mouse [55].

CB2

The peripheral cannabinoid receptor, CB2, was first identified pharmacologically in murine spleen cell membranes [56]. A fragment of cDNA encoding this receptor was fortuitously amplified by degenerate primer PCR from cDNA derived from HL60 cells (a human leukemia cell line) in an attempt to identify G-protein-coupled receptors that are involved in granulocyte differentiation. The PCR fragment was used to screen and isolate a complete CB2 coding sequence from an HL60 cDNA library [11].

The human CB2 receptor is shorter than CB1: 360 amino acids vs. 472. Most of this difference is accounted for by a reduction in the size of extracellular amino-terminal tail domain of CB2. The remaining human CB2 sequence is 61% identical to the human CB1. Despite these sequence differences, the pharmacology of CB1 and CB2 receptors are remarkably similar. Both receptors effect a reduction in adenylate cyclase activity that is consistent with activation of G_i and the pharmacological signature of the receptors as defined by rank order of affinities for most cannabinoid ligands are identical.

Molecular Pharmacology

To date, two studies have attempted to identify specific amino acids within CB1 and CB2 receptors that are critical for ligand binding and subtype selectivity. The first of these employed wild-type and mutated forms of human CB1 in combination with cannabinoid agonists of different structural classes. Results revealed that lysine[192], an amino acid within the third transmembrane spanning domain region (TMD) of the receptor, is critical for the specific binding of the bicyclic cannabinoids HU-210 and CP-55940 and the eicosanoid cannabinoid anandamide but not the aminoalkylindole WIN 55212-2. Replacement of lysine[192] with an alanine residue had little effect on high-affinity specific binding of WIN 55212-2 [57].

In the second study, the CB1-selective properties of the cannabinoid antagonist SR141716A was used to evaluate the ligand binding properties of CB1/CB2 chimeric receptors in order to determine regions involved in antagonist interaction. These studies were hampered by lack of proper receptor processing evidenced by intracellular sequestration of several of the chimeric receptors. Despite these problems, a broad region extending from TMD4 through TMD5 and including the intervening extracellular loop was found to be important for SR141716A specific binding. A CB1 receptor modified to contain the CB2 version of this TMD4-TMD5 region had no affinity for SR141716A but bound all cannabinoid agonists tested with wild type affinity [58].

These mutational studies are complemented by a theoretical 3-D model of the human CB1 receptor proposed by Bramblett, *et al* [59]. This model is based on the

crystal structure of rhodopsin [60] and proposes specific amino acids within TMD3, TMD5 and TMD6 that may be critical for binding the cannabinoid agonist, CP-55940. Additional mutational and structural studies will be required to more fully understand the biophysics of CB1 and CB2 receptors.

Distribution

CB1

The distribution of CB1 receptors within the central nervous system has been evaluated with both radioligand binding and in situ hybridization. In rat brain, highest levels of specific [^{3}H]CP-55940 binding are detected in structures of the basal ganglia followed by the hippocampus and cerebellum [9]. Binding in cerebellum is restricted to the molecular layer and is associated with receptors present on pre-synaptic terminals of granule cell neurons [61]. This pattern of distribution is maintained across several mammalian species including human, monkey, dog and rat [62]. These brain areas are most notably associated with learning and memory and motor control, suggesting possible roles for cannabinoid systems. Diffuse but significant numbers of CB1 receptors are detected within the cerebral cortex which may be associated with the psychoactive effects of cannabinoids. Low numbers of receptors are present in the medulla which may explain the lack of respiratory and cardiac effects produced by even high doses of cannabinoids. The distribution of CB1 receptors within the nervous systems of non-mammalian species has not been reported.

The highest densities of CB1 receptors are restricted to the central nervous systems of all species evaluated to this point. Under northern blotting conditions that allowed CB1 mRNA to be readily detected in total RNA prepared from rat brain, none was detected in samples prepared from rat heart, liver, kidney, spleen, thymus, small intestine, testes and ovary [8]. Later studies reported northern blot detection of CB1 mRNA in testes [50] and uterus [63] although mRNAs in these peripheral tissues were much less abundant than within the CNS.

CB1 expression was not detected in mouse spleen cells by northern blotting but was found to be expressed using the more sensitive method of reverse transcription coupled to the polymerase chain reaction (RT-PCR) [56]. RT-PCR has allowed detection of CB1 mRNA in adrenal gland, heart, lung, prostate, uterus, ovary, testis, bone marrow, thymus and tonsils [64], colon, stomach, liver, pancreas, placenta, kidney, and leukocytes [51] and vas deferens [65].

CB2

In situ hybridization of CB2-specific oligonucleotides with mouse brain and spleen slices demonstrated lack of CNS representation and significant presence of splenic mRNA [11]. These findings were extended by northern blot analysis which demonstrated that HL60 leukemia cells as well as monocytes and macrophages isolated from mouse spleen also express the mRNA. The same northern blot failed to detect CB2 mRNA in samples prepared from liver, nasal epithelium, thymus, brain, lung and kidney.

RT-PCR demonstrated that CB2 mRNA was present spleen, tonsil and the following blood cells in rank order of density: B-cells > natural killer cells >> monocytes > polymorphonuclear neutrophil cells > T8 cells > T4 cells, suggesting CB2 involvement in immune system modulation [64].

Pharmacology

Models

The pharmacology of CB1 ligands have been evaluated using behavioral models, a variety of which have been developed employing monkeys, rats, mice, and pigeons. The most thorough and widely-used of these models is based on the mouse and is referred to as the "Martin Multiparameter Mouse Model" or the "Mouse Tetrad Model" [66]. This model includes measures of antinocioception, decreased locomotor behavior, hypothermia and catalepsy. Cannabinoid effects on these parameters measured individually can be mimicked by drugs of other classes, but when combined the four measures are diagnostic of cannabinoid agonism - no other class of drug produces the predicted effect on all four parameters.

Other bioassays of CB1 activity include measurement of inhibition of smooth muscle contractions in isolated mouse vas deferens, guinea pig myenteric plexus-longitudinal muscle [67], and mouse urinary bladder. Prevention of mouse urinary bladder contractions by treatment with the sodium channel blocker tetrodotoxin

suggests presence of pre-synaptic CB1 receptors in this isolated tissue which modulates release of excitatory transmitters [68].

Perhaps due to lack of selective ligands, behavioral models and bioassays of CB2 activity have not been developed. The recent development of a CB2-selective antagonist, SR144528 [34] may lead to investigation of potential CB2-mediated behavioral effects and more thorough evaluation of CB2-mediated effects on immune system function.

Availability of cDNAs encoding CB1 and CB2 receptors has allowed transfection and expression of these receptors in mammalian lines. Heterologous expression of these receptors has allowed detailed elucidation of their ligand binding properties. Two studies have directly compared the rank order of affinity for displacement of specific [^{3}H]CP-55940 binding of a structurally-diverse series of cannabinoids for CB1 and CB2 receptors expressed in mammalian cell lines [48], [69]. The results of these experiments are summarized in Table 1 below.

Table 1: Displacement of [3H]CP-55940 from human CB1 and CB2 receptors by cannabinoids

Author	Cell Line	K_i (nM)					
		HU-210	CP-55940	SR141716A	WIN 55212-2	THC	Anandamide
Felder et al., 1995	CB1-L cell	0.06	3.7	11.8	62.3	53	543
Felder et al., 1995	CB2-At20	0.52	2.55	973	3.3	75.3	1940
Showalter et al., 1996	CB1-CHO	0.73	0.58	12.3	1.89	40.7	89
Showalter et al., 1996	CB2-CHO	0.22	0.69	702	0.28	36.4	371

From these and other competition binding experiments using CB1- and CB2-expressing cell lines and various tissue preparations, a consensus rank order of affinity of several cannabinoid ligands has emerged [70]. For CB1 receptors this rank order is: HU-210 > CP-55940 > SR141716A > WIN 55212-2 > Δ^9-THC > anandamide. For CB2 receptors the rank order of affinity of this series of structurally-diverse cannabinoids is: HU-210 > WIN 55212-2 ≈ CP-55940 > Δ^9-THC > anandamide ≈ SR141716A.

Although CB1 and CB2 receptors have similar affinities for most cannabinoids, subtype-selective agonists and antagonists have been identified. These cannabinoids are summarized in Table 2 below.

The results summarized in Table 2 suggest that fluroethyl-anandamide and SR141716A are CB1-selective, JWH-015 and SR144528 are CB2-selective, and that SR141716A and SR144528 are CB1- and CB2-selective antagonists respectively.

Cell Signaling

Among the earliest evidence that cannabinoids exert their effects through specific interaction with receptors was the observation that Δ^9-THC and synthetic cannabinoids reduce the activity of adenylate cyclase [71]. This reduction is affected by guanyl nucleotides [72], and sensitive to the effects of pertussis toxin, implicating involvement of G-proteins of the G_i/G_o subtype [49]. Similar effects on adenylate cyclase activity are produced by CB2 activation [73].

Table 2: Affinity and efficacy of various cannabinoids at CB1 and CB2

Ligand	K_i (nM) CB1	K_i (nM) CB2	Inhibition of AC EC_{50} (nM) CB1	Inhibition of AC EC_{50} (nM) CB2	Class
THC	40.7 a	36.4 a	11 g	>1000 d	tricyclic
CP-55940	8.9 a	1 a	2 g	0.72 e	tricyclic
HU-210	0.18 e	0.36 e	0.2 h	0.37 e	tricyclic
HU-211	466 e	585 e	N/A	286 e	tricyclic
HU-243	0.43 c	0.61 c	N/A	N/A	tricyclic
anandamide	89 a	371 a	315 f	>1000 c	eicosanoid
fluoroethyl-anandamide	8.6 a	324 a	N/A	N/A	eicosanoid
WIN 55212-2	1.9 a	0.28 a	44 g	0.63 e	indole
SR141716A	12.3 a	702 a	>1000 g	>1000 h	pyrrazole
SR144528	400 I	0.6 i	>1000 i	>1000 i	pyrrazole
JWH-015	383 a	14 a	N/A	N/A	pyrrole

a Showalter, et al. 1996, CHO-human CB2, CHO-human CB1

b Devane et al. 1992, rat brain

c Bayewitch et al. 1995, CHO-human CB2

d Bayewitch et al. 1996, CHO-human CB2, COS-rat CB1

e Slipetz et al 1995, CHO- human CB2

f Priller et al. 1995 CHO-human CB1

g Rinaldi-Carmona et al. 1996, CHO-human CB1

h Felder et al. 1995, CHO-human CB1, CHO-human CB2

i Rinaldi-Carmona 1998, CHO-human CB1, CHO- human CB2

In addition to reduction in adenylate cyclase activity, CB1 activation is associated with inhibition of N-type [74] and Q-type calcium channels, and activation of inward-rectifying potassium channels [75]. Similar effects on ion channels has not been reported for CB2 activation.

Two recent reports indicate that CB1 receptors are also positively coupled to adenylate cyclase activity [76], [77]. The first of these studies demonstrates that activation of CB1 and dopamine D2 receptors both resulted in a reduction of forskolin-stimulated adenylate cyclase activity. These reductions were both reversed by respective antagonists. Reductions were also reversed in both cases by pertussis toxin

treatment, which in the case of CB1 but not D2 activation, also resulted in a stimulation of adenylate cyclase activity.

Both CB1 and CB2 activation have been associated with mitogen-activated protein kinase (MAPK) activation [78], [79] implying a possible interaction of cannabinoid signaling with that produced by growth factors and activation of other receptors coupled to the MAPK signaling pathway [80].

Activation of mammalian CB1 and CB2 receptors expressed by CHO cell lines results in an increase in the immediate-early gene product krox-24. The increase in expression of this protein is pertussis toxin-sensitive, but does not require activation of adenylate cyclase [81].

Non-receptor-mediated cannabinoid effects have been reported to include the release of arachidonic acid, and increases in the concentration of intracellular calcium [82]. Anandamide, but not other cannabinoid agonists, has been reported to inhibit gap junction conductance in astrocytes, implying an additional role for the endogenous cannabinoid in regulating neuron-glial interaction [83].

Taricha granulosa: The Roughskin Newt

The amphibian *Taricha granulosa* or roughskin newt is indigenous to the Pacific Northwest region of North America [84]. It and two closely-related species including *Taricha torosa* and *Taricha sierra* which inhabit more southern regions including parts of California have been useful models for the study of phylogeny and biogeography [85]. A related genus, *Notophtalamus viridescens*, native to the

Northeastern parts of the United States has been central to the study of limb regeneration [86] and the involvement of retinoic acid signaling in this phenomenon [87].

In addition to its use in phylogenetic studies, *Taricha granulosa* has also been employed as a physiological model for the study of mitotic events [88], the function of lung ciliated cells [89], white blood cells [90], red blood cells [91] and various blood proteins [92].

The roughskin newt has also served as a model system for the study of various neurochemical and endocrine systems including those involving the actions of luteinizing hormone-releasing hormone [93], testosterone-binding protein [94], corticotropin [95], gonadotropin [96], corticosterone [96], vasotocin, [97], GABA [98] and opioids [99]. The relationship of some of these systems to newt spontaneous locomotor and courtship behaviors have also been investigated. Electrophysiological correlates of the effects of vasotocin and corticosterone on locomotor and courtship clasping behaviors have also been investigated [100].

Overall, the combination of well-studied neurophysiology, with behavioral and electrophysiological correlates make the roughskin newt a compelling choice for the development of a model of cannabinoid pharmacology in a lower vertebrate species. Through studying cannabinoid pharmacology in an animal with neurophysiology that is simpler than mammalian species it may be possible to better understand the physiological significance of the relatively newly-discovered cannabinoid neurochemical system.

CHAPTER II. CANNABINOID EFFECTS ON NEWT BEHAVIORS

Introduction

The first step in evaluating the roughskin newt as a potential model for

cannabinoid pharmacology was to determine if cannabinoid agonists are effective in

altering newt behaviors. As discussed above, methods for the evaluation of drug

effects on two newt behaviors, spontaneous locomotor activity and courtship clasping,

have been developed in the study of other neurochemical systems. These methods

were adapted for the investigation of cannabinoid effects on newt behaviors.

Methods

Spontaneous Locomotor Behavior

Male roughskin newts (*Taricha granulosa*) were collected from various ponds

in Benton county, OR. These animals were transported to a laboratory where they

were maintained in large fiberglass tanks containing dechlorinated water at 17° C.

After locomotor behavior experiments, animals were returned to the ponds from which

they were captured.

Animals were randomly assigned to treatment groups. Injections of 100mcl

were made into the peritoneal cavity. Levonantradol was suspended at various

concentrations into a vehicle of 1% ETOH in H_2O.

Thirty minutes post-injection animals were placed into 15-liter buckets filled with about 5 liters of water at 17° C. Dark lines drawn on the bottom of the testing bucket created 8 sectors of equal area in a radial pattern. The center of each bucket was obstructed with a large Styrofoam cup. Animals were scored for locomotor behavior according to the number of times their heads crossed a sector line. Counting began one minute after animals were placed into the testing bucket, and continued for a total of three minutes. The observer in these experiments was blind to treatment. Significance of results were assessed by Student's t-test.

Courtship Clasping Behavior

During mating season which extends from January through March, roughskin newts display a mating behavior that is characterized by males vigorously clasping smaller females from the back using forearms and hind legs. This clasping position is easily identified and measured and is maintained for long periods, often hours. Cannabinoid effects on male clasping behavior were measured in the field at a lake in the coastal mountains near Benton county, OR.

Female roughskin newts were captured prior to each experiment and transported to a laboratory where they were maintained in large fiberglass tanks containing dechlorinated water at 17° C. These females were injected with 100 mcg progesterone the day prior to clasping behavior experiments and transported back to the field for use as sexual stimuli.

The day of experiments, male newts were collected from the lake constituting the experiment site and randomly assigned to treatment groups. These male newts were then placed in buckets prepared with perforations that allowed free circulation of pond water. The perforated buckets were then suspended from a raft floating in the lake.

All treatments were administered by intraperitoneal injection of 100 mcl. After an hour equilibration period following capture and assignment to treatment groups, males were treated with levonantradol or a vehicle control (1% ETOH in H_2O). Fifteen minutes after treatment, female targets were introduced into testing buckets, and observation and recording of clasping behavior commenced. Numbers of males clasping and the latency to clasp were recorded.

Results

Spontaneous Locomotor Behavior

Three experiments investigating the effect of levonantradol on newt spontaneous locomotor activity were conducted. The first two experiments failed to produce statistically-significant results due to highly-complex experimental design or too few subjects within treatment groups. The third experiment produced significant results through employing a large number of subjects (50 newts per group) in a simply-designed experiment (two treatment groups). The results of the third experiment confirmed trends observed in the first two.

In the third experiment, animals were administered either vehicle or 5 mcg levonantradol as detailed in the methods section above. As shown in Figure 7, animals treated with levonantradol crossed fewer lines (4.1) during the three minute testing period than did animals receiving vehicle only (11.4). This difference was found to be statistically-significant after t-test analysis (p < 0.05, two-tailed t-test).
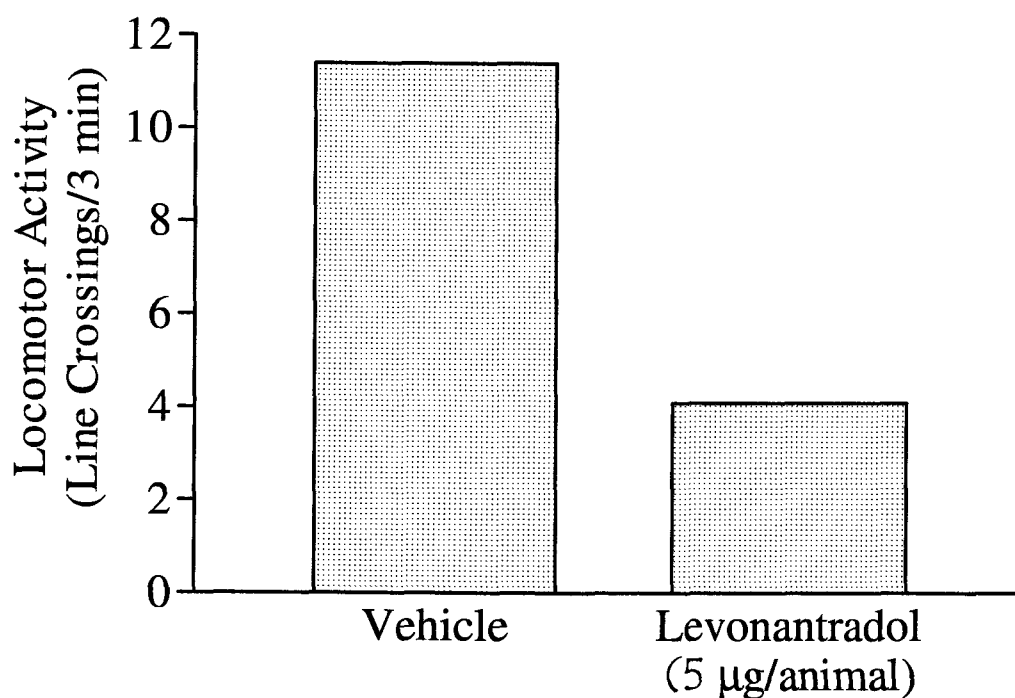
Figure 7. Levonantradol significantly reduces newt spontaneous locomotor activity. Activity was tested 30 minutes after injections of vehicle or 5 mcg levonantradol (n = 50). The difference in mean number of line crossings observed in treatment and control groups was significant (p = 0.012, two-tailed t-test).

Courtship Clasping Behavior

Two experiments investigating the effects of levonantradol on newt courtship clasping behavior were done.

The first of these experiments was a simple, two-treatment group experiment which tested the ability of single 5 mcg doses of levonantradol to alter the incidence, and latency of incidence of newt courtship clasping behavior. Newts were collected and treated as described in the methods section above.

Results presented in Figure 8 demonstrate that injections of 5 mcg of levonantradol were effective in reducing the incidence of newt clasping behavior. Seventeen of 25 animals in the vehicle control group demonstrated clasping behavior while only five of 25 animals administered levonantradol displayed the behavior. This difference was found to be significant upon analysis with the Fisher exact probability test ($p < 0.01$).

Latency results showed that of levonantradol treated animals, none initiated clasping after 45 minutes into recording. The lack of incidence of clasping after 45 minutes in the treatment group may reflect the period separating the levonantradol injection and development of its full effect. If this is the case, levonantradol injections may not have been fully-effective when recording had been initiated in this experiment. Future experiments may benefit from increasing the time between injections and initiation of recording.

The second newt clasping behavior experiment investigated the effect of six levonantradol dosages on the incidence of the behavior. Groups of 12 newts each

received injections of 0, 0.1, 0.32, 1, 3.2, or 5.6 mcg levonantradol in 100 mcl as

described in the methods section above.
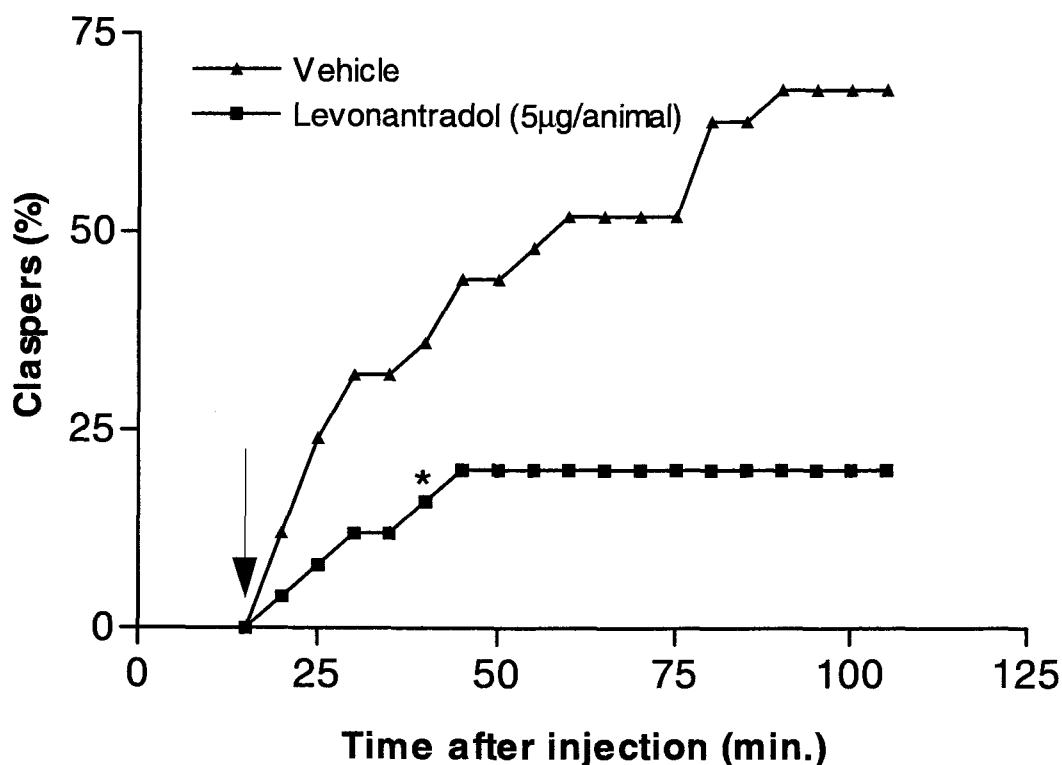
Figure 8. Levonantradol effects on incidence and latency to incidence of male clasping behavior. The arrow indicates the time at which females were added to testing buckets. Data are presented as cumulative percentage of clasping males at 5 min intervals. Males injected with levonantradol were significantly (*) inhibited within 40 min (Fisher exact probability test, p = 0.036).

Results are summarized in Figure 9 and demonstrate that levonantradol-

mediated inhibition of courtship clasping is dose-dependent and occurs at a very low

concentration (IC_{50} = 0.09 mcg/animal). Significant inhibition of clasping was

observed in the 1.0 and 5.6 mcg/animal dosage groups (Fisher exact probability test, p < 0.05).
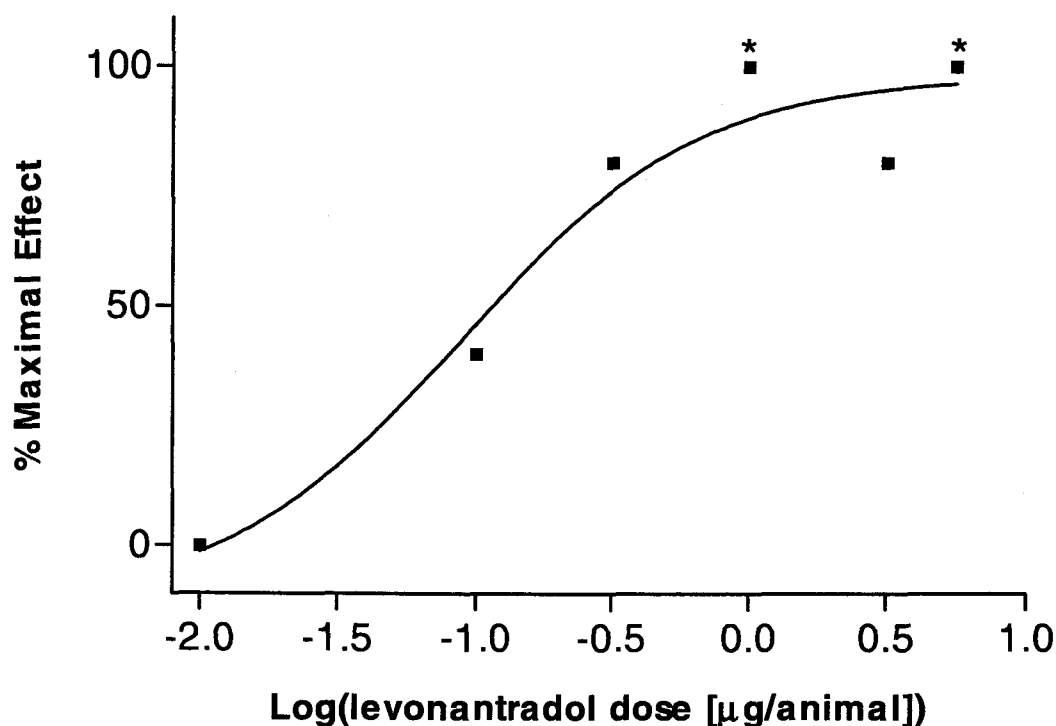
Figure 9. Levonantradol inhibition of clasping behavior is dose-dependent and occurs at a low concentration. Inhibition of clasping was significant when compared to controls (*) at the 1 and 5.6 mcg dosage levels (Fisher exact probability test, p < 0.05). The EC_{50} was 0.09 mcg/animal (95% CI = 0.01 - 0.59 mcg/animal).

Discussion

The inhibition of newt spontaneous locomotor behavior by levonantradol is

consistent with cannabinoid agonist production of hypomobility in mammalian species

[101], [102], [103]. These results are also similar to the effect of clonidine on locomotor activity in newts [104].

Levonantradol suppression of male courtship clasping has no mammalian correlate and is the first documented direct cannabinoid alteration of a sex behavior. Investigation of cannabinoid effects on mammalian sex behaviors have primarily been limited to investigation of the effects of perinatal cannabinoid exposure on sex behaviors after development to adulthood. Such perinatal exposure has demasculinizing effects on male mice [105] and rats [106] and little effect on similar behaviors in females of either species. Demasculinizing effects in male rats have been associated with changes in catecholaminergic development [107] and responsiveness to dopaminergic agonists [108].

Increases in incidence of clasping behavior have been observed after treatment with vasotocin [109] and testosterone [110]. Inhibition of newt courtship clasping (consistent with that observed after cannabinoid treatment) has also been observed after treatment with corticosterone [111], and the κ-opioid agonist, bremazocine [99], although the mechanisms of these agents probably differ.

High densities of both cannabinoid receptors and glucocorticoid receptors are observed in areas of the mammalian hippocampus and striatum. This overlapping pattern of distribution suggests possible similar mechanisms in the mediation of newt behaviors. Also, a membrane receptor for corticosterone has been characterized in newt brain tissue. Activation of this membrane receptor is associated with inhibition of newt clasping behavior [112].

The ability of the cannabinoid agonist levonantradol to alter newt behaviors strongly suggests the presence of a cannabinoid neurochemical system within the central nervous system of this amphibian.

CHAPTER III. PHARMACOLOGY OF CANNABINOID BINDING SITES
IN NEWT NEURONAL MEMBRANES

Introduction

The ability of the cannabinoid agonist, levonantradol, to reduce newt

spontaneous locomotor behavior and potently and dose-dependently suppress clasping

behavior suggested that specific cannabinoid receptors might be present within the

central nervous system of this lower vertebrate. To test this hypothesis a series of

radioligand binding experiments using newt neuronal membranes were initiated.

These experiments were designed to determine if specific cannabinoid receptors are

expressed within newt brain, the number and pharmacological properties of these

binding sites, and how these properties might compare to results obtained in similar

experiments investigating mammalian CB1 receptors.

Methods

Preparation of Newt Neuronal Membranes

Well-washed newt neuronal membranes were used in radioligand binding

assays. To prepare these membranes newt brains were homogenized using a glass and

Teflon homogenizer in 25 volumes (based on tissue weight) of cold 0.32 M sucrose

containing 5 mM HEPES. This homogenate was then centrifuged at 1000 x g for 15

minutes at 4° C. The supernatant from this low-speed centrifugation was collected and

centrifuged at 30,000 x g for 30 minutes at 4° C. The pellet from this second

centrifugation was snap-frozen at -70° C, thawed, and resuspended using a glass and

Teflon homogenizer in 150 volumes of cold buffer containing 25 mM HEPES and 10

mM EDTA at pH = 7.45. This suspension was centrifuged at 30,000 x g for 30

minutes at 4° C, the resulting pellet resuspended in 150 volumes of 25 mM HEPES

buffer, and this suspension centrifuged again at 30,000 x g for 30 minutes at 4° C.

Pellets resulting from this final centrifuging step were stored at -70° C until needed for

binding assays.

Radioligand Binding Assays

The synthetic cannabinoid agonist CP-55940 in tritiated form (103 or 131

Ci/mmol; New England Nuclear, Boston, MA) was used in the binding studies

described. Binding reactions were conducted in a final volume of 500 mcl containing:

25 mM HEPES, 10 mM MgCl2, 1 % BSA, 0.1 % ethanol, and 60 to 185 mcg

membrane protein. Non-specific binding was defined as that occurring in the presence

of 1 mcM levonantradol (diluted from a 10 mM ETOH stock). Equilibrium binding

experiments were routinely carried out for 480 min and terminated by rapid filtration

over GF/C glass fiber filters using Brandel Cell Harvesters (Gaithersburg, MD).

Filters were washed immediately after termination of binding reactions with 6 ml ice-

cold buffer containing 25 mM HEPES and 10 mM $MgCl_2$. Kinetic experiments were

carried out over multiple time periods, using ligand concentrations greater than 10-fold

the concentration of receptor, and terminated similarly. Filter-trapped radioactivity was quantified by use of a Beckman LS 6000SC scintillation counter.

Data Analysis

Radioligand binding data were analyzed by computer-assisted nonlinear regression analysis using GraphPad Prism software (San Diego, CA). This program fits data to appropriate equations using iterative least-squares curve fitting techniques. The equations that data were fit to are summarized below.

Data from equilibrium saturation binding studies were fit to the equation for a rectangular hyperbola where [B] is the concentration of radioligand bound, B_{max} is the total receptor concentration, [L] is the amount of free radioligand, and K_d is the equilibrium dissociation constant:

$$[B] = B_{max} \bullet [L] / (K_d + [L])$$

For evaluation of binding to two or more sites the data were fit to the following equation where K_{di} and B_{maxi} are the constants for radioligand binding to site i:

$$[B] = \sum_{i=1}^{i=n} \frac{B_{maxi} \bullet [L]}{K_{di} + [L]}$$

The relative appropriateness of a one site model compared with a multiple site model was evaluated through F tests which determine if additional parameters improve the fit of the data to the more complex equation.

The dissociation rate constant (k_{-1}) was derived by fitting the data to the first-order rate equation where [B_t] is the amount of radioligand bound at time t after the

start of dissociation, [B$_0$] is the amount bound at time 0 and k$_{-1i}$ is the dissociation rate constant for each site i out of a possible n sites:

$$[\mathrm{B}_t] = \sum_{i=1}^{i=n} [B_{0i}] \bullet e^{k_{-1i}t}$$

The association rate constant (k$_{+1}$) is estimated by fitting the data to a pseudo-first order rate equation where [B$_t$] is the amount of radioligand bound at time t, K_{obs} is the observed association rate, and [B_{Eqi}] is the amount of radioligand bound at equilibrium to site i out of a possible n sites:

$$[\mathrm{B}_t] = \sum_{i=1}^{i=n} [B_{Eqi}] \bullet \left(1 - e^{k_{obsi}t}\right)$$

The association rate constant may then be determined using the following equation where k$_{-1i}$ is the empirically-determined dissociation rate constant for site i, and [L] is the radioligand concentration used.:

$$k_{+1i} = \frac{k_{obsi} - k_{-1i}}{[L]}$$

Data generated in competition binding experiments were analyzed by fitting a logistic equation to data points. The equation used was:

$$Bound = min + \frac{(max - min)}{1 + \left(10^{[L]} / 10^{IC_{50}}\right)}$$

where max represents binding in the absence of competitor, min represents in the presence of an excess concentration of competitor, [L] represents the concentration of competitor, and IC$_{50}$ represents the [L] that will produce a 50% percent inhibition of binding. For analysis of specific binding in equilibrium competition binding

experiments, min and max were fixed at 0% and 100%, respectively. Inhibitory

binding constants (K_i) were calculated from IC_{50} values using the Cheng-Prusoff

equation:

$$K_i = IC_{50} / \left[1 + \left([L] / K_d \right) \right]$$

where [L] is the concentration of radioligand and K_d is the empirically-determined

equilibrium dissociation constant for the radioligand.

Results

Equilibrium Saturation Binding

Results of equilibrium saturation binding of [³H]CP-55940 to newt neuronal

membranes demonstrate a specific interaction that is saturable and of high affinity.

The experiment presented in Figure 10 was performed in triplicate for 480 minutes at

15° C and employed radioligand concentrations ranging from 0.1 to 16.7 nM. Results

obtained through this experiment are consistent with those of two others. Over the

concentration range employed, an apparently single population of sites was labeled as

reflected in a linear Scatchard replot of the data (Figure 10, inset). Labeling occurred

with high affinity ($K_d = 6.5 \pm 1.3$ nM) and the density of binding sites in these

membranes is high ($B_{max} = 1853 \pm 161$ fmol/mg protein). At a concentration of

radioligand approximating the K_d, approximately 50% of total binding was specific.
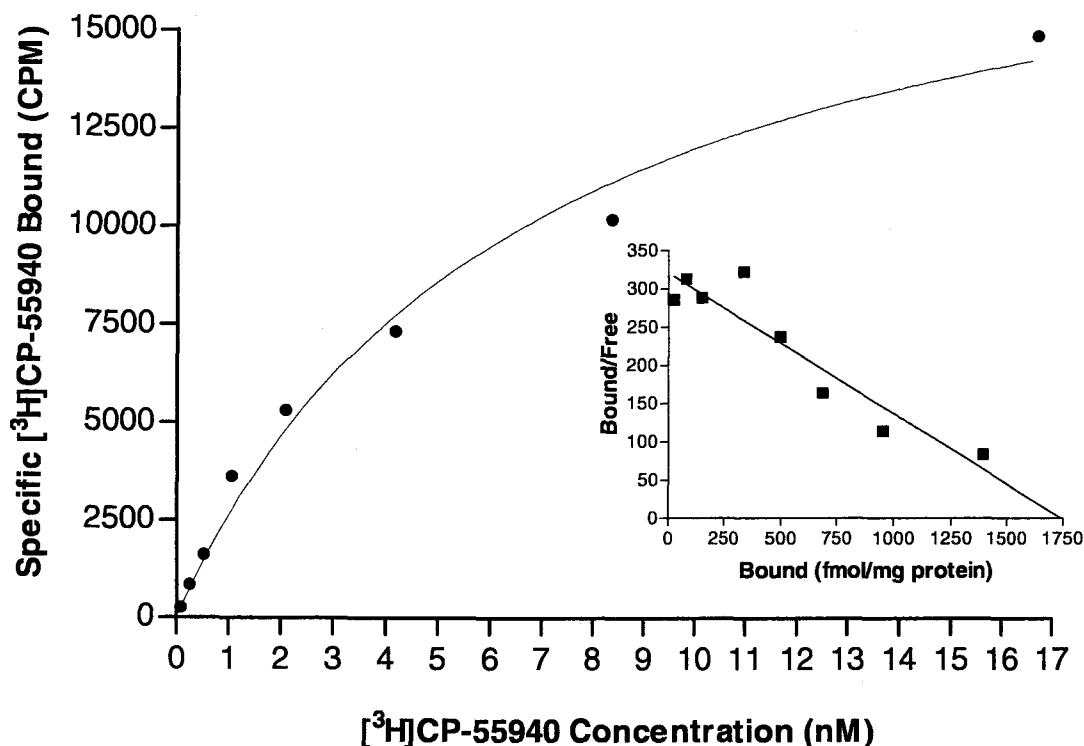
Figure 10. Equilibrium saturation binding of [^{3}H]CP-55940 to newt neuronal membranes (74 mcg protein). Membranes were incubated at the radioligand concentrations shown at 15° C for 480 min. Data were best fit with an equation describing interaction with a single binding site (K_d = 6.5 nM, B_{max} = 1853 fmol/mg protein). Inset: Scatchard replot of specific binding data was linear.

Kinetic Studies

Kinetic analysis of the binding of [^{3}H]CP-55940 to *Taricha* neuronal

membranes revealed that equilibrium binding was reached by 480 minutes at 15 °C

(Figure 11). Association and dissociation of [^{3}H]CP-55940 to the binding site was

monophasic. The k_{-1} estimated from the fit of the dissociation data was 6.84 x 10-3 ±

7.91 x 10-4 min $^{-1}$. The K_{obs} determined from the association data was 7.07 x 10-3 ±

7.71 x 10-4 min $^{-1}$. With a radioligand concentration of 0.094 nM, these parameters

resulted in a kinetically-derived $K_d = 2.7$ nM, a value in reasonable agreement with

that obtained through equilibrium saturation binding experiments. The agreement of

affinity values obtained through equilibrium saturation binding and kinetic studies

support the validity of the methods used for these binding experiments.

Equilibrium Competition Binding Experiments

The specificity of the cannabinoid binding site in newt neuronal membranes

was evaluated through a series of equilibrium competition binding experiments. These

experiments employed several cannabinoids with diverse structures. The cannabinoids

displaced [^{3}H]CP-55940 from an apparently single binding site with a distinct rank-

order of affinity, establishing a pharmacological profile for this amphibian

cannabinoid receptor (Figure 12).

The rank order of affinity of the cannabinoids used was (K_d, nM): CP-55940

(3.8) > levonantradol (13.0) > WIN55212-2 (25.7) >> anandamide (1665) ≈

anandamide + 100 mcM PMSF (2398). These experiments were performed three

times in triplicate. Results are summarized in Table 3 below.

Table 3: Displacement of specific [^{3}H]CP-55940 binding from newt neuronal
membranes

	CP-55940	levonantradol	WIN55212-2	anandamide	anadamide + PMSF
K_i, nM	3.8	13.0	25.7	1665	2398
95% CI	3.1-4.6	10.7-16.0	20.0-33.0	1437-1929	1749-3286
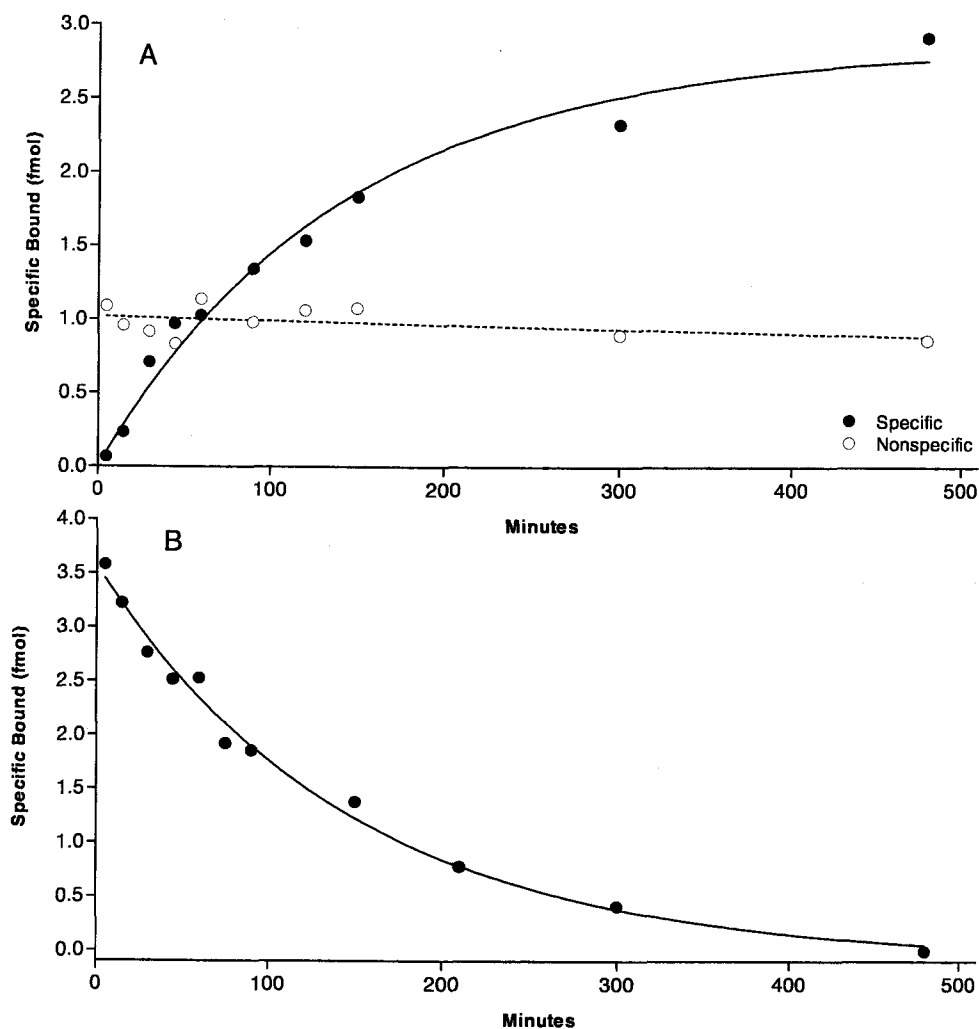
Figure 11. Kinetics of specific [³H]CP-55940 (94 pM) binding to newt neuronal membranes (50 mcg) at 15° C. (A) Association proceeded for the times indicated. Data were best fit by an equation describing a one-site association with $K_{obs} = 7.07$ x 10^{-3}/min. (B) Dissociation after incubation with radioligand for 480 min before addition of 100 mcM levonantradol. Data were best described using a one-site model with $K_{-1} = 6.84$ x 10^{-3}/min.

<u>Discussion</u>

The saturation and kinetic binding experiments presented demonstrate that an apparently single high-affinity cannabinoid binding site is present within newt neuronal membranes. The equilibrium competition experiments demonstrate the pharmacologic specificity of this binding site. The specificity of the binding site for various cannabinoids is consistent with that observed using mammalian tissue [70]. Taken together, these binding data are consistent with the expression of a specific CB1-like cannabinoid receptor in newt brain tissue.

The affinity of this newt brain cannabinoid receptor for [^{3}H]CP-55940 (6.5 nM) is somewhat lower than that reported for mammalian species (e.g. rat K_d = 0.13 nM [7]. This lower affinity may be partially-attributable to a lower incubation temperature used for binding experiments with newt tissue (15° C). This lower incubation temperature was employed to approximate physiologically-relevant conditions.
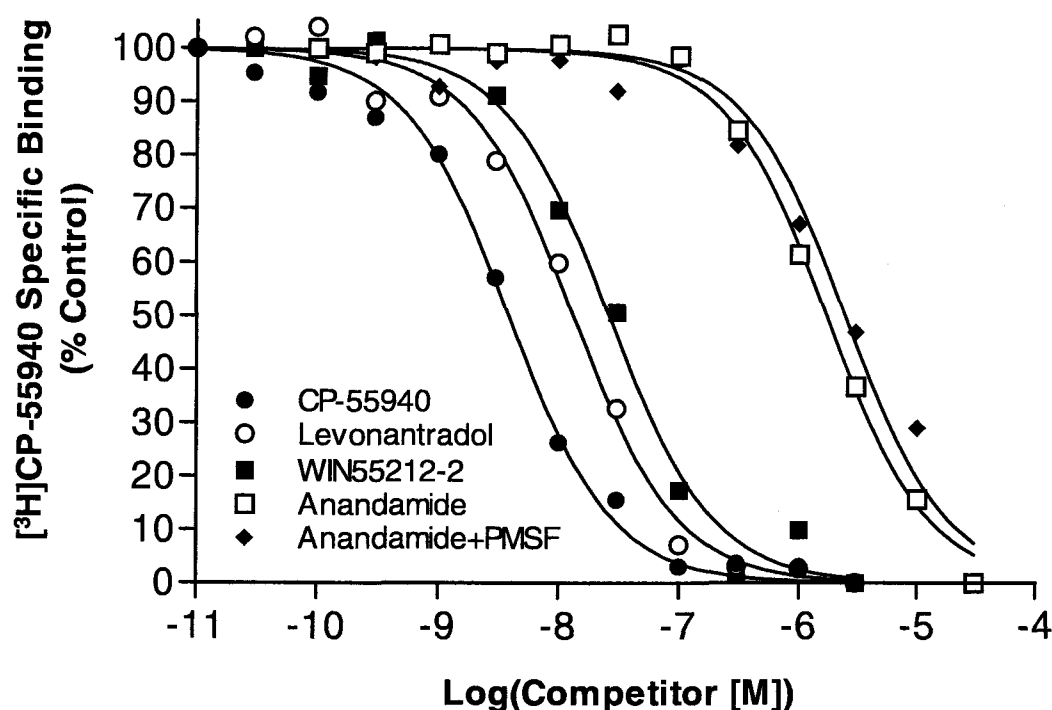
Figure 12. Specificity of displacement of [^{3}H]CP-55940 binding to newt neuronal membranes by various cannabinoids. Membranes (80-120 mcg protein) were incubated for 480 min at 15° C with 0.1 nM radioligand and the concentration of competitor shown.

The only notable inconsistency in the newt pharmacological profile as compared to that of mammalian CB1 receptors involves the interaction of the endogenous cannabinoid, anandamide. Anandamide effectively displaces [^{3}H]CP-55940 binding from both newt and mammalian neuronal membranes, but interacts with newt neuronal membranes with a lower affinity (newt K_i = 1651 nM vs. rat K_i = 52 nM [23]). Again, this apparent lower affinity may be due, in part, to different incubation temperatures used in binding experiments. In addition to apparent reduced anandamide affinity, the potentiating effect of the serine protease inhibitor,

phenylmethylsulfonyl fluoride (PMSF), on the ability of anandamide to displace

specific [^{3}H]CP-55940 binding from mammalian neuronal membranes was not seen

with newt neuronal membranes. PMSF [43] and a variety of other compounds [113]

inhibit an amidase activity present within preparations of mammalian neuronal

membranes. This amidase is retained during preparations of neuronal membranes and

catalyzes the metabolism of anandamide to arachidonic acid and ethanolamine.

Inhibition of this amidase is essential for detecting anandamide displacement of

cannabinoid radioligand binding to mammalian neuronal membranes at 30° C.

The lack of a dramatic effect of amidase inhibition in newt neuronal membrane

binding reactions employing anandamide is due to the low incubation temperatures

(15° C). When anandamide competition was evaluated with newt neuronal

membranes at 30° C, PMSF had a potentiating effect similar to that reported for

binding experiments with mammalian membranes (Figure 13). The lack of activity of

this amidase at temperatures approximating those physiologically-relevant for the newt

may indicate that this enzyme is not involved in the inactivation of anandamide

signaling in the newt *in vivo*. The PMSF-inactivated amidase activity as well as a

specific anandamide re-uptake system have been suggested to be involved in

cannabinoid signal termination in mammalian species [40], [114].
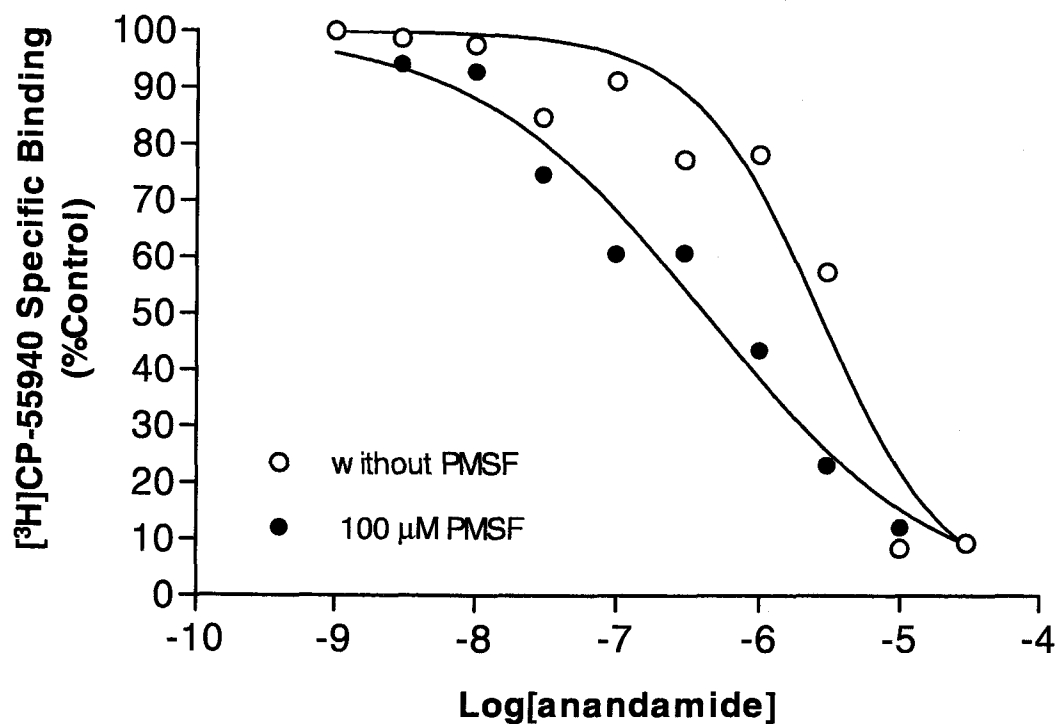
Figure 13. Potentiation of anandamide displacement of [^{3}H]CP-55940 specific binding to newt neuronal membranes by PMSF at 30° C. Similar potentiation was not seen at 15° C (Figure 12). K_i for anandamide in the presence of 100 mcM PMSF = 418 nM, for anandamide without PMSF = 2671 nM.

CHAPTER IV. MOLECULAR CLONING OF THE NEWT CB1
CANNABINIOD RECEPTOR

Introduction

The ability of cannabinoids to inhibit newt spontaneous locomotor activity and clasping behavior, combined with identification of a specific cannabinoid binding site in newt neuronal membranes with pharmacological specificity similar to that reported for mammalian species indicated the presence of an amphibian cannabinoid neurochemical system. To further characterize this system, experiments were designed to clone and heterologously express a cDNA encoding the newt cannabinoid receptor.

Methods

Construction of Newt Brain Complementary DNA Libraries

Isolation of Newt Head and Newt Brain Total RNA

Male roughskin newts were rapidly decapitated and heads were either immediately immersed in liquid nitrogen (newt head total RNA) or brains were dissected from the heads and immediately frozen in liquid nitrogen (newt brain total RNA). The nitrogen was evaporated and the frozen tissue (approximately 500 mg) was quickly homogenized by Polytron in 25 ml of a choatropic buffer consisting of

4M guanidinium isothiocyanate, 20 mM sodium acetate, 0.1 mM DTT and 0.5%

Sarkosyl. The homogenate was carefully layered over 5.7 M CsCl and centrifuged 20

hr at 150,000 x g at 18° C. The resulting total RNA pellet was resuspended in 500 mcl

RNAase-free water. The concentration of RNA was determined by UV absorbance at

260 nm. The average yield of total RNA from 500 mg of tissue was 700 mcg. Quality

was assessed by the sharpness of ribosomal RNA bands after separation by

electrophoresis through an ethidium bromide-stained, formaldehyde-containing

agarose gel. Total RNA was stored at -70° C as an ethanol precipitate.

Isolation of Polyadenylated RNA

Polyadenylated RNA was isolated from total RNA using the mRNA

Purification Kit manufactured by Pharmacia (catalog # 27-9258-01). This kit uses an

oligo(dT)-cellulose column-based strategy to selectively retain and isolate

polyadenylated RNA from other RNAs. Polyadenylated RNA used for cDNA library

construction was purified twice over oligo(dT)-cellulose columns. The average yield

of polyadenylated RNA from 700 mcg total RNA was 15 mcg. Yields were

determined by ethidium bromide plate assays. Quality of the polyadenylated RNA was

determined by its ability to provide a template for the synthesis of cDNA.

Synthesis and Cloning of Newt Head and Newt Brain cDNA

Newt head and brain cDNA was synthesized from about 5 mcg polyadenylated RNA using oligo(dT)12-18 as a primer for Moloney murine leukemia virus (MMLV) reverse transcriptase. Products of these reactions were treated with RNAase H and the second strand of cDNA synthesized by nick translation with *E. coli* DNA polymerase I in the presence of *E. coli* DNA ligase.

The resulting double stranded cDNA was precipitated with ETOH, resuspended, and the ends polished using *Pfu* polymerase (Stratagene). Polished cDNA was precipitated with ETOH, resuspended in T4 ligase buffer, and blunt ligated to adapters with EcoR1 cohesive ends and internal Not1 restriction sites. Excess adapters were removed and cDNAs were size-selected using CL-4B Sepharose spun columns (Pharmacia) which retain DNA < 350 base pairs in length. Some newt brain cDNA was synthesized using a kit (Pharmacia catalog # XY-033-00-07) that employs a strategy similar to that described above with the exception that cDNA ends were blunted with T4 DNA polymerase.

The concentration of cDNA was estimated by ethidium bromide plate assay. Complementary DNA (about 100 ng) was ligated into EcoR1-cut, phosphatase-treated lambda ZAPII or lambda gt11 phage arms (1 mcg, Stratagene). The resulting recombinant phage DNAs were packaged into viable bacteriophage using commercially-available extracts (Stratagene).

The number of primary clones in each library was determined by serial dilution of packaging reactions followed by infection of an appropriate bacterial strain

(Stratagene) and plating on LB-agarose plates. The number of primary plaque-forming units per unit volume of each library was determined. Libraries consisting of at least 1 x 10^6 were amplified, aliquoted and stored.

Polymerase Chain Reaction Using Degenerate Primers

To generate a template for the synthesis of newt cannabinoid receptor-specific nucleotide probes that could be used for high-stringency screening of cDNA libraries, degenerate primer PCR was attempted. This technique takes advantage of knowledge of amino acid sequences of the gene of interest which have been cloned from other species. At the time that this technique was applied to amplification of a newt cannabinoid receptor sequence, the amino acid sequences of human, rat, mouse, and pufferfish CB1 were available. Highly-conserved regions encoding portions of TMD2, TMD3, TMD6 and TMD7 of CB1 of these species were selected and degenerate primers were designed.

Two 5' sense primers were created, corresponding to the human CB1 amino acids 153-157 (YHFIG, designated "5CB1dpA") and 211-216 (AIDRYI, designated "5CB1dpB"). The degenerate DNA sequence encoding 5CB1dpA was: TAC CAC TTC AT(C/T/A) GG. The degenerate DNA sequence encoding 5CB1dpB was: GCC AT(C/T) GAC (A/C)G(G/C/A) TAC (A/G)T. Addition of 5' spacers and HindIII restriction sites resulted in the following primers: 5CB1dpA - ATG AAG CTT TAC CAC TTC AT(C/T/A) GG; 5CB1dpB - TTG AAG CTT GCC AT(C/T) GAC (A/C)G(G/C/A) TAC (A/G)T.

Two 3' anti-sense primers were designed based on amino acids corresponding
to human CB1 373-378 (ICWGP, designated 3CB1dpA) and 400-406 (FCSMLC,
designated 3CB1dpB). The degenerate DNA sequence used for 3CB1dpA was:
AT(C/T/A) TG(C/T) TGG GGC CCT. The degenerate DNA sequence used for
3CB1dpB was: TT(C/T) TG(C/T) AG (C/T) ATG CTG TGC. Taking the
complement of these DNA sequences and adding 5' spacers and XbaI restriction sites
resulted in the following degenerate primers: 3CB1dpA - CAT TCT AGA AGG
GCC CCA (G/A)CA (G/A/T)AT; 3CB1dpB - CAT TCT AGA GCA CAG CAT
(A/G)CT (G/A)CA (G/A)AA.

All four combinations of 5CB1dpA, 5CB1dpB, 3CB1dpA and 3CB1dpB
primers were used for 40 rounds of *Taq* polymerase-catalyzed PCR. The cDNA used
to construct NBL3 was used as a template. Annealing temperatures of 40°C were used
for the first five cycles, followed by 48°C for the remaining 35.

A third 5' sense degenerate primer was designed to amplify the 5' coding
sequence of CB1. This primer was useful in cloning the 5' coding sequence of the
newt cannabinoid receptor by PCR when library screening resulted in isolation of only
a 3' fragment. The first six amino acids of the rat CB1 was used for the design of this
primer: MKSILD. The degenerate sequence corresponding to these amino acids was
ATG AA(G/A) (A/G)T(G/C) (C/T)T(A/G) GA. Addition of a spacer and HindIII
restriction site resulted in the following primer designated 5CB1dpC: ATG AAG CTT
ATG AA(G/A) (A/G)T(G/C) (C/T)T(A/G) GA.

Products of degenerate PCR reactions were separated from excess primers by electrophoresis through an ethidium bromide-stained agarose gel. Bands corresponding to newt cannabinoid receptor sequence fragments were excised from gels and the DNA was isolated by centrifugation through a paper slurry. The resulting purified PCR fragments were digested overnight with appropriate restriction enzymes, phenol/chloroform extracted, and ligated into appropriately-digested, phosphatased, pBluescript (KS-) plasmid (Stratagene). Chemically-competent DH5α bacteria were transformed with the resulting recombinant plasmids and clones isolated. Clones containing cDNAs were confirmed by restriction mapping of small-scale plasmid DNA preparations. The DNA sequences of positive clones were determined by the Oregon State University Central Services Laboratory.

Evaluation of Newt CB1 Cannabinoid Receptor Expression in Various Tissues

Northern Blot Analysis

Total RNA from various newt tissues including lung, heart, testes, digestive tract, skeletal muscle, liver and spleen was isolated as described above for brain. These total RNAs (25 mcg each) were separated by electrophoresis through a formaldehyde-containing agarose gel and transferred to a nylon membrane (Brightstar-Plus, Ambion, Inc.).

The membrane was baked at 80° C for two hours and pre-hybridized for two hours at 42° C in 10 ml of a solution containing: 50 % formamide, 25 mM KPO_4, 5X

SSC, 5X Denharts solution, and 50 mg/ml sonicated herring sperm DNA. For hybridization, the solution was replaced with an equal volume of the same hybridization solution containing 1×10^6 CPM/ mcl of a [^{32}P]-labeled newt cannabinoid receptor probe. This probe was made as described below for plaque-lift library screening using Klenow fragment to incorporate [^{32}P]-dCTP using random hexamer primers and a 715 bp degenerate primer PCR fragment of the newt cannabinoid receptor as a template (described below).

Hybridization proceeded for 18 hr at 42 °C and was terminated by removal of the probe-containing solution followed by several room-temperature washes with 2X SSC/2 % SDS. Additional 10-minute stringent washes were done at 65° C in 0.1X SSC/0.1 % SDS until background counts were reduced to 100 CPM/minute. The membrane was then wrapped in plastic wrap, placed in an X-ray cassette with two intensifying screens and opposed to film for about 18 hr.

After a suitable film image had been obtained using the newt cannabinoid receptor probe, the membrane was stripped and probed again with a [^{32}P]-labeled probe synthesized using a cDNA encoding mouse 18S RNA as a template. This additional hybridization was done to demonstrate that equal amounts of RNA had been loaded from each tissue type.

Reverse-Transcription Coupled to PCR (RT-PCR)

One microgram each of the total RNAs isolated from the various tissues as described above were treated with RNAase-free DNAase I, phenol/chloroform

extracted, and used as templates for MMLV reverse transcriptase-mediated synthesis of oligo(dT)1-18-primed cDNAs in a reaction volume of 10 mcl. A 1 mcl aliquot of each of these cDNA synthesis reactions were then used as templates for PCR using newt CB1-specific primers.

The 5' primer used corresponds to bases 1012-1030 of the newt CB1 cannabinoid receptor coding sequence and contains a 5' three-base spacer followed by a BamHI restriction site. This primer was designated "nCB1L" and its sequence is: TTG GGA TCC GCA TGG ACA TCC GGT TAG. The 3' primer was designed to complement the last 21 coding bases of the newt CB1 cDNA and contains an XhoI restriction site followed by a three base spacer. This primer was designated "3FLnCB1", and its sequence is: CAT CTC GAG CTA TAC TGC TTC GCC AGA TGT. The expected size of the fragment produced by these primers is 428 bp.

The primers described above were used with 1 mcl of the cDNA synthesis reactions for 30 cycles of PCR using *Taq* polymerase and a "touchdown PCR" annealing temperature reduction program. Touchdown PCR is described in more detail in the cloning section below, for these reactions an initial annealing temperature of 60° C was decreased each cycle until 50° C was reached, after which remaining cycles were conducted at this 50° C "touchdown" temperature. Five mcl of 20 mcl PCR reactions were used for gel electrophoresis. Products were analyzed after ethidium bromide-staining and photography.

Complementary DNA Library Screening

Newt brain cDNA libraries were titered on XL1-Blue bacteria (Stratagene) and 50,000 plaque forming units were plated on each of six 150 mm LB agarose plates; 300,000 plaque forming units were screened at once. Cultures were grown at 37° C until plaques were about 1 mm in diameter. Duplicate lifts were made onto 120 mm nitrocellulose disks (Schleicher and Schuell). The orientation of each lift was recorded by stabbing through the disks into the underlying LB agarose media with a needle containing India ink.

The 715 base pair newt cannabinoid receptor fragment synthesized by PCR using 5CB1dpA and 3CB1dpB degenerate primers was used as a template for the synthesis of a radio-labeled DNA probe. Klenow fragment was used for random hexamer primed synthesis of this probe in the presence of [^{32}P]-dCTP (DuPont-NEN). This reaction resulted in production of DNA fragments encoding the newt cannabinoid receptor labeled to high specific activity. Probes were purified from excess primers and unincorporated [^{32}P]-dCTP over Sepharose G-50 spun columns and used for hybridization at 1×10^6 CPM/mcl of hybridization buffer.

Hybridization reactions were conducted overnight at 42°C in buffer containing 50% formamide, 1% SDS, 5X SSC, and 2 mg/ml salmon sperm DNA. After hybridization, excess probe was removed by several room temperature washes with 2X SSC/1% SDS. These washes were followed by several 15 minute high-stringency washes in 0.1X SSC/0.1% SDS at 65°C. High-stringency washes were repeated until background counts on the nitrocellulose disks were reduced to about 100 CPM/minute

as determined by a hand-held monitor. About five high-stringency washes were usually required.

After stringent washing, the nitrocellulose disks were wrapped in plastic wrap and placed into X-ray film cassettes between intensifying screens. Orientations of disks were recorded with tape marked with ink containing ^{35}S. The disks exposed film overnight at -80°C. Putative clones (as determined by signals present on duplicate lifts) were isolated from LB-agarose plates by excising about a 5 mm square chunk of agarose plate media and dispersing into 500 mcl SM buffer. These initial isolates each contained several clones and therefore were subjected to second and occasionally third rounds of plaque lift screening.

When isolation of a single lambda phage clone had been achieved, subcloning of cDNA inserts was commenced. For clones isolated from NBL3 which was made with the lambda ZAPII vector, subcloning was done by phagemid excision of a cDNA insert-containing Bluescript plasmid by co-infection of bacteria with a single-stranded helper phage.

Clones derived from lambda gt11-based libraries were amplified to high titer and the lambda DNA isolated using a kit (Qiagen). Complementary DNA was isolated from lambda arms by digestion with Not1 (the internal restriction site present in the adapters used during cDNA library construction) followed by separation by electrophoresis through an ethidium bromide-stained agarose gel. Bands corresponding to cDNA inserts were excised from the gel and the DNA was isolated by centrifugation through a paper slurry.

The resulting purified cDNA fragments were ligated into Not1 digested,

phosphatased pBluescript (KS-) plasmid. Chemically-competent DH5α bacteria were

transformed with the resulting recombinant plasmids and clones isolated. Clones

containing cDNAs were confirmed by restriction mapping of small-scale plasmid

DNA preparations. The DNA sequences of positive clones were determined by the

Oregon State University Central Services Laboratory. Large-scale plasmid DNA

preparations and glycerol storage stocks were made of selected plasmid clones.

Cloning of Complementary DNA Encoding the Complete Newt CB1 Amino Acid Sequence for Heterologous Expression

The cDNAs isolated from library screening were subcloned into the Bluescript

plasmid as described above. These sequences were further subcloned into the

eukaryotic expression vector, pTL1 through 3-way ligations taking advantage of the

presence of unique restriction sites in overlapping sequences. These 3-way ligations

resulted in formation of contiguous cDNAs encoding the complete newt CB1

cannabinoid receptor.

In order to remove untranslated regions, PCR primers were designed

corresponding to the extreme 5' and 3' ends of the newt CB1 receptor coding

sequence. Use of these primers resulted in amplification of cDNAs consisting of only

the newt CB1 receptor coding bases. One of the 5' PCR primers used was designed to

modify the newt CB1 receptor to include an N-terminal amino acid sequence

recognized by a commercially-available anti-myc antibody (Invitrogen). The amino

acids corresponding to the epitope tag encoded by this primer were: EQKLISEEDLN. This epitope sequence was placed between the first two amino acids of the newt CB1 receptor.

The PCRs described above were done using *Pfu* polymerase (Stratagene). This thermostable polymerase has error correcting activity that results in significantly better fidelity of transcription than that produced by *Taq* polymerase. Reactions were conducted in a total volume of 100 mcl in the buffer supplied by the manufacturer supplemented with 200 nM dNTP and 5 % DMSO. The template used was 10 ng of pTL1nCB1Lib (Figure 19). Primers were used at 1 mcM. Cycle temperature steps were conducted for the following times: denaturing temperature (94° C) for one minute, annealing temperature (variable, discussed below) for two minutes, extension (72° C) for three minutes.

Annealing temperatures varied according to a "touchdown PCR" annealing temperature reduction program. In this program, a total of 25 cycles are conducted starting with an annealing temperature of 60° C. This initial annealing temperature is reduced by one degree in succeeding cycles until a final temperature of 50° C is reached. An additional 15 cycles are then conducted at this "touchdown" temperature.

The rationale of this annealing temperature reduction program involves problems associated with balancing a robust amplification with production of a specific DNA product. At the initial higher annealing temperatures used in touchdown PCR the likelihood of non-specific annealing is low. Amplification of specific sequences may also be reduced. The gradual reduction in annealing temperature

increases the probability that an optimal temperature for specific amplification will be used. This results in an early production of specific products which will, over the course of the chain reaction, dilute any non-specific products that may be produced in following lower temperature cycles.

Chinese Hamster Ovary Cell Transfections

Chinese hamster ovary (CHO) cell cultures were transfected by a standard calcium phosphate-based method [115]. Briefly, 10 mcg of plasmid DNA encoding the newt CB1 receptor and 250 ng of pRC/RSV(-) (Invitrogen) which encodes a neomycin resistance factor were precipitated in 250 mcl HEPES-buffered saline (pH = 7.10) with 250 mM $CaCl_2$. This precipitate was spread evenly over CHO cell cultures at about 60 % confluence in 100 mm dishes. Cultures were incubated with precipitates for four hours. After removal of precipitates, the cultures were shocked for 3 minutes by addition of 2 ml of 10 % glycerol in complete media. Cells were then washed three times with sterile phosphate buffered saline solution (PBS) and grown to confluence in complete media (about two days). Confluent 100 mm dishes were split into four 150 mm plates and cultured in media containing G418 (750 mcg/ml). Well-isolated, G418-resistant colonies became visible after 10-14 days and were isolated by scraping with a sterile pipette tip and transfer to 35 mm dishes. Clones were allowed to grow to confluence under selection in 35 mm dishes, after which they were split, still under selection, into T-75 flasks. Clonal cultures grown to confluence in flasks were either harvested in complete media containing 10 % DMSO

and samples stored in liquid nitrogen, or further cultured for screening for newt CB1 receptor expression.

A non-clonal cell line expressing a non-myc-epitope tagged version of the newt cannabinoid receptor was made as described above with the following exceptions: 1) Transfected cells that had become confluent in 100 mm dishes were split into a single 150 mm plate and cultured under selection. Colonies resulting from this dense plating were not generally well isolated and consisted of numerous independent clones. These clones were all harvested together and aliquots were prepared and stored cryogenically. The resulting non-clonal cell line was handled as described for clonal cell lines above.

In Vitro Translation of Cannabinoid Receptors

Expression vectors (pTL1) containing cDNAs encoding myc-epitope-tagged newt CB1 and the human CB2 receptors (Figure 19) were evaluated for ability to direct synthesis of proteins of expected size by in vitro translation.

These experiments were done using a rabbit reticulocyte lysate-based kit manufactured by Promega, Inc. (TnT Coupled Reticulocyte Lysate System). Transcription and translation of cannabinoid receptor sequences were accomplished in the presence of [^{35}S]-labeled methionine. Products of these reactions were separated by polyacrylamide gel electrophoresis (PAGE) as described in more detail in the following section. The resulting gel was laid on chromatography paper, dried, covered with plastic wrap, and allowed to expose film overnight.

Western Blot Detection of Newt CB1 Cannabinoid Receptor Expression

For purposes of screening cell lines, samples of stable CHO cell cultures were prepared by scraping confluent 100 mm dish cultures in PBS into a tube and centrifuging for 10 minutes at 3000 x g followed by addition of 2X Laemmli sample buffer [116]. For analysis of subcellular localization, samples of membranes were prepared as described above for preparation of neuronal membranes for binding experiments, or total particulate preparations were made. For total particulate preparation, CHO cultures were collected by scraping in 50 mM Tris buffer (pH 7.4), and homogenized by three 10 second bursts of a Polytron homogenizer and pelleted at 30,000 x g for 15 minutes. These membranes were resuspended by Polytron and pelleted two additional times. Protein concentrations were assayed by the method described by Lowry [117].

Proteins were separated by PAGE on 10 % or 12.5 % minigels and transferred electrophoretically to nitrocellulose membranes.

Immunoblots were blocked by incubation with 5 % non-fat dried milk in Tris-buffered saline (TBS) and reacted with commercially-available anti-myc primary antibody and goat anti-mouse IgG-HRP conjugate (Invitrogen). Immunoblots were visualized by Enhanced Chemiluminescence (Amersham) and allowed to expose film.

Adenylate Cyclase Assays

Adenylate cyclase assays were performed according to a modified version of

the Salomon method [118]. Newt CB1 receptor-expressing CHO cell cultures were

washed twice with serum-free F12 Ham's media and then incubated for 4 hours in 1

ml of the same media containing 1.2 mcCi [^{3}H]adenine. The tritium-containing media

was then aspirated and replaced with serum-free F12 Ham's media containing a

phosphodiesterase inhibitor (50 mcM Ro 20-1724). These cultures were incubated at

37° for 40 min in the presence of 25 mcM forskolin and various concentrations of

cannabinoids. Incubations were terminated by the addition of 300 mcl of Stop

Solution (2% SDS, 1.3 mM cyclic AMP), followed by addition of 100 mcl

concentrated perchloric acid, and 750 mcl water. [^{14}C]cyclic AMP (5000 CPM in 50

mcl) was added to each plate to correct for recovery. After transferring the contents of

culture dishes to 1.5 ml centrifuge tubes, 12 M KOH was added to neutralize the

samples. The resulting precipitate was pelleted by centrifuging at 10,000 g for 10

minutes. Cyclic AMP in the supernatants was isolated by sequential chromatography

over Bio-Rad AG-50W-X4 cation exchange resin and neutral alumina. Concentrations

of [^{3}H]cyclic AMP and [^{14}C]cyclic AMP in eluates were determined simultaneously

using a Beckman LS 6000SC scintillation counter (^{3}H channels 0 - 250, ^{14}C channels

350 - 670). Counts were corrected for crossover and recovery.

Results

Newt Head and Newt Brain Complementary DNA Library Construction

Total RNA of good quality was isolated from newt head and newt brain tissue

as determined by the lack of degradation of ribosomal RNA bands after separation

through a formaldehyde-containing agarose gel. RNA was blotted to a nitrocellulose

filter, stained with methylene blue and photographed (Figure 14).
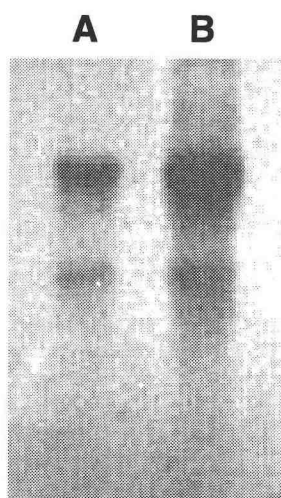
Figure 14. Northern blot detection of total RNA with distinct ribosomal bands. (A) 5
mcg newt brain total RNA. (B) 10 mcg newt head total RNA. RNAs were separated
by electrophoresis through a formaldehyde-containing agarose gel, blotted to
nitrocellulose, stained with methylene blue and photographed. The presence of sharp
ribosomal RNA bands in each sample indicates a lack of degradation and suitability
for further use in cDNA library construction.

The quality of cDNA used for library construction was evaluated by southern blots of aliquots of synthesis reactions containing a small amount of $[^{32}P]$-dCTP. Examples of these southern blots are presented in Figure 15.

Several initial attempts to construct newt head and newt brain cDNA libraries resulted in production of libraries based on a low number of primary clones (10,000 - 25,000 Pfu). The third attempt to produce a newt brain cDNA library resulted in production of a large number of recombinant phage. 1.3×10^6 plaque-forming units of this library were amplified by infection of XL1-Blue bacteria (Stratagene), aliquoted, and designated "newt brain library 3" or "NBL3". The cDNA used for this library was synthesized using oligo(dT)12-18 primers.

Three additional newt brain libraries were constructed using a Pharmacia cDNA synthesis kit and the lambda gt11 phage vector (Stratagene), each using different primers for first strand synthesis: NBL6 was primed with a combination of random hexamers and a newt cannabinoid receptor-specific primer, NBL7 was primed with random hexamers, and NBL8 was primed with a combination of oligo(dT)12-18 and newt cannabinoid receptor-specific primer. NBL6, 7 and 8 were each amplified from 1×10^6 plaque-forming units of primary recombinant phage.

The quality of all libraries described were assessed by the ability of each to serve as a template for the amplification of a portion of the newt cannabinoid receptor using degenerate PCR primers. NBL8 has also been used as a template for degenerate primer PCR amplification of cDNAs encoding newt homologues of NAP-22, GAP-43, calcineurin and vasotocin/neurophysin precursor protein.

Polymerase Chain Reaction Using Degenerate Primers

Amplification of DNA fragments of expected size in all four of the reactions

possible using combinations of 5CB1dpA, 5CB1dpB, 3CB1dpA and 3CB1dpB

degenerate primers were observed. The reaction employing 5CB1dpA and 3CB1dpB

gave the largest fragment (715 bp). This fragment was subcloned into the HindIII and

XbaI sites of pBluescript (KS-). A large-scale plasmid DNA preparation of this

construct was made. Digestion of this plasmid with HindIII and XbaI followed by gel

isolation of the 715 base-pair newt cannabinoid receptor cDNA fragment resulted in

DNA which was used as a template for Klenow-mediated synthesis of $[^{32}P]$-dCTP-

labeled probes for stringent library screening and northern blotting.
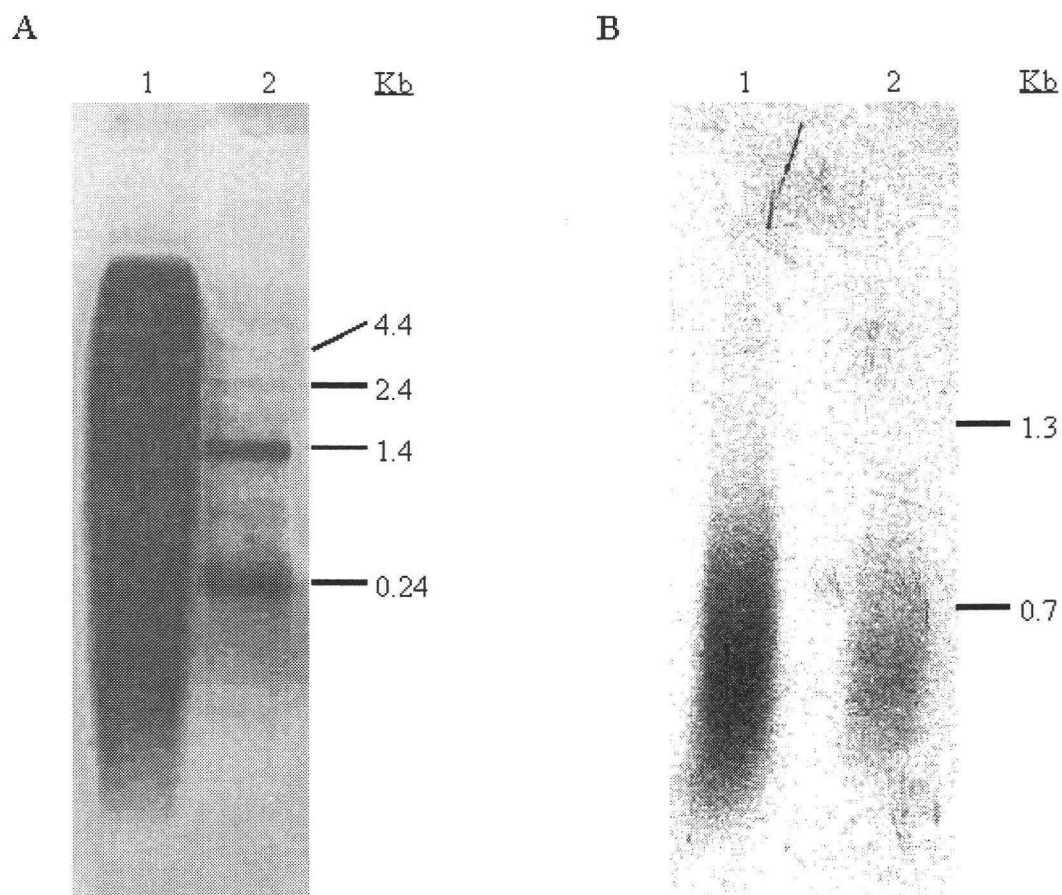
Figure 15. Southern blot detection of cDNA synthesis control reactions. Complementary DNAs labeled with [^{32}P]-dCTP were separated by electrophoresis through agarose gels, transferred to nitrocellulose membranes, and allowed to expose film. (A) Newt brain cDNA: (lane 1) second strand cDNA synthesized from newt brain polyadenylated RNA and (lane 2) cDNA synthesized from control polyadenylated RNAs of various lengths. (B) Newt head cDNA: (lane 1) first and (lane 2) second strand cDNA synthesized from newt head polyadenylated RNA.

Determination of Tissue Distribution of Newt CB1 Cannabinoid Receptor Expression

Northern blot analysis

Results of northern blot analysis of total RNA isolated from various newt tissues are presented in Figure 16. These results indicate that the newt CB1 cannabinoid receptor is expressed in brain at much higher levels than in lung, heart, testes, digestive tract, skeletal muscle, liver or spleen. Re-probing of the blot with a probe specific for 18S rRNA demonstrates that similar amounts of RNA were loaded for each tissue type. Based on generation of a standard curve based on the migration of the RNA molecular weight standards used, the size of the newt CB1 cannabinoid receptor transcript is estimated to be 5.9 Kb.

Reverse-transcription coupled to PCR (RT-PCR)

Results of northern blot analysis of the expression of the newt CB1 cannabinoid receptor gene in various tissues demonstrated that highest expression occurs in brain. These results did not exclude the possibility that expression does occur in the other tissues at levels too low to detect under the northern blotting conditions employed. To further evaluate potential expression in other tissues, RT-PCR experiments were done. The results of these RT-PCR experiments are presented in Figure 17. These results suggest that, in addition to brain, the newt CB1 receptor may be expressed in newt digestive tract.

Identification of a newt gene that is equally-expressed across these tissue types will be required to control for amounts of cDNA used for different tissues and allow quantitative comparisons to be made. These results do indicate, however, that the newt CB1 is expressed at some level in tissues of the digestive tract.

Complementary DNA Library Screening

As several additional attempts to isolate NBL3 clones encoding the remaining 5' sequence of the newt CB1 cannabinoid receptor were unproductive, additional libraries were constructed as described in the methods section above. The cDNAs used for these libraries were primed with various oligonucleotides in an attempt to ensure the representation of sequences encoding the 5' sequence of newt CB1: NBL6 was primed with a combination of random hexamers and a newt cannabinoid receptor-specific primer, NBL7 was primed with random hexamers, and NBL8 was primed with a combination of oligo(dT)12-18 and newt cannabinoid receptor-specific primer. Each of the cDNAs synthesized for these second generation libraries were cloned into the lambda gt11 vector and 1×10^6 primary clones of each were amplified, aliquoted and stored.
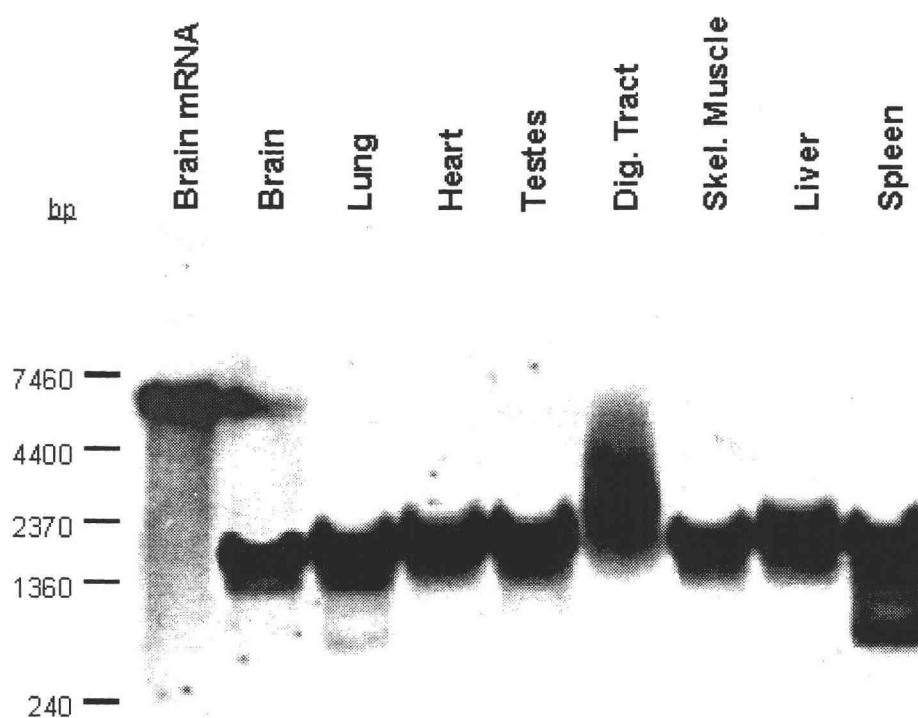
Figure 16. Northern blot analysis of tissue expression of the newt CB1 cannabinoid receptor gene. Numbers on the left indicate migration of RNA molecular weight standards. Shown are superimposed images of the same blot probed with a newt CB1 receptor probe and an 18s rRNA probe. Bands corresponding newt CB1 transcripts are estimated to be 5.9 Kb and are only visible in brain samples. Faster migrating transcripts present in all tissues except brain mRNA indicate expression of 18s rRNA and demonstrate that similar amounts of total RNA (25 mcg) were loaded across tissue types.

Figure 17. RT-PCR analysis of newt CB1 receptor expression in various tissues. Total RNA (1 mcg) from newt brain (B), lung (L), heart (H), testes (T), digestive tract (D), skeletal muscle (M), liver (V) and spleen (S) were reverse-transcribed into cDNA using MMLV and oligo(dT) primers. *Taq*-catalyzed PCR was done using newt CB1-specific primers for 30 cycles using annealing temperatures decreasing from 60° C to 50° C. A no-reverse transcriptase brain RNA control is shown (-). The arrow indicates migration of a 700 bp DNA standard.

Plaque-lift screening of NBL6, NBL7 and NBL8 each produced several positive clones. Each of these clones was subjected to additional screening by PCR using a combination of 5CB1dpC (a degenerate primer encoding the extreme 5' end of the CB1 coding sequence, discussed in detail in the methods section above) and a 3' anti-sense newt CB1-specific primer. These primers resulted in amplification of a promising fragment from a clone isolated from NBL6. This fragment was subcloned into a Bluescript plasmid and sequenced by the OSU Central Services Laboratory.

Sequencing confirmed the fragment's identity as a cDNA encoding the 5' portion of the newt CB1. This 5' clone overlapped "library clone 1" by 80 nucleotides. Within this overlapping sequence is a unique restriction site recognized by the blunt-cutting restriction enzyme, BstZ17I. The NBL6 lambda gt11 clone from which this PCR clone was derived was amplified to high titer and a mid-scale

preparation of its DNA was made. This lambda DNA was digested with NotI (the internal restriction site present in the adapters used for cDNA cloning) which allowed separation of the cDNA insert from the lambda vector arms and isolation after agarose gel electrophoresis. This gel-purified cDNA was subcloned into a Bluescript plasmid and designated "library clone 2".

Sequencing of "library clone 2" revealed that the cDNA consisted of 1594 bases, the first 644 of which represent a 5' untranslated region, while the remaining 950 bases encode a portion of the newt CB1 receptor beginning with the 5' initiator codon, "ATG". As with the PCR fragment amplified with the degenerate primer, 5nCB1dpC and a 3' newt CB1-specific primer (described above), "library clone 2" overlaps "library clone 1" by 80 bases. This similarity indicates that this clone was derived from cDNA made with the newt CB1-specific primer used both in construction of NBL6 and the PCR amplification described.

Cloning of Complementary DNA Encoding the Complete Newt CB1 Amino Acid Sequence for Heterologous Expression

The unique BstZ17I restriction site present in both cDNAs isolated from plaque lift screening (library clone 1 and library clone 2) was used to join the two into a complete, contiguous, coding sequence through a 3-way ligation into the eukaryotic expression vector, pTL1. The resulting expression vector construct was designated "pTL1nCB1Lib" and was sequenced by the OSU Central Services Laboratory. The

DNA sequence of the complete newt CB1 cDNA encoded by pTL1nCB1Lib is

presented in Figure 18.

```
   1 gagaggcgctgggagagacactgagcaaaggaacacccaggggagcaggaagcacacagtaggcgcaggggaggatgaggggaagctttg 90
  91 tggtgcaacatccccaagacgctgcgcacagagaaagccgttgaagaggacgacaggcaaaagagaaatctactccacccctgcacccc 180
 181 caggcttctgctacgagagtgacacctcgtgaaagaagaggttccagcacccctttcactgcccccaggctgcccgcggcagagtctttc 270
 271 ctgcctctcgcgctctgccgctgggctgccaggtcttgcactgtcagggaagccggcttaaccaagctcccccctctgccggcgaagcca 360
 361 agtactgcagccaagtagttctccgcagcacgggaggaccagctcatgtatatagctccacaaagacacagtgcggagcatctccagtcc 450
 451 aggaggaccacccctgcctgagctccagagagtaacagtgcgacagcatctccagcccaggacgaccacccctgcctgaactcagagtgt 540
 541 aacagtgcgggagcgatgcagccggagcggggcgagcgatgtgactggcatacttctacattctttcattttcgaagatgctcatgtgat 630
 631 caaaaacaaaggttATGAAGTCGATCTTGGATGGCCTTGCAGACACAACTTTTCGAACCATTACAACTGACCTTCTCTACATGGGTTCCA 720
 721 ACGACGTTCAGTACGAAGACACTAAGGGCGAAATGGCCTCCAAACTTGGGTATTTTCCACAAAAGTTACCTTTGTCCTCCTTCAGGAGTG 810
 811 ATCACTCTCCAGACAAAATGACTATAGGAGATGATAATCTGCTCAGTTTCTATCCTCTAGATCAGTTTAATGTCACTGAGTTTTTTAATC 900
 901 GGTCTGTATCGACATTCAAGGAAAATGACGATAACTTAAAATGTGGGGAAAATTTCATGGACATGGAGTGCTTCATGATTCTAACTGCAA 990
 991 GCCAACAGCTGATCATTGCAGTCCTTTCCCTTACCCTAGGCACCTTCACAGTCCTGGAGAACTTTTTAGTACTGTGTGTCATTCTACAAT 1080
1081 CTAGGACCCTCCGATGCAGACCCTCCTACCACTTCATTGGCAGCTTAGCTGTGGCTGATCTCCTTGGAAGTGTCATTTTTGTCTACAGTT 1170
1171 TTCTTGACTTTCATGTGTTCCATCGAAAAGATAGTTCCAATGTCTTTTTGTTCAAATTGGGAGGAGTTACAGCCTCATTCACAGCTTCAG 1260
1261 TAGGTAGCCTTTTTCTCACTGCCATAGACCGGTATATTTCTATACATAGGCCACTTGCTTATAAACGGATAGTGACAAGGACAAAAGCGG 1350
1351 TCATCGCATTCTGCGTGATGTGGACCATTGCTATTATTATTGCTGTACTTCCTTTACTTGGCTGGAACTGCAAAAAACTCAAATCGGTCT 1440
1441 GCTCCGACATATTCCCACTTATTGATGAGAACTATTTGATGTTCTGGATTGGGGTCACAAGTATACTCCTGCTGTTCATTGTGTATGCTT 1530
1531 ATGTTTACATACTCTGGAAGGCCCACAGTCATGCTGTTCGAATGTTGCAACGGGGCACTCAAAAGAGTATAATTATTCACACTTCAGAAG 1620
1621 ATGGCAAAGTACAGATCACTAGACCGGAACAGACGCGCATGGACATCCGGTTAGCCAAAACCCTGGTCCTTATTCTGGTGGTCCTCATTA 1710
1711 TCTGCTGGGGCCCGCTCCTTGCCATTATGGTCTACGATGTCTTTGGAAAGATGAACAACCCCATCAAGACTGTTTTTGCCTTTTGCAGCA 1800
1801 TGCTCTGCCTAATGAATTCTACAGTGAATCCCATCATCTATGCTCTGCGGAGCCAAGACTTGAGGCATGCTTTCTTGGAGCAGTGCCCCC 1890
1891 CTTGCGAAGGGACCTCGCAACCTCTTGATAACAGTATGGAATCAGACTGTCAGCACAGGCATGGGAATAATGCAGGAAATGTTCACAGGG 1980
1981 CTGCTGAAAACTGCATTAAGAGCACGGTTAAAATCGCCAAAGTGACCATGTCTGTCTCCACAGAAACATCTGGCGAAGCAGTATAGgttg 2070
2071 tagaataatattcggtctacacatctataaatctttgaaaaaaagtaaacaggatgtgttcaagttcgacccttctggattatataatta 2160
2161 acaatcacattgcctaccctcttcaatatctcaaaagactacaactgtgatggatgcacatttaaaaaaatcaaatcaagattagaggtt 2250
2251  ggattgatcagtgatcagagaaacccctaacaagtaaaaaaaaaaaaaagcggccgc                                 2308
```

Figure 18. cDNA sequence encoding the newt CB1 cannabinoid receptor. Coding sequence is designated as uppercase type (1422 bases). Untranslated regions (UTR) are in lowercase type (5' UTR = 644 bp, 3' UTR = 242 bp). The BstZ17I restriction enzyme site used to join the two cDNA clones is underlined.

Two additional newt CB1 receptor-encoding expression vector constructs were

made in an attempt to remove untranslated regions that may reduce levels of protein

expression. The untranslated region-free newt CB1-encoding sequences used to make

these additional constructs were obtained through PCR amplification of complete

coding sequences as described in the methods section above.

In the first of these "trimmed" constructs, the newt CB1 sequence was

modified to include a sequence encoding an N-terminal myc epitope tag. This

construct was designated "pTL1nCB1myc". The second construct was designated

"pTL1nCB1". Maps of the constructs used for CHO cell transfections are presented in

Figure 19.

In Vitro Translation of Newt CB1 Cannabinoid Receptors

In order to determine if the cDNA encoded by pTL1nCB1myc was capable of

directing expression of the newt cannabinoid receptor protein, it was used as a

template for in vitro transcription and translation reactions. A cDNA encoding the

human CB2 receptor subcloned into pTL1 (pTL1hCB2) was used as a positive control.

The results of these experiments are presented in Figure 20. This experiment

demonstrates that both pTL1nCB1myc and pTL1hCB2 were effective templates for

the production of proteins consistent with the size expected based on deduced amino

acid sequences encoded by each.
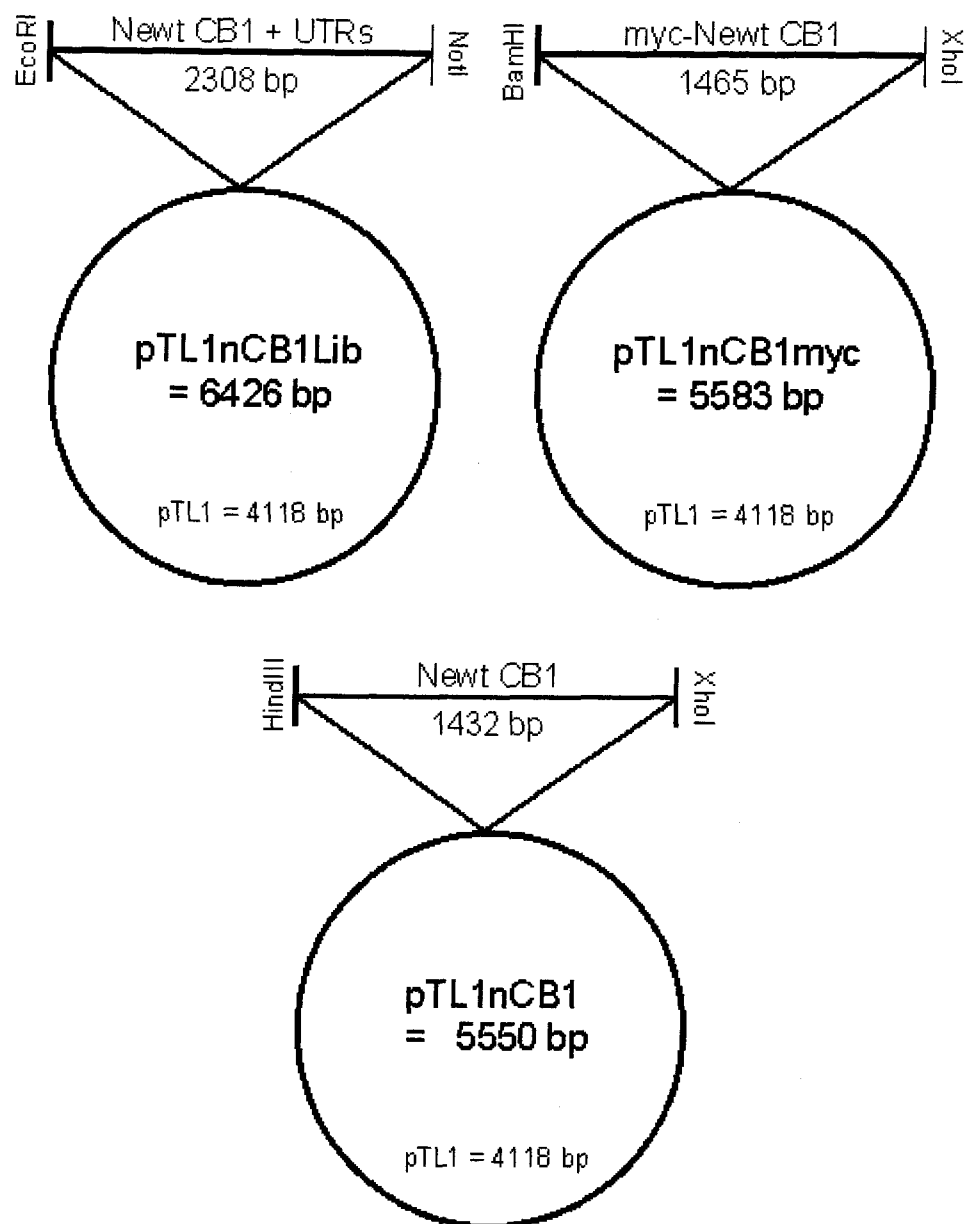
Figure 19. Vector maps of newt cannabinoid receptor-encoding constructs used to transfect CHO cells.
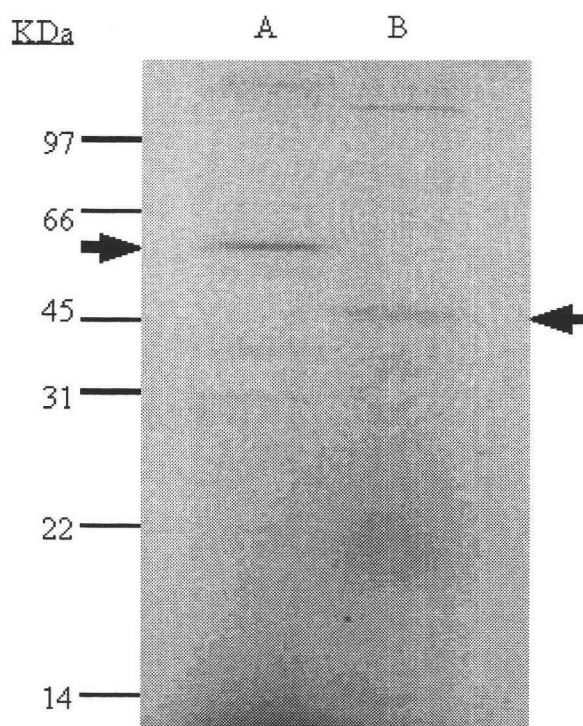
Figure 20. SDS-PAGE analysis of [^{35}S] methionine-labeled protein translated *in vitro*. (A) pTL1nCB1myc used as a template. (B) pTL1hCB2 used as a template. Arrows indicate migration of predominant bands.

Western Blot Detection of Newt CB1 Cannabinoid Receptor Expression

Western blot analysis of pTL1nCB1myc expression in CHO cells was used for two purposes: (1) To screen stable cell lines for expression of receptor protein. (2) To investigate subcellular localization of the receptor protein. The western blot presented in Figure 21 demonstrates that localization of the newt CB1 cannabinoid receptor encoded by pTL1nCB1 is primarily restricted to non-membrane portions.
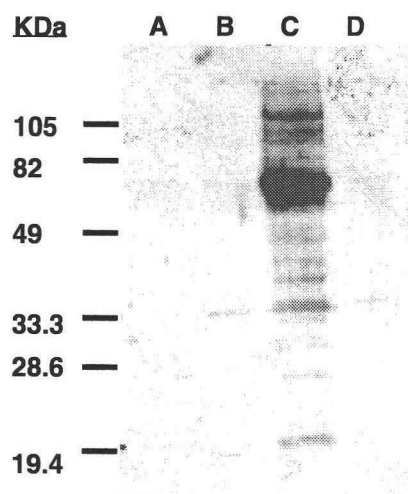
Figure 21. Western blot detection of myc epitope-tagged newt CB1 cannabinoid receptor stably expressed in CHO cells. (A) P2 membrane preparation (10 mcg protein). (B) Total particulate membrane preparation (10 mcg protein). (C) Crude lysate (about 50 mcg protein). (D) Untransfected CHO cell lysate (about 10 mcg protein).

Adenylate Cyclase Assays

Functional expression of the newt cannabinoid receptor was detected through adenylate cyclase assays performed as described in the Methods section above. The CHO cell line used in these assays was transfected with the pTL1nCB1 construct and G418-resistant colonies were cultured without clonal selection. Results of these experiments are presented in Figure 22.
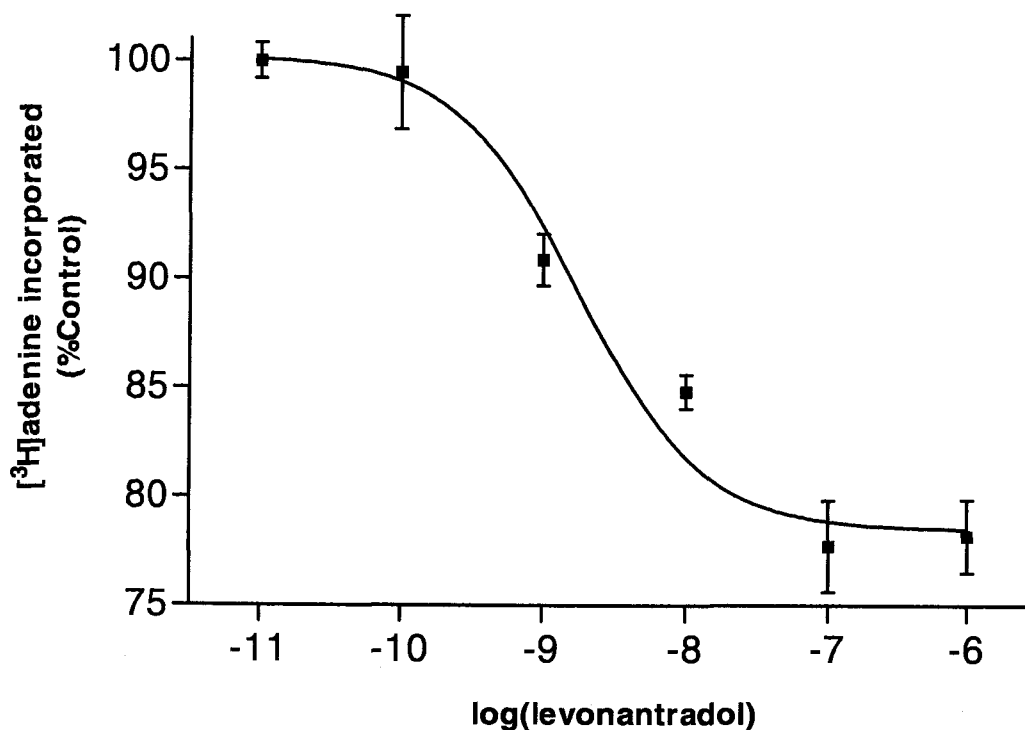
Figure 22. Inhibition of forskolin-stimulated [³H]adenine incorporation to cyclic AMP. CHO cells expressing the newt CB1 cannabinoid receptor were treated for 20 min with 25 mcM forskolin (100 % of control) and the concentrations of levonantradol shown. Data points represent the means of two pooled experiments performed in triplicate.

Treatment of this cell line with the synthetic cannabinoid agonist levonantradol

resulted in a modest inhibition of forskolin-stimulated (25 mcM) adenylate cyclase

activity (21.5 %). This level of inhibition of adenylate cyclase activity was not

observed in untransfected CHO cell cultures treated with 1 mcM levonantradol.

The newt CB1 cannabinoid receptor-mediated inhibition occurred with an IC_{50}

= 1.8 nM, a value which is lower than its affinity as determined in competition binding

experiments with newt neuronal membranes (K_i = 13.0 nM). The difference between

these apparent affinities may be attributable to differences in the temperature used for cannabinoid treatment of CHO cells (37° C) and the low incubation temperatures (15° C) used in the binding experiments. The lower temperature used in binding experiments was employed in an attempt to approximate physiological conditions.

Discussion

Construction of Newt Brain Complementary DNA Libraries

Several initial attempts to produce cDNA libraries using mRNA isolated from newt head and brain tissue resulted in production of few primary clones (<100,000 pfu). These initial problems may have been related to differences in quality of cDNA produced using a manufactured kit vs. that synthesized using enzymes and reagents purchased or obtained separately (e.g. brain cDNA vs. head cDNA, (Figure 15). Improvement in cDNA quality is probably responsible for the final production of several high quality newt brain cDNA libraries which include NBL3, NBL6, NBL7 and NBL8.

These libraries have all been successfully used as templates for degenerate primer PCR of cannabinoid receptor sequences. In addition, NBL8 has been used to for isolation of cDNAs encoding amphibian homologues of NAP-22, GAP-43, glucocorticoid receptor, calcineurin and vasotocin/neurophysin precursor protein.

The lambda ZAPII vector used to construct NBL3 allows for convenient subcloning of cDNA inserts through *in vivo* excision of a pBluescript phagemid which

contains the EcoRI cloning site. Negative aspects of using this vector include its cost, and a low cloning efficiency relative to that of the more economical lambda gt11. This low cloning efficiency may be general problem with this vector, or a specific problem with the lot used for newt cDNA library synthesis. A lambda gt11 vector was used in the construction of NBL6, 7 and 8.

This second series of lambda gt11-based libraries were constructed in an attempt to isolate portions of the newt CB1 cDNA that were not isolated after several attempts screening of NBL3. The missing 5' sequences were finally isolated from NBL6 as a cDNA clone designated "library clone 2". Sequencing of this clone demonstrated that it was a transcript primed with a newt CB1-specific primer. Construction of this type of cDNA library using gene-specific primers was initiated after several attempts to isolate missing 5' sequences using PCR-based methods failed. The PCR-based methods attempted included Rapid Amplification of cDNA Ends (5'-RACE) [119] and Uneven PCR [120].

The problem experienced with cloning the complete newt CB1 coding sequence is common with cDNA libraries made from oligo(dT)-primed cDNA. These problems are related to an under-representation of 5' sequences. This under-representation is due to a combination of the moderate processivity of the viral reverse transcriptase enzymes used in first strand cDNA synthesis, and the fact that almost all sequences are primed at the extreme 3' end. This problem was encountered in the screening of NBL3 and resulted in isolation of only a partial newt CB1 coding sequence.

Polymerase Chain Reaction Using Degenerate Primers

Degenerate primer PCR was a very important technique in the successful

screening of the newt cDNA libraries and for the probing of the northern blot of

various newt tissues (Figure 16). The degenerate PCR fragments used represent

perfect newt CB1 sequence templates for the synthesis of radiolabeled probes. The

high specificity of these probes allowed for high-stringency plaque-lift screening. All

clones identified by duplicate plaque lifts contained newt CB1 cDNA; there were no

false positives.

Evaluation of Newt CB1 Cannabinoid Receptor Expression in Various Tissues

The tissue distribution results obtained through northern blotting techniques

clearly demonstrate that, of the tissues evaluated, highest expression of the newt CB1

cannabinoid receptor gene occurs in brain (Figure 16). It is possible that significant

expression does occur in the other tissues tested. This expression may occur at levels

undetectable under the northern blotting conditions employed. To evaluate this

possibility, the more sensitive technique of RT-PCR was used. The results of RT-PCR

experiments corroborated northern blotting results and, in addition, suggested that

significant expression may occur in tissues of the digestive tract (Figure 21). Before

definite conclusions based on such RT-PCR experiments can be made, suitable

controls for cDNA template amounts used for the PCRs will have to be developed, and

more extensive set controls will have to be used. These controls may allow for quantitative evaluation of relative expression levels.

The determination that highest levels of newt CB1 expression occurs in brain is consistent with results obtained with mammalian species. Northern blots using RNA isolated from mammalian tissue have only detected CB1 expression in CNS, testes [50], and uterus [63]. The signals obtained with the peripheral tissues were modest relative to those obtained with brain.

Use of RT-PCR techniques have allowed detection of CB1 expression in a wide array of mammalian tissues including adrenal gland, heart, lung, prostate, uterus, ovary, testis, bone marrow, thymus and tonsils [64], colon, stomach, liver, pancreas, placenta, kidney, and leukocytes [51] and vas deferens [65].

Complementary DNA Library Screening

Plaque-lift screening of the cDNA libraries was generally trouble-free and productive. This success may be attributable to the use of a specific probe that was synthesized using a fragment of the newt CB1 cDNA amplified with degenerate primers.

In order to obtain the 5' coding sequence that wasn't isolated from NBL3, additional libraries were constructed using random hexamer primers and newt CB1-specific primers. Ultimately, the use of a gene-specific primer proved effective as "library clone 2" incorporates the sequence of this primer as its extreme 3' end. The use of random hexamer-primed libraries may also have been a successful strategy.

The relationships of cDNAs isolated and used to clone the newt CB1 cDNA is presented schematically in Figure 23.
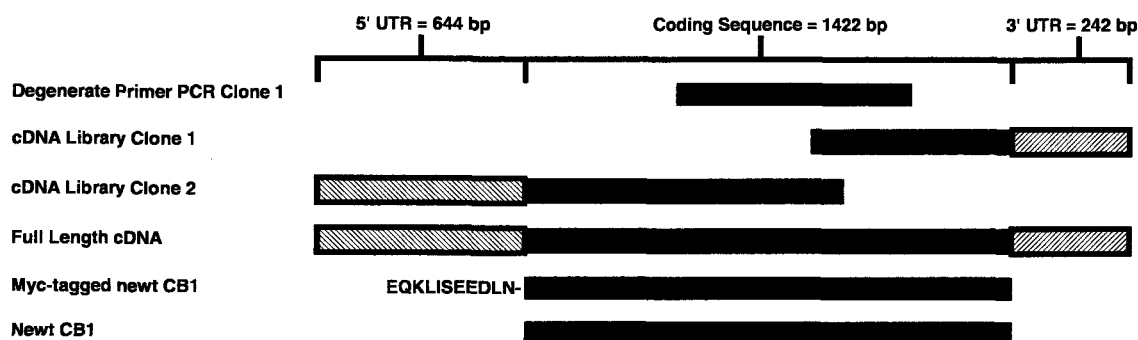
Figure 23. Schematic representation of relationships between cDNAs used for cloning and expression of the newt CB1 cannabinoid receptor.

Cloning of Complementary DNA Encoding the Complete Newt CB1 Amino Acid Sequence For Heterologous Expression

The DNA sequence encoding the newt CB1 receptor is shown in Figure 18. In this figure, untranslated bases are presented in lower case text, while the coding sequence is in uppercase text. The sequence corresponding to the BstZ17I restriction site that was used to join "library clone 1" with "library clone 2" into a contiguous, complete newt CB1 cDNA sequence is underlined.

Other notable portions of this sequence include bases 101-107 which are analogous to the splice donor site identified in the human CB1 sequence [51], and responsible for producing the splice variant, CB1A. The splice donor site for human

CB1A is not present in the newt CB1 sequence. An alignment of the human donor CB1A splice and the analogous sequence for the newt are presented below.

human CB1: 100-AAGGTGA-108

newt CB1:   100-AGGGCGA-108

This alignment demonstrates that the thymine base in the human sequence, which is 100 percent conserved across splice donor sites, is not present in the newt CB1. There are other sites in the newt CB1 sequence that may serve as donor sites, but none in the immediate vicinity of the analogous human site, and none that have high homology to the consensus donor sequence.

The acceptor sequence for CB1A is a better match between the human and newt sequences, but is still closer to consensus in the human sequence. This is demonstrated in the following alignment.

human CB1: 253-TCTCTCTCGTCCTTCAAG-271

newt CB1:   259-TCTGTATCGACATTCAAG-277

The 3' adenine and guanine bases in the sequences of both species are 100 percent conserved in the consensus acceptor sequence. The other important feature of the consensus is the 5' tract of pyrimidine bases which is perfect in the human sequence except for a guanine base (underlined) and interrupted by 2 guanine and 3 adenine bases (also underlined) in the case of the newt sequence. Despite significant lack of conformity to the consensus sequence, the newt sequence still represents a potential acceptor site.

The deduced amino-acid sequence of the newt CB1 cannabinoid receptor is presented in Figure 24 and compared to all other CB1 receptors for which complete protein sequence information is available. In this figure, predicted transmembrane domains (TMD) are numbered and their locations indicated by heavy lines. Extracellular domains are italicized which distinguishes them from intracellular segments. Other features that are highly conserved between the receptors include: 1) dual sites for N-linked glycosylation in the same region of the N-terminal extracellular tail domain (indicated in bold type). 2) A potential site for protein kinase C (PKC) phosphorylation within the region between TMDV and TMDVI which corresponds to the third cytoplasmic loop (indicated in bold italics). 3) A potential PKC phosphorylation site within the intracellular tail region of the receptor.

The location of these cytoplasmic tail PKC sites (indicated in bold italics) are conserved across species except in the cases of the cat CB1 and the pufferfish CB1B. The high degree of conservation of these PKC sites across species is consistent with functional importance.

Comparison of the predicted amino acid sequence of the newt CB1 with cannabinoid receptor sequences available from other species reveals a high degree of conservation (Table 4). In the case of human and mouse cannabinoid receptors where protein sequence for both CB1 and CB2 receptor subtype are known, this homology is highest within receptor subtype, suggesting that separate CB1 and CB2 receptor subtypes had evolved prior to divergence of the species.

Table 4: Percentage of amino acid sequence identity between cannabinoid receptors of known sequence

	CB1 Rat	CB1 Mouse	CB1 Human	CB1 Cat	CB1 Newt	CB1A Fish	CB1B Fish	CB2 Human	CB2 Mouse
CB1 Rat	100								
CB1 Mouse	99.8	100							
CB1 Human	97.3	97.0	100						
CB1 Cat	96.8	96.6	96.2	100					
CB1 Newt	84.2	84.4	84.2	83.8	100				
CB1A Fish	73.5	73.5	72.6	72.8	75.5	100			
CB1B Fish	61.4	61.1	59.8	60.1	61.6	66.1	100		
CB2 Human	48.5	48.5	48.0	48.5	46.9	47.2	42.2	100	
CB2 Mouse	49.5	49.5	48.5	49.5	49.2	49.7	44.9	82.7	100

The newt CB1 sequence shares about 10% more identity with the mammalian proteins than the fish CB1A and about 20% more identity than the fish CB1B. This higher degree of identity suggests that there is less evolutionary distance between mammalian and amphibian CB1 receptors than between mammalian and fish CB1 receptors. This is supported by phylogenetic analyses and the resulting dendrogram presented in Figure 25.

Figure 24. Amino acid alignment of CB1 cannabinoid receptors with deduced protein sequence. Predicted transmembrane domains are numbered and locations indicated by heavy lines. Extracellular domains are distinguished from italicized intracellular segments. Other notable regions and residues are indicated and described in the text.

```
Newt_CB1          MKSILDGLADTTFRTITTDLLYMGSNDVQYEDTKGEMASKLGYFPQKLPLSSFRSDHSPD 60
Human_CB1         MKSILDGLADTTFRTITTDLLYVGSNDIQYEDIKGDMASKLGYFPQKFPLTSFRGSPFQE 60
Cat_CB1           MKSILDGLADTTFRTITTDLLYVGSNDIQYEDIKGDMASKLGYFPQKFPLTSFRGSPFQE 60
Rat_CB1           MKSILDGLADTTFRTITTDLLYVGSNDIQYEDIKGDMASKLGYFPQKFPLTSFRGSPFQE 60
Mouse_CB1         MKSILDGLADTTFRTITTDLLYVGSNDIQYEDIKGDMASKLGYFPQKFPLTSFRGSPFQE 60
Pufferfish_CB1A   MKSVLDGVADTTFRTITSGLQYLGSNDANYDDPLNDAAFKTGFSLQK-PLSAFRSNSFPN 59
Pufferfish_CB1B   MKLALHRIAGATMAALTTEVQYLGSNDASYEDPQADAALMKSRFNFEKPYS--ASSSLHR 58
                  **   *. :*.:*: ::*: : *:**** .*:*   : *   .   : *  .   ..

Newt_CB1          KMTIGDDNLLSFYPL-DQFNVTEFFNRSVSTFKENDDNLKCGENFMD-MECFMILTASQQ 118
Human_CB1         KMTAGDNPQL--VPA-DQVNITEFYNKSLSSFKENEENIQCGENFMD-IECFMVLNPSQQ 116
Cat_CB1           KMTAGDNSQL--VPA-DQVNITEFYNKSLSSYKENEENIQCGENFMD-MECFMILNPSQQ 116
Rat_CB1           KMTAGDNSPL--VPAGDTTNITEFYNKSLSSFKENEENIQCGENFMD-MECFMILNPSQQ 117
Mouse_CB1         KMTAGDNSPL--VPAGDTTNITEFYNKSLSSFKENEDNIQCGENFMD-MECFMILNPSQQ 117
Pufferfish_CB1A   KVPADEELIFKGIPF-FPTNSTDLFGNRNTTRDEN--SIQCGENFMD-MECFMILTPSQQ 115
Pufferfish_CB1B   LIPGNKELIYGGLSTILPTNASDFPLSNGSG--E---ATQCGEDIVDNMECFMILTPAQQ 113
                  .:.  ..:       * ::.      :  *    :***::.* :****:*...:**
                          I                                           II
Newt_CB1          LIIAVLSLTLGTFTVLENFLVLCVILQSRTLRCRPSYHFIGSLAVADLLGSVIFVYSFLD 178
Human_CB1         LAIAVLSLTLGTFTVLENLLVLCVILHSRSLRCRPSYHFIGSLAVADLLGSVIFVYSFID 176
Cat_CB1           LAIAVLSLTLGTFTVLENLLVLCVILHSRSLRCRPSYHFIGSLAVADLLGSVIFVYSFVD 176
Rat_CB1           LAIAVLSLTLGTFTVLENLLVLCVILHSRSLRCRPSYHFIGSLAVADLLGSVIFVYSFVD 177
Mouse_CB1         LAIAVLSLTLGTFTVLENLLVLCVILHSRSLRCRPSYHFIGSLAVADLLGSVIFVYSFVD 177
Pufferfish_CB1A   LAVAVLSLTLGTFTVLENLVVLCVIFQSRTLRCRPSYHFIGSLAVADLLGSVIFVYSFLD 175
Pufferfish_CB1B   LVIVILAITLGTFTVLENFVVLCVILHSHTLRSRPSYHFIGSLAVADLIGSIIFVYSFLD 173
                  * :..:*:.**********::*****.:*.:**.*************.**.:******.*
                            III
Newt_CB1          FHVFHRKDSSNVFLFKLGGVTASFTASVGSLFLTAIDRYISIHRPLAYKRIVTRTKAVIA 238
Human_CB1         FHVFHRKDSRNVFLFKLGGVTASFTASVGSLFLTAIDRYISIHRPLAYKRIVTRPKAVVA 236
Cat_CB1           FHVFHRKDSPNVFLFKLGGVTASFTASVGSLFLTAIDRYISIHRPLAYKKIVTRPKAVVA 236
Rat_CB1           FHVFHRKDSPNVFLFKLGGVTASFTASVGSLFLTAIDRYISIHRPLAYKRIVTRPKAVVA 237
Mouse_CB1         FHVFHRKDSPNVFLFKLGGVTASFTASVGSLFLTAIDRYISIHRPLAYKRIVTRPKAVVA 237
Pufferfish_CB1A   FHVFHKKDSPNVFLFKLGGVTASFTASVGSLFLTAIDRYISIHRPLAYRRIVTRTKAVIA 235
Pufferfish_CB1B   FHVLHRKDSPSIFLFKLAGVIASFTASVGSLFLTAIDRYVSIHRPMAYKRIITKTKAVIA 233
                  ***.*:***  .:*****.** *****************:*****:**::*.*:.***:*
                     IV                                    V
Newt_CB1          FCVMWTIAIIIAVLPLLGWNCKKLKSVCSDIFPLIDENYLMFWIGVTSILLLFIVYAYVY 298
Human_CB1         FCLMWTIAIVIAVLPLLGWNCEKLQSVCSDIFPHIDETYLMFWIGVTSVLLLFIVYAYMY 296
Cat_CB1           FCLMWTIAIVIAVLPLLGWNCKKLQSVCSDIFPLIDETYLMFWIGVTSVLLLFIVYAYMY 296
Rat_CB1           FCLMWTIAIVIAVLPLLGWNCKKLQSVCSDIFPLIDETYLMFWIGVTSVLLLFIVYAYMY 297
Mouse_CB1         FCLMWTIAIVIAVLPLLGWNCKKLQSVCSDIFPLIDETYLMFWIGVTSVLLLFIVYAYMY 297
Pufferfish_CB1A   FCMMWTISIIIAVLPLLGWNCKRLNSVCSDIFPLIDENYLMFWIGVTSVLVLFIIYAYIY 295
Pufferfish_CB1B   FSVMWAISIEFSLLPLLGWNCKRLHSVCSDIFPLIDEKYLMFWIGMTTVLLLFIIYAYMF 293
                  *.:**:*:* :::*********::*:********* ***.*******:*::*:***:***::
                  VI
Newt_CB1          ILWKAHSHAVRMLQRGTQKSIIIHTSEDGKVQITRPEQTRMDIRLAKTLVLILVVLIICW 358
Human_CB1         ILWKAHSHAVRMIQRGTQKSIIIHTSEDGKVQVTRPDQARMDIRLAKTLVLILVVLIICW 356
Cat_CB1           ILWKAHIHAVRMIQRGTQKSIIIHTSEDGKVQVTRPDQARMDIRLAKTLVLILVVLIICW 356
Rat_CB1           ILWKAHSHAVRMIQRGTQKSIIIHTSEDGKVQVTRPDQARMDIRLAKTLVLILVVLIICW 357
Mouse_CB1         ILWKAHSHAVRMIQRGTQKSIIIHTSEDGKVQVTRPDQARMDIRLAKTLVLILVVLIICW 357
Pufferfish_CB1A   ILWKAHHHAVRMLSRTSQKSLVVYSAEGTKVQTTRPEQTRMDIRLAKTLVLILAVLVICW 355
Pufferfish_CB1B   ILWKSHHHAVRMLSRSSQRSIIVYTSEGTKVQTVRPEQAQMDLRLAKTLVLILVALIICW 353
                  ****:* *****:.* :*:*::::::*. *** .**:*:***:*********..*:***
                                      VII
Newt_CB1          GPLLAIMVYDVFGKMNNPIKTVFAFCSMLCLMNSTVNPIIYALRSQDLRHAFLEQCPPCE 418
Human_CB1         GPLLAIMVYDVFGKMNKLIKTVFAFCSMLCLLNSTVNPIIYALRSKDLRHAFRSMFPSCE 416
Cat_CB1           GPLLAIMVYDVFGKMNKLIKTVFAFCSMLCLLNSTVNPIIYALRSKDLRHAFRSMFPSCE 416
Rat_CB1           GPLLAIMVYDVFGKMNKLIKTVFAFCSMLCLLNSTVNPIIYALRSKDLRHAFRSMFPSCE 417
Mouse_CB1         GPLLAIMVYDVFGKMNKLIKTVFAFCSMLCLLNSTVNPIIYALRSKDLRHAFRSMFPSCE 417
Pufferfish_CB1A   GPLLAIMVYDLFWKMDDNIKTVFAFCSMLCLLNSTVNPIIYALRSRDLRHAFLSSCHACR 415
Pufferfish_CB1B   GPLLAIMVYDLFGRVNDFIKTVFAFCSMLCLLNSTINPVIYAMRSKDLRRAFVNICHMCR 413
                  **********:* ::. ************.***:**:***:**:** :.       *.
Newt_CB1          GTSQPLDNSM-ESDCQHRHGNNAGNVHRAAEN-CI--KSTVKIAKVTMS-VSTETSGEAV 473
Human_CB1         GTAQPLDNSMGDSDCLHKHANNAASVHRAAES-CI--KSTVKIAKVTMS-VSTDTSAEAL 472
Cat_CB1           GTAQPLDNSMGDSDCLHKHANNTANVHRAAEN-CI--KNTVQIAKVTIS-VSTNTSAKAL 472
Rat_CB1           GTAQPLDNSMGDSDCLHKHANNTASMHRAAES-CI--KSTVKIAKVTMS-VSTDTSAEAL 473
Mouse_CB1         GTAQPLDNSMGDSDCLHKHANNTASMHRAAES-CI--KSTVKIAKVTMS-VSTDTSAEAL 473
Pufferfish_CB1A   GSAQQLDNSL-ESDCQNRNVN--ISANRAAES-CV--KTTVKIAKVTMS-VSTETSAEAV 468
Pufferfish_CB1B   GTTQSLDSSA-ESDWNSRSVR--STGGRAGKDRSVGGKPQVKVAQVTVSGVTASSPAEAV 470
                  *:.* **.* :** *     :     . **.:. .:  *  *:.*:**:* *::.:...*:
```

Figure 24

Figure 25. Estimated phylogenetic relationship between cannabinoid receptors of known sequence. Branch lengths are additive and approximate evolutionary distance between receptors. Bar units are in terms of expected substitutions per site as described in the text. Estimates were generated from protein sequences using PROTDIST and FITCH computer programs which are part of the PHYLIP set of phylogenetic analysis tools (J. Felsenstein, Department of Genetics, University of Washington, Seattle).

The phylogenetic relationships of cannabinoid receptors of known complete amino acid sequence were analyzed in a three-step process: First, amino acid sequence alignments were made by hand, assisted by the ClustalW multiple alignment computer program (accessible on the Internet at http://www2.ebi.ac.uk/clustalw). Second, genetic distances were estimated using the PROTDIST computer program, and finally a dendrogram was computed from genetic distance estimates using the FITCH computer program. The PROTDIST and FITCH computer programs are available as part of the PHYLIP set of phylogenetic analysis tools developed by Joseph Felsenstein [121].

PROTDIST generates a matrix of estimated genetic distances based on protein sequences. The algorithm used to calculate these matrices takes into consideration the degeneracy of the genetic code through use of a model of amino acid substitution based on the PAM001 model [122]. This model is empirically-based and scales probabilities of change of one amino acid to another in terms of an expected 1% change between two amino acid sequences. Matrix estimates produced by PROTDIST are expressed as the expected number of amino acid substitutions per site. The number of sites used for this analysis was 473, the maximum number of amino acids encoded by known cannabinoid receptor genes. For the shorter CB2 receptors, gaps were introduced to maintain alignment with longer CB1 sequences. The matrix used for generation of the dendrogram presented as Figure 25 is presented in Table 5.

Table 5: Genetic distance matrix generated by PROTDIST for cannabinoid receptors

	Human_CB2	Mouse_CB2	Newt_CB1	Human_CB1	Cat_CB1	Rat_CB1	Mouse_CB1	PFish_CB1A	PFish_CB1B
Human_CB2	0	0.20004	1.07	1.09344	1.07659	1.07441	1.07441	1.08929	1.17224
Mouse_CB2	0.20004	0	1.00315	1.03074	1.01398	1.00129	1.00129	1.01401	1.14641
Newt_CB1	1.07	1.00315	0	0.16199	0.16426	0.15839	0.156	0.3165	0.51169
Human_CB1	1.09344	1.03074	0.16199	0	0.03439	0.02567	0.02783	0.34444	0.5343
Cat_CB1	1.07659	1.01398	0.16426	0.03439	0	0.02573	0.02789	0.34552	0.52495
Rat_CB1	1.07441	1.00129	0.15839	0.02567	0.02573	0	0.00208	0.33017	0.52136
Mouse_CB1	1.07441	1.00129	0.156	0.02783	0.02789	0.00208	0	0.33017	0.52136
PFish_CB1A	1.08929	1.01401	0.3165	0.34444	0.34552	0.33017	0.33017	0	0.44941
PFish_CB1B	1.17224	1.14641	0.51169	0.5343	0.52495	0.52136	0.52136	0.44941	0

The FITCH computer program fits dendrograms to distance matrices. The program accomplishes this through a least squares algorithm based on the method described by Fitch and Margolish [123]. This method infers phylogenies based on the principle of maximum parsimony; more complicated trees are rejected in favor of simpler models. Optimal values calculated based on varying the extent of branching and branch lengths are used for comparisons of trees. Clearly, as the number of sequences evaluated increases, the total number of tree comparisons multiply, rendering these analyses potentially computationally-intensive. Also, there is no assurance that the simplest tree describing the relationship between protein sequences reflects the course by which evolution actually occurred.

This program does not assume the operation of a molecular clock. This means that substitution rates are not constrained after divergence, and branch lengths to common ancestors may vary. Without invoking a molecular clock, the dendrogram calculated is unrooted. With an unrooted dendrogram, branch lengths represent sequence-to-sequence genetic distances; these branch lengths have additive properties and can be summed to calculate estimated genetic distances between divergent

sequences. In Figure 25, branch lengths are expressed in units of expected number of substitutions per site. Use of this measure may overestimate the genetic differences between CB1 and CB2 receptors as the event responsible for their dissimilarity was most likely an insertion or deletion of large portions of sequence rather than the single substitution changes implied by the distance units used. Despite this possibility of an overestimate, the phylogenetic analysis is still consistent with what is known of the time of divergence of fish and terrestrial vertebrates [124] and implies that divergence of CB1 and CB2 receptors was an ancient event.

The methods selected for the phylogenetic analysis presented here are among a large number of alternate methods that have been proposed. The relative appropriateness of individual methods are vigorously debated. A balanced review of competing strategies for phylogenetic reconstruction has been written by Swofford and Olsen [125].

Newt CB1 Cannabinoid Receptor Expression

In order to more fully characterize the pharmacology of the newt CB1 cannabinoid receptor, attempts were made to heterologously express it in CHO cells. Before transfections, in vitro translation experiments were performed using the pTL1nCB1myc construct (Figure 19) which confirmed its ability to direct production of protein of the expected size (Figure 20).

Transfection of CHO cells with the pTL1nCB1myc construct allowed for screening of receptor-expressing clones by western blots probed with an anti-myc

antibody. A stable clone was identified by these western immunoblots and isolated and used for further evaluation in binding experiments. Using membranes prepared from this CHO cell line, specific [^{3}H]CP-55940 binding was not observed. Together, the western immunoblot and radioligand binding results seemed to indicate that although the cell line was expressing the receptor protein, the protein was not functional. To assess whether this lack of function might be attributable to improper cellular localization, subcellular fractions of the CHO cell line were prepared and investigated by immunoblotting (Figure 21).

Results of this subcellular localization experiment suggested that little of the total newt CB1 receptor protein produced is present within membrane fractions. A lack of receptor processing to the plasma membrane of these cells is consistent with the non-functional expression observed.

The high level of non-membrane-associated newt CB1 receptor observed with the CHO cell line is also consistent with recent findings obtained in localization experiments using N18TG2 neuroblastoma cells [126]. Using N18TG2 cells and an antibody directed to the N-terminal extracellular domain of the CB1 receptor, this group found that only about 10 % of CB1 was liable to trypsin digestion of the extracellular epitope. This 10 % fraction did not change over the course of 24 hours. These results indicate that most CB1 protein produced by N18TG2 cells is intracellular. Despite the fact that most CB1 protein in this cell line was restricted in intracellular compartments, membranes prepared from these cells contained specific cannabinoid binding sites, indicating functional expression. Also, using subcellular

fractions in binding assays employing the antagonist radioligand [³H]SR141716A, the same group demonstrated that high affinity binding sites are more abundant within membrane fractions than within intracellular fractions.

Increased levels of membrane expression of G-protein-coupled receptors has been achieved using cleavable membrane insertion signal sequences [127]. These cleavable signal sequences are composed of an N-terminal domain of 20-25 predominantly hydrophobic amino acids. These hydrophobic amino acids are cleaved by a specific protease after membrane insertion at the level of endoplasmic reticulum [128]. Use of a cleavable membrane insertion signal sequence has been used to functionally-express G-protein-coupled receptors from lower vertebrates in mammalian cells [129].

The hydrophobic nature of membrane insertion signal sequences is in contrast to the hydrophilic nature of the myc epitope used in pTL1nCB1myc (Figure 19). This epitope consists of a total of 11 amino acids, five of which are acidic or basic and three of which are hydrophilic. The amino acid sequence of the myc epitope used is: EQKLISEEDLN.

The contrasting chemical natures of the N-terminal sequences known to direct membrane insertion and the myc epitope used to tag the N-terminus of the newt CB1 receptor expressed by the CHO cell cultures described above, make it reasonable to suspect that the myc epitope itself may be at least partially responsible for the lack of functional expression observed.

Functional expression of the newt CB1 cannabinoid receptor was achieved after stable transfection of CHO cells with the pTL1nCB1 construct (Figure 19). This was determined through adenylate cyclase assays using a non-clonal, G418-resistant culture. Non-clonal cell lines stably-expressing G-protein-coupled receptors have been used with other systems including expression of a mu-opioid receptor from a lower vertebrate [130]. Advantages of non-clonal cell lines include the fact that they are more rapidly and economically produced. Potential disadvantages of non-clonal cell lines include low-level expression, possibly related to a significant population of non- or under-expressing cells, and instability of the culture. Instability may be related to different growth rates of individual cells within the culture. Over-expression of a foreign protein may result in lower growth rates, leading eventually to a dilution of expressing cells over the course of several passages.

The inhibition of adenylate cyclase activity in the newt CB1-transfected CHO cell line was modest (Figure 22), possibly due to only a fraction of the cells in the non-clonal culture expressing the newt CB1 receptor. Although the inhibition of cyclase by levonantradol was modest, it occurred with an IC_{50} consistent with levonantradol's binding affinity determined through competition binding experiments using newt neuronal membranes (Table 3). Further investigation using this cell line, perhaps including isolation and characterization of individual clones, will allow a more-complete analysis of the pharmacology of the newt CB1 cannabinoid receptor.

CHAPTER V. SUMMARY

The first chapter of this thesis presented the history and current state of cannabinoid pharmacology. Despite the long history of cannabinoid use, an understanding of basis of cannabinoid activity has only recently been developed. Currently it is known that specific G-protein-coupled receptors mediate cannabinoid activity. Two subtypes of these receptors have been identified: CB1 is associated with the central nervous system (although peripheral expression has been detected), and CB2 which may be exclusively associated with tissues of the immune system.

Both of these receptors alter cellular activity through activation of G-proteins of the $G_{i/o}$ subtype. Activation of these G-proteins by CB1 and CB2 receptors has been associated with reductions in the activity of adenylate cyclase, thereby lowering intracellular concentrations of cAMP. G-protein activation by both cannabinoid receptors has also been implicated in modulating the MAP kinase signaling pathway. CB1 but not CB2 activation has been shown to be negatively coupled through $G_{i/o}$ to N-type and P/Q-type calcium channels, and positively coupled to inward rectifying potassium channels.

A variety of cannabinoid ligands of different classes have been developed and include classic cannabinoids with structures related to Δ^9-THC, aminoalkylindole cannabinoids (e.g., WIN55212-2), and fatty acid cannabinoids such as the endogenous ligand, anandamide. The array of available ligands also now includes subtype specific antagonists: CB1 = SR-141716A, CB2 = SR-144528.

Better appreciation of cannabinoid neuropharmacology may allow the development of cannabinoid-based therapies that are effective while minimizing toxicity, which is primarily restricted to psychoactivity. Current therapeutic uses of cannabinoids include treatment of nausea and vomiting associated with cancer chemotherapy and anorexia associated with AIDS. Cannabinoids hold promise for the management of glaucoma, chronic pain, epilepsy, multiple sclerosis, and inflammation. The psychoactivity associated with currently-available cannabinoid-based therapies has limited their usefulness in these areas.

Toxicity problems have been resolved in other systems through production of receptor subtype-specific ligands. This type of strategy may not be productive in the case of cannabinoids due to an apparent lack of CB1 receptor subtypes. It may be unlikely that populations of such subtypes have so far escaped detection. Toxicity problems in other systems have also been addressed through production of partial agonists. Partial opioid agonists have been developed that are effective analgesics, but have side-effect profiles more favorable than morphine (e.g., pentazocine, butorphanol, nalbuphine). Development of additional cannabinoid ligands with partial efficacy or perhaps antagonist properties may allow production of useful cannabinoid-based therapies.

Despite progress over the last decade, a clear pharmacologic role for the systems mediated by cannabinoid receptor activation has not emerged. It is possible that the study of cannabinoid neurochemistry in lower vertebrates and other animals with relatively simple neurophysiology may allow a better understanding of the

physiological role of cannabinoid systems. Characterization of the newt cannabinoid receptor represents progress toward developing such a system in an amphibian.

It is clear from the data presented in the second chapter of this thesis that cannabinoids are capable of modulating well-characterized behaviors in the newt. Levonantradol reduces spontaneous locomotor activity, an effect which is consistent with cannabinoid-induced hypomobility in mice. Levonantradol also effectively inhibited courtship clasping behavior in male newts. The inhibition of clasping behavior was concentration-dependent and occurred at a low dose.

In the third chapter of this thesis, data were presented that clearly demonstrate that a specific cannabinoid binding site is present in newt neuronal membranes. This binding site has high affinity and is present in numbers similar to CB1 in mammalian neuronal tissue. The pharmacological specificity of the cannabinoid binding site in newt neuronal membranes was investigated and is also similar to that of mammalian CB1.

The final chapter of data presented here documents the construction of newt brain cDNA libraries and their use in isolating and expressing a cDNA that encodes the newt CB1 cannabinoid receptor. Multiple cDNA libraries were made and have been used to clone sequences encoding several amphibian proteins.

One of the more significant obstacles involved in cloning cDNAs from libraries is development of a method to screen for the sequences of interest. In cloning the newt CB1 receptor, use of degenerate PCR primers allowed use of a perfect

template to make radiolabeled probes for high stringency screening. Degenerate primer PCR fragments were also useful in the probing of northern blots.

Northern blotting techniques allowed labeling of the mRNA transcript encoding the newt CB1. This transcript appears to be approximately 5900 bp in length. Northern blots of various tissues demonstrated that (of the tissues tested) levels of expression of the newt CB1 cannabinoid receptor gene is highest in brain. The more sensitive technique of RT-PCR was also applied to the question of distribution of expression. RT-PCR results were not quantitative, but corroborated significant brain expression and were also consistent with CB1 expression in the tissues of the digestive tract.

Complementary DNA library screening resulted in isolation of two cDNAs, each encoding a portion of the newt CB1 cannabinoid receptor. These cDNAs were joined through use of a unique restriction site in the sequence shared between them. PCR amplification of the complete coding sequence, followed by subcloning into a eukaryotic expression vector allowed transfection and heterologous expression of the newt CB1 cannabinoid receptor.

Heterologous expression of a myc epitope-tagged version of the newt CB1 allowed immunoblotting techniques to be employed. These immunoblots demonstrated that most myc-tagged newt CB1 receptors stably-expressed by CHO cells were intracellular. This distribution may have resulted in an inability to detect specific [^{3}H]CP-55940 binding to membranes prepared from this cell line.

Functional expression of a non-epitope-tagged newt CB1 receptor was accomplished through stable transfection of CHO cells. A stable CHO cell line was produced, without clonal selection, and used for assays of adenylate cyclase activity. In this non-clonal cell line levonantradol produced a modest, although dose-dependent inhibition of forskolin-stimulated adenylate cyclase activity. Functional expression confirmed the identity of the of the cDNA cloned as encoding a newt CB1 cannabinoid receptor.

Overall, as a result of the experiments presented in this thesis, we know that the amphibian, *Taricha granulosa* has a behaviorally-relevant cannabinoid-mediated neurochemical system. This system is regulated by a specific G-protein-coupled receptor that is similar in both ligand binding affinity and expression levels to that present in mammalian CNS. The structure of the newt CB1 cannabinoid receptor is also very similar to that identified in other species, including another lower vertebrate, the pufferfish. The high degree of cross-species homology of CB1 receptors indicates that cannabinoid neurochemical systems have been maintained over the course of vertebrate evolution. This maintenance implies that cannabinoid receptor-mediated signaling is of critical functional importance. A clear understanding of the nature of this functional importance is dependent upon further cannabinoid research, perhaps employing lower vertebrate models such as that described here using *Taricha granulosa.*

BIBLIOGRAPHY

1.   Abel, E., *A Comprehensive guide to the Cannabis Literature*. 1979, Westport, CN: Greenwood Press.

2.   Abel, E.A., *Marijuana: The First Twelve Thousand Years*. 1980, New York and London: Plenum Press.

3.   Gaoni, A. and R. Mechoulam, *Isolation, structure, and partial synthesis of an active constituent of hashish*. Journal of the American Chemical Society, 1964. **86**: p. 1646-1647.

4.   Martin, B.R., *et al.*, *Pharmacological potency of R- and S-3'-hydroxy-delta 9-tetrahydrocannabinol: additional structural requirement for cannabinoid activity*. Pharmacol Biochem Behav, 1984. **21**(1): p. 61-65.

5.   Howlett, A.C. and R.M. Fleming, *Cannabinoid inhibition of adenylate cyclase. Pharmacology of the response in neuroblastoma cell membranes*. Mol Pharmacol, 1984. **26**(3): p. 532-538.

6.   Johnson, M., *et al.*, *Structural studies leading to the discovery of a cannabinoid binding site*. NIDA Res Monogr, 1988. **90**: p. 129-135.

7.   Devane, W.A., *et al.*, *Determination and characterization of a cannabinoid receptor in rat brain*. Mol Pharmacol, 1988. **34**(5): p. 605-613.

8.   Matsuda, L.A., *et al.*, *Structure of a cannabinoid receptor and functional expression of the cloned cDNA*. Nature, 1990. **346**(6284): p. 561-564.

9.   Herkenham, M., *et al.*, *Characterization and localization of cannabinoid receptors in rat brain: a quantitative in vitro autoradiographic study*. J Neurosci, 1991. **11**(2): p. 563-583.

10.   Mailleux, P. and J.J. Vanderhaeghen, *Localization of cannabinoid receptor in the human developing and adult basal ganglia. Higher levels in the striatonigral neurons*. Neurosci Lett, 1992. **148**(1-2): p. 173-176.

11.   Munro, S., K.L. Thomas, and M. Abu-Shaar, *Molecular characterization of a peripheral receptor for cannabinoids*. Nature, 1993. **365**(6441): p. 61-65.

12.   Mechoulam, R., *Marijuana chemistry*. Science, 1970. **168**: p. 1159-1166.

13.   Martin, B.R., *Cellular effects of cannabinoids*. Pharmacol Rev, 1986. **38**(1): p. 45-74.

14.   Johnson, M.R., *et al.*, *Selective and potent analgetics derived from cannabinoids*. J Clin Pharmacol, 1981. **21**(8-9): p. 271S-282S.

15.   Howlett, A.C., *et al.*, *Nonclassical cannabinoid analgetics inhibit adenylate cyclase: development of a cannabinoid receptor model*. Mol Pharmacol, 1988. **33**(3): p. 297-302.

16.   Titishov, N., R. Mechoulam, and A.M. Zimmerman, *Stereospecific effects of (-)- and (+)-7-hydroxy-delta-6- tetrahydrocannabinol-dimethylheptyl on the immune system of mice*. Pharmacology, 1989. **39**(6): p. 337-349.

17.   Burstein, S.H., *et al.*, *Synthetic nonpsychotropic cannabinoids with potent antiinflammatory, analgesic, and leukocyte antiadhesion activities*. Journal of Medicinal Chemistry, 1992. **35**: p. 3135-3141.

18.   Feigenbaum, J.J., *et al.*, *Nonpsychotropic cannabinoid acts as a functional N-methyl-D-aspartate receptor blocker*. Proc Natl Acad Sci U S A, 1989. **86**(23): p. 9584-9587.

19.   Shohami, E., M. Novikov, and R. Mechoulam, *A nonpsychotropic cannabinoid, HU-211, has cerebroprotective effects after closed head injury in the rat*. J Neurotrauma, 1993. **10**(2): p. 109-119.

20.   Nadler, V., R. Mechoulam, and M. Sokolovsky, *The non-psychotropic cannabinoid (+)-(3S,4S)-7-hydroxy-delta 6- tetrahydrocannabinol 1,1-dimethylheptyl (HU-211) attenuates N-methyl-D- aspartate receptor-mediated neurotoxicity in primary cultures of rat forebrain*. Neurosci Lett, 1993. **162**(1-2): p. 43-45.

21.   Eshhar, N., S. Striem, and A. Biegon, *HU-211, a non-psychotropic cannabinoid, rescues cortical neurones from excitatory amino acid toxicity in culture*. Neuroreport, 1993. **5**(3): p. 237-240.

22.   Thomas, B.F., X. Wei, and B.R. Martin, *Characterization and autoradiographic localization of the cannabinoid binding site in rat brain using [3H]11-OH-delta 9-THC-DMH*. J Pharmacol Exp Ther, 1992. **263**(3): p. 1383-1390.

23.   Devane, W.A., *et al.*, *A novel probe for the cannabinoid receptor*. J Med Chem, 1992. **35**(11): p. 2065-2069.

24.   Eissenstat, M.A., *et al.*, *Aminoalkylindoles (AAIs): structurally novel cannabinoid-mimetics*. NIDA Res Monogr, 1991. **105**: p. 427-428.

25.   Kuster, J.E., *et al.*, *Aminoalkylindole binding in rat cerebellum: selective displacement by natural and synthetic cannabinoids*. J Pharmacol Exp Ther, 1993. **264**(3): p. 1352-1363.

26.   Ward, S.J., *et al.*, *Aminoalkylindoles (AAIs): a new route to the cannabinoid receptor?* NIDA Res Monogr, 1991. **105**: p. 425-426.

27.   Pacheco, M., *et al.*, *Aminoalkylindoles: actions on specific G-protein-linked receptors.* J. Pharmacol. Exp. Ther, 1991. **257**: p. 170-183.

28.   Casiano, F.M., *et al.*, *Putative aminoalkylindoles (AAI) antagonists.* NIDA Res Monogr, 1991. **105**: p. 295-296.

29.   Huffman, J.W., *et al.*, *Design, synthesis and pharmacology of cannabimimetic indoles.* Bioorganic Medicinal Chemistry Letters, 1994. **4**: p. 563-566.

30.   Rinaldi-Carmona, M., *et al.*, *SR141716A, a potent and selective antagonist of the brain cannabinoid receptor.* FEBS Lett, 1994. **350**(2-3): p. 240-244.

31.   Rinaldi-Carmona, M., *et al.*, *Biochemical and pharmacological characterisation of SR141716A, the first potent and selective brain cannabinoid receptor antagonist.* Life Sci, 1995. **56**(23-24): p. 1941-1947.

32.   Rinaldi-Carmona, M., *et al.*, *Characterization and distribution of binding sites for [3H]-SR 141716A, a selective brain (CB1) cannabinoid receptor antagonist, in rodent brain.* Life Sci, 1996. **58**(15): p. 1239-1247.

33.   Landsman, R.S., *et al.*, *SR141716A is an inverse agonist at the human cannabinoid CB1 receptor.* Eur J Pharmacol, 1997. **334**(1): p. R1-R2.

34.   Rinaldi-Carmona, M., *et al.*, *SR 144528, the first potent and selective antagonist of the CB2 cannabinoid receptor.* J Pharmacol Exp Ther, 1998. **284**: p. 644-650.

35.   Devane, W.A., *et al.*, *Isolation and structure of a brain constituent that binds to the cannabinoid receptor.* Science, 1992. **258**(5090): p. 1946-1949.

36.   Sugiura, T., *et al.*, *2-Arachidonoylglycerol: a possible endogenous cannabinoid receptor ligand in brain.* Biochem Biophys Res Commun, 1995. **215**(1): p. 89-97.

37.   Mechoulam, R., *et al.*, *Identification of an endogenous 2-monoglyceride, present in canine gut, that binds to cannabinoid receptors.* Biochem Pharmacol, 1995. **50**(1): p. 83-90.

38.   Priller, J., *et al.*, *Mead ethanolamide, a novel eicosanoid, is an agonist for the central (CB1) and peripheral (CB2) cannabinoid receptors.* Mol Pharmacol, 1995. **48**(2): p. 288-292.

39.   Felder, C.C., et al., Anandamide, an endogenous cannabimimetic eicosanoid, binds to the cloned human cannabinoid receptor and stimulates receptor-mediated signal transduction. Proc Natl Acad Sci U S A, 1993. **90**(16): p. 7656-7660.

40.   Devane, W.A. and J. Axelrod, Enzymatic synthesis of anandamide, an endogenous ligand for the cannabinoid receptor, by brain membranes. Proc Natl Acad Sci U S A, 1994. **91**(14): p. 6698-6701.

41.   Di Marzo, V., et al., Formation and inactivation of endogenous cannabinoid anandamide in central neurons. Nature, 1994. **372**(6507): p. 686-691.

42.   Hillard, C.J., et al., Accumulation of N-arachidonoylethanolamine (anandamide) into cerebellar granule cells occurs via facilitated diffusion. J Neurochem, 1997. **69**(2): p. 631-638.

43.   Deutsch, D.G. and S.A. Chin, Enzymatic synthesis and degradation of anandamide, a cannabinoid receptor agonist. Biochem Pharmacol, 1993. **46**(5): p. 791-796.

44.   Facci, L., et al., Mast cells express a peripheral cannabinoid receptor with differential sensitivity to anandamide and palmitoylethanolamide. Proc Natl Acad Sci U S A, 1995. **92**(8): p. 3376-3380.

45.   Skaper, S.D., et al., The ALIAmide palmitoylethanolamide and cannabinoids, but not anandamide, are protective in a delayed postglutamate paradigm of excitotoxic death in cerebellar granule neurons. Proc Natl Acad Sci U S A, 1996. **93**(9): p. 3984-3989.

46.   Evans, D.M., M.R. Johnson, and A.C. Howlett, Ca(2+)-dependent release from rat brain of cannabinoid receptor binding activity. J Neurochem, 1992. **58**(2): p. 780-782.

47.   Evans, D.M., et al., Endogenous cannabinoid receptor binding activity released from rat brain slices by depolarization. J Pharmacol Exp Ther, 1994. **268**(3): p. 1271-1277.

48.   Felder, C.C., et al., Comparison of the pharmacology and signal transduction of the human cannabinoid CB1 and CB2 receptors. Mol Pharmacol, 1995. **48**(3): p. 443-450.

49.   Howlett, A.C., J.M. Qualy, and L.L. Khachatrian, Involvement of Gi in the inhibition of adenylate cyclase by cannabimimetic drugs. Mol Pharmacol, 1986. **29**(3): p. 307-313.

50.   Gerard, C.M., et al., Molecular cloning of a human cannabinoid receptor which is also expressed in testis. Biochem J, 1991. **279**(Pt 1): p. 129-134.

51.   Shire, D., *et al.*, *An amino-terminal variant of the central cannabinoid receptor resulting from alternative splicing.* J Biol Chem, 1995. **270**(8): p. 3726-3731.

52.   Rinaldi-Carmona, M., *et al.*, *Characterization of two cloned human CB1 cannabinoid receptor isoforms.* J Pharmacol Exp Ther, 1996. **278**(2): p. 871-878.

53.   Yamaguchi, F., A.D. Macrae, and S. Brenner, *Molecular cloning of two cannabinoid type 1-like receptor genes from the puffer fish Fugu rubripes.* Genomics, 1996. **35**(3): p. 603-605.

54.   Stefano, G.B., B. Salzet, and M. Salzet, *Identification and characterization of the leech CNS cannabinoid receptor: coupling to nitric oxide release.* Brain Res, 1997. **753**(2): p. 219-224.

55.   Chakrabarti, A., E.S. Onaivi, and G. Chaudhuri, *Cloning and sequencing of a cDNA encoding the mouse brain-type cannabinoid receptor protein.* DNA Seq, 1995. **5**(6): p. 385-388.

56.   Kaminski, N.E., *et al.*, *Identification of a functionally relevant cannabinoid receptor on mouse spleen cells that is involved in cannabinoid-mediated immune modulation.* Mol Pharmacol, 1992. **42**(5): p. 736-742.

57.   Song, Z.H. and T.I. Bonner, *A lysine residue of the cannabinoid receptor is critical for receptor recognition by several agonists but not WIN55212-2.* Mol Pharmacol, 1996. **49**(5): p. 891-896.

58.   Shire, D., *et al.*, *Structural features of the central cannabinoid CB1 receptor involved in the binding of the specific CB1 antagonist SR 141716A.* J Biol Chem, 1996. **271**(12): p. 6941-6946.

59.   Bramblett, R.D., *et al.*, *Construction of a 3D model of the cannabinoid CB1 receptor: determination of helix ends and helix orientation.* Life Sci, 1995. **56**(23-24): p. 1971-1982.

60.   Baldwin, J.M., *Structure and function of receptors coupled to G proteins.* Curr Opin Cell Biol, 1994. **6**(2): p. 180-190.

61.   Herkenham, M., *et al.*, *Neuronal localization of cannabinoid receptors and second messengers in mutant mouse cerebellum.* Brain Res, 1991. **552**(2): p. 301-310.

62.   Herkenham, M., *et al.*, *Cannabinoid receptor localization in brain.* Proc Natl Acad Sci U S A, 1990. **87**(5): p. 1932-1936.

63.   Das, S.K., *et al.*, *Cannabinoid ligand-receptor signaling in the mouse uterus.* Proc Natl Acad Sci U S A, 1995. **92**(10): p. 4332-4336.

64.   Galiegue, S., *et al., Expression of central and peripheral cannabinoid receptors in human immune tissues and leukocyte subpopulations.* Eur J Biochem, 1995. **232**(1): p. 54-61.

65.   Ishac, E.J., *et al., Inhibition of exocytotic noradrenaline release by presynaptic cannabinoid CB1 receptors on peripheral sympathetic nerves.* Br J Pharmacol, 1996. **118**(8): p. 2023-2028.

66.   Martin, B.R., *et al., Pharmacological evaluation of agonistic and antagonistic activity of cannabinoids.* NIDA Res Monogr, 1987. **79**: p. 108-122.

67.   Pertwee, R.G., *et al., Inhibitory effects of certain enantiomeric cannabinoids in the mouse vas deferens and the myenteric plexus preparation of guinea-pig small intestine.* Br J Pharmacol, 1992. **105**(4): p. 980-984.

68.   Pertwee, R.G. and S.R. Fernando, *Evidence for the presence of cannabinoid CB1 receptors in mouse urinary bladder.* Br J Pharmacol, 1996. **118**(8): p. 2053-2058.

69.   Showalter, V.M., *et al., Evaluation of binding in a transfected cell line expressing a peripheral cannabinoid receptor (CB2): identification of cannabinoid receptor subtype selective ligands.* J Pharmacol Exp Ther, 1996. **278**(3): p. 989-999.

70.   Pertwee, R.G., *Pharmacology of cannabinoid CB1 and CB2 receptors.* Pharmacol Ther, 1997. **74**(2): p. 129-180.

71.   Howlett, A.C., *Inhibition of neuroblastoma adenylate cyclase by cannabinoid and nantradol compounds.* Life Sci, 1984. **35**(17): p. 1803-1810.

72.   Howlett, A.C., *Cannabinoid inhibition of adenylate cyclase. Biochemistry of the response in neuroblastoma cell membranes.* Mol Pharmacol, 1985. **27**(4): p. 429-436.

73.   Bayewitch, M., *et al., The peripheral cannabinoid receptor: adenylate cyclase inhibition and G protein coupling.* FEBS Lett, 1995. **375**(1-2): p. 143-147.

74.   Mackie, K., W.A. Devane, and B. Hille, *Anandamide, an endogenous cannabinoid, inhibits calcium currents as a partial agonist in N18 neuroblastoma cells.* Mol Pharmacol, 1993. **44**(3): p. 498-503.

75.   Mackie, K., *et al., Cannabinoids activate an inwardly rectifying potassium conductance and inhibit Q-type calcium currents in AtT20 cells transfected with rat brain cannabinoid receptor.* J Neurosci, 1995. **15**(10): p. 6552-6561.

76.   Glass, M. and C.C. Felder, *Concurrent stimulation of cannabinoid CB1 and dopamine D2 receptors augments cAMP accumulation in striatal neurons: evidence for a Gs linkage to the CB1 receptor.* J Neurosci, 1997. **17**(14): p. 5327-5333.

77.   Felder, C.C., *et al.*, *LY320135, a novel cannabinoid CB1 receptor antagonist, unmasks coupling of the CB1 receptor to stimulation of cAMP accumulation.* J Pharmacol Exp Ther, 1998. **284**(1): p. 291-297.

78.   Bouaboula, M., *et al.*, *Activation of mitogen-activated protein kinases by stimulation of the central cannabinoid receptor CB1.* Biochem J, 1995. **312**(Pt 2): p. 637-641.

79.   Bouaboula, M., *et al.*, *Signaling pathway associated with stimulation of CB2 peripheral cannabinoid receptor. Involvement of both mitogen-activated protein kinase and induction of Krox-24 expression.* Eur J Biochem, 1996. **237**(3): p. 704-711.

80.   Bouaboula, M., *et al.*, *A selective inverse agonist for central cannabinoid receptor inhibits mitogen-activated protein kinase activation stimulated by insulin or insulin-like growth factor 1. Evidence for a new model of receptor/ligand interactions.* J Biol Chem, 1997. **272**(35): p. 22330-22339.

81.   Bouaboula, M., *et al.*, *Stimulation of cannabinoid receptor CB1 induces krox-24 expression in human astrocytoma cells.* J Biol Chem, 1995. **270**(23): p. 13973-13980.

82.   Felder, C.C., *et al.*, *Cannabinoid agonists stimulate both receptor- and non-receptor-mediated signal transduction pathways in cells transfected with and expressing cannabinoid receptor clones.* Mol Pharmacol, 1992. **42**(5): p. 838-845.

83.   Venance, L., *et al.*, *Inhibition by anandamide of gap junctions and intercellular calcium signalling in striatal astrocytes.* Nature, 1995. **376**(6541): p. 590-594.

84.   Oliver, M.G. and H.M. McCurdy, *Migration, overwintering, and reproductive patterns of Taricha.* Can J Zool, 1974. **52**(4): p. 541-545.

85.   Tan, A.M., *Chromosomal variation in the northwestern American newts of the genus.* Chromosome Res, 1994. **2**(4): p. 281-292.

86.   Thoms, S.D. and D.L. Stocum, *Retinoic acid-induced pattern duplication in regenerating urodele limbs.* Dev Biol, 1984. **103**(2): p. 319-328.

87.   Brockes, J.P., *Retinoid signalling and retinoid receptors in amphibian limb.* Biochem Soc Symp, 1996. **62**: p. 137-142.

88.   Bajer, A.S., *Functional autonomy of monopolar spindle and evidence for oscillatory.* J Cell Biol, 1982. **93**(1): p. 33-48.

89. Weaver, A. and R. Hard, *Isolation of newt lung ciliated cell models: characterization of motility and coordination thresholds.* Cell Motil, 1985. **5**(5): p. 355-375.

90. Friedmann, G.B., *Differential white blood cell counts for the urodele Taricha granulosa.* Can J Zool, 1970. **48**(2): p. 271-274.

91. Friedmann, G.B., *The annual cycle of red blood cell count and haemoglobin level in the urodele Taricha granulosa on southern Vancouver Island.* Can J Zool, 1974. **52**(4): p. 487-494.

92. Francis, R.T., Jr. and R.R. Becker, *Two hemoglobin-binding proteins identified in the plasma of the amphibian Taricha granulosa.* Comp Biochem Physiol [B], 1984. **77**(2): p. 341-347.

93. Moore, F.L., *et al.*, *Luteinizing hormone-releasing hormone involvement in the reproductive behavior of a male amphibian.* Neuroendocrinology, 1982. **35**(3): p. 212-216.

94. Moore, F.L., *et al.*, *Testosterone-binding protein in a seasonally breeding amphibian.* Gen Comp Endocrinol, 1983. **49**(1): p. 15-21.

95. Miller, L.J. and F.L. Moore, *Intracranial administration of corticotropin-like peptides increases.* Peptides, 1983. **4**(5): p. 729-733.

96. Muske, L.E., *et al.*, *Gonadotropin-releasing hormones in microdissected brain regions of an amphibian: concentration and anatomical distribution of immunoreactive mammalian GnRH and chicken GnRH II.* Regul Pept, 1994. **54**(2-3): p. 373-384.

97. Lowry, C.A., *et al.*, *Neuroanatomical distribution of vasotocin in a urodele amphibian.* J Comp Neurol, 1997. **385**(1): p. 43-70.

98. Orchinik, M., T.F. Murray, and F.L. Moore, *Steroid modulation of GABAA receptors in an amphibian brain.* Brain Res, 1994. **646**(2): p. 258-266.

99. Deviche, P. and F.L. Moore, *Opioid kappa-receptor agonists suppress sexual behaviors in male rough-skinned newts (Taricha granulosa).* Horm Behav, 1987. **21**(3): p. 371-383.

100. Rose, J.D., J.R. Kinnaird, and F.L. Moore, *Neurophysiological effects of vasotocin and corticosterone on medullary neurons: implications for hormonal control of amphibian courtship behavior.* Neuroendocrinology, 1995. **62**(4): p. 406-417.

101. Wiley, J., R. Balster, and B. Martin, *Discriminative stimulus effects of anandamide in rats.* Eur J Pharmacol, 1995. **276**(1-2): p. 49-54.

102. Martin, B.R., *et al.*, *Pharmacological evaluation of dimethylheptyl analogs of delta 9-THC: reassessment of the putative three-point cannabinoid-receptor interaction.* Drug Alcohol Depend, 1995. **37**(3): p. 231-240.

103. Martin, B.R., *et al.*, *Behavioral, biochemical, and molecular modeling evaluations of cannabinoid analogs.* Pharmacol Biochem Behav, 1991. **40**(3): p. 471-478.

104. Lowry, C.A. and F.L. Moore, *Corticotropin-releasing factor (CRF) antagonist suppresses stress-induced locomotor activity in an amphibian.* Horm Behav, 1991. **25**(1): p. 84-96.

105. Dalterio, S.L., S.D. Michael, and P.J. Thomford, *Perinatal cannabinoid exposure: demasculinization in male mice.* Neurobehav Toxicol Teratol, 1986. **8**(4): p. 391-397.

106. Navarro, M., P. Rubio, and F.R. de Fonseca, *Behavioural consequences of maternal exposure to natural cannabinoids in rats.* Psychopharmacology (Berl), 1995. **122**(1): p. 1-14.

107. Bonnin, A., *et al.*, *Effects of perinatal exposure to delta 9-tetrahydrocannabinol on the fetal and early postnatal development of tyrosine hydroxylase- containing neurons in rat brain.* J Mol Neurosci, 1996. **7**(4): p. 291-308.

108. Garcia, L., *et al.*, *Perinatal delta 9-tetrahydrocannabinol exposure in rats modifies the responsiveness of midbrain dopaminergic neurons in adulthood to a variety of challenges with dopaminergic drugs.* Drug Alcohol Depend, 1996. **42**(3): p. 155-166.

109. Moore, F.L. and L.J. Miller, *Arginine vasotocin induces sexual behavior of newts by acting on cells in the brain.* Peptides, 1983. **4**(1): p. 97-102.

110. Deviche, P. and F.L. Moore, *Steroidal control of sexual behavior in the rough-skinned newt (Taricha granulosa).* Horm Behav, 1988. **22**(1): p. 26-34.

111. Moore, F.L. and L.J. Miller, *Stress-induced inhibition of sexual behavior: corticosterone inhibits courtship behaviors of a male amphibian (Taricha granulosa).* Horm Behav, 1984. **18**(4): p. 400-410.

112. Orchinik, M., T.F. Murray, and F.L. Moore, *A Corticosteroid Receptor in Neuronal Membranes.* Science, 1991. **252**: p. 1848-1851.

113.   Deutsch, D.G., *et al.*, *Fatty acid sulfonyl fluorides inhibit anandamide metabolism and bind to the cannabinoid receptor.* Biochem Biophys Res Commun, 1997. **231**(1): p. 217-221.

114.   Beltramo, M., *et al.*, *Functional role of high-affinity anandamide transport, as revealed by selective inhibition.* Science, 1997. **277**(5329): p. 1094-1097.

115.   Kingston, R.E., C.E. Chen, and H. Okayama, *Calcium Phosphate Transfection.* 2 ed. Short Protocols in Molecular Biology, ed. F.M. Ausubel. 1992, New York: John Wiley & Sons.

116.   Laemmli, U.K., *Cleavage of structural proteins during the assembly of the head of bacteriophage T4.* Nature, 1970. **227**: p. 680-685.

117.   Lowry, O., *et al.*, *Protein measurement with the Folin phenol reagent.* Journal of Biological Chemistry, 1959. **193**: p. 265-275.

118.   Salomon, Y., *Adenylate Cyclase Assay.* Advances in Cyclic Nucleotide Research, 1979. **10**: p. 35-55.

119.   Ohara, O., R.L. Dorit, and W. Gilbert, *One-sided polymerase chain reaction: the amplification of cDNA.* Proc Natl Acad Sci U S A, 1989. **86**(15): p. 5673-5677.

120.   Chen, X. and R. Wu, *Direct amplification of unknown genes and fragments by Uneven polymerase chain reaction.* Gene, 1997. **185**(2): p. 195-199.

121.   Felsenstein, J., *Phylogenies from molecular sequences: Inference and reliability*, in *Annual Review of Genetics*, A. Campbell, Editor. 1988, Annual Reviews, Inc.: Palo Alto, CA. p. 521-565.

122.   Dayhoff, M.O., *Atlas of Protein Sequence and Structure*, . 1979, National Biomedical Research Foundation: Washington, D.C. p. 348.

123.   Fitch, W.M. and Margoliash, *Construction of phylogenetic trees.* Science, 1967. **155**: p. 279-284.

124.   Carroll, R.H., *Vertebrate paleontology and evolution.* 1988, New York: H. Freeman & Co.

125.   Swofford, D.L. and G.J. Olsen, *Phylogeny Reconstruction*, in *Molecular Systematics*, D.M.H.a.C. Moritz, Editor. 1990, Sinauer Associates, Inc.: Sunderland, MA. p. 411-501.

126.   McIntosh, H.H., C. Song, and A.C. Howlett, *CB1 cannabinoid receptor: cellular regulation and distribution in N18TG2 neuroblastoma cells.* Molecular Brain Research, 1998. **53**: p. 163-173.

127. Guan, X.M., T.S. Koblika, and B.K. Koblika, *Enhancement of membrane insertion and function in a type IIIb membrane protein following introduction of a cleavable signal peptide.* The Journal of Biological Chemistry, 1992. **267**(31): p. 21995-21998.

128. Von Heijne, G., *Patterns of amino acids near signal-sequence cleavage sites.* European Journal of Biochemistry, 1983. **133**: p. 17-22.

129. Wellerdieck, C., *et al.*, *Functional expression of odorant receptors of the zebrafish Danio rerio and of the nematode C. elegans in HEK293 cells.* Chemical Senses, 1997. **22**(4): p. 467-476.

130. Darlison, M.G., *et al.*, *Opioid receptors from a lower vertebrate (Catostomus commersoni): sequence, pharmacology, coupling to a G-protein-gated inward-rectifying potassium channel (GIRK1), and evolution.* Proc Natl Acad Sci U S A, 1997. **94**(15): p. 8214-8219.

131. Rafferty, K.A., Jr., ed. *Mass culture of amphibian cells: Methods and observations concerning stability of cell type.* Biology of Amphibian Tumors, ed. M. Mizell. 1968, Springer-Verlag: New York.

132. Bradford, C.S., *et al.*, *Characterization of cell cultures derived from Fugu, the Japanese pufferfish.* Mol Mar Biol Biotechnol, 1997. **6**(4): p. 279-288.

133. Teifel, M., *et al.*, *Optimization of transfection of human endothelial cells.* Endothelium, 1997. **5**(1): p. 21-35.

APPENDIX

CULTURE AND TRANSFECTION OF *XENOPUS* A6 CELLS

Introduction

The observation that most of the myc-tagged newt CB1 protein synthesized by CHO cells stably-expressing the receptor remained intracellular (Figure 21) led to the hypothesis that potential differences in mammalian and amphibian protein-processing enzymes may be responsible. To test this hypothesis, experiments were designed to stably-express the myc-tagged newt CB1 construct, pTL1nCB1myc (Figure 19), in an amphibian cell line.

Methods

Cell Culture

Xenopus A6 cells were purchased from ATCC (ATCC number CCL-102). These cells were submitted by Keen A. Rafferty, Jr., who developed them for use as a model for the study of vertebrate aging [131]. These epithelioid cells are derived from kidney tissue obtained from an adult male and grow as a monolayer.

Under 5% CO_2

For growth in a CO_2 incubator, these cells were cultured at 26-28° C in sterile media consisting of: Media 199 (60 %), fetal bovine serum (10 %), Supplementary

saline (SS)-A: (12 %), SS-B: (12 %), SS-C (6 %), and glutamine to 2 mM. The pH of this media was adjusted to 6.8 with 1 N NaOH. SSA is composed of (120 ml): 35 mg $CaCl_2 \cdot 2H_2O$, 53 mg $MgSO_4$. SSB is composed of (120 ml): 70 mg Na_2HPO_4, 20 mg KH_2PO_4, 140 mg glucose. SSC is composed of (60 ml): 100 mg $NaHCO_3$.

Without CO_2

For growth outside of an incubator cultures were grown in the dark at ambient temperature in media consisting of: DLF [132] (74 %), H_2O (14.5 %), fetal calf serum (10%), and 0.5 % each of: 10 mcg/ml insulin, 1 mM L-glutamine, 25 mcM non-essential amino acids.

Transfection

Calcium Phosphate Precipitate-Based Method

Calcium phosphate precipitate-based transfection of *Xenopus* A6 cells was attempted as described above for the generation of CHO stable cell lines with the following exceptions: 1) four HeBS solutions of were used for precipitate formation, pH=6.9, 7.0, 7.1, and 7.2. 2) a plasmid encoding a green fluorescent protein sequence (pEGFP-C, Clontech) was transfected alone to assess transfection efficiency or was co-transfected (1:40) with pTL1nCB1myc to confer G418 resistance. 3) Precipitate volume was scaled-down to accommodate the smaller plate sizes of 24-well plates.

Each of the four HeBS solutions were evaluated for transfection efficiency using six different amounts of DNA: 1.5 mcg, 0.75 mcg, 0.38 mcg, 0.2 mcg, 0.1 mcg, 0.05 mcg. Precipitates of these amounts of DNA were spread on *Xenopus* A6 cells cultured to about 70% confluence in 24-well plates (~ 2 cm^2/well surface area). Transfection efficiency was evaluated by counting fluorescent cells.

Electroporation

An attempt was made to optimize field strength in electroporation-mediated transfection of *Xenopus* A6 cells using a BTX model 600 electroporator. For these experiments, adherent cells were treated with trypsin and collected in PBS and pelleted by centrifugation for 10 minutes at 1500 rpm. Pellets were resuspended in PBS to a concentration of 8 million cells per ml. Four-hundred mcl of cells were mixed with 10 mcg of plasmid DNA and transferred to an electroporation cuvette (2 mm gap). At a fixed pulse length of 3 msec, the following field strengths were evaluated (KV/cm): 0.25, 0.5, 1.5, 2.5. After manipulation, contents of cuvettes were transferred to 100 mm plates containing 15 ml of complete media. Cells were allowed to grow to confluence before assessment of transfection efficiency by counting fluorescent protein-expressing cells.

Lipid-Based Method

Four lipid reagents were evaluated for transfection efficiency of *Xenopus* A6 cells cultured to about 60% confluence in 24-well plates (well surface area ≈ 2 cm^2). Six lipid volumes were used: 7.5, 4, 2, 1, 0.5 and 0.25 mcl. 1.5 mcg of pEGFP-C was used for these transfections. The lipid reagents used were part of a kit sold by Life Technologies (#10552-016), and included lipofectamine, lipofectin, cellfectin and DMRIE-C.

For transfections, the volumes of lipids outlined above were suspended in 100 mcl of serum-free culture media. Plasmid DNA was suspended in an equal volume and the two mixtures were combined, mixed by pipeting, and allowed to sit for 30 minutes at room temperature. The 200 mcl DNA/lipid mixtures were then layered over cultures and allowed to incubate at 26-28 °C for four hours. After the incubation period, the DNA/lipid mixture was removed, and the cultures fed with 1 ml of complete media. Cultures were evaluated for transfection by counting fluorescent cells 48 hours after transfection.

Transfections used for stable selection and assays of adenylate cyclase activity were done using 10 mcl of lipofectamine reagent and 3 mcg of plasmid DNA. Plasmid/DNA mixtures were layered on cells cultured in 35 mm plates as described above for 24-well plate cultures.

Selection of Stable *Xenopus* A6 Cell Lines

To select *Xenopus* A6 cells that had stably-integrated the pEGFP-C plasmid,
cultures transfected by the lipid-based method in 35 mm plates were allowed to grow
to confluence (about 3 days), monolayers were removed by treatment with 0.25 %
trypsin, and cells were transferred to 100 mm plates containing 10 ml of selection
media.

Initial attempts to select stable colonies with 750 mcg/ml G418 failed due to
apparent resistance to the antibiotic. To determine an effective G418 concentration, a
dose-response experiment was designed. This experiment employed G418
concentrations of 750, 1000, 1250, 1500, 2000, and 3000 mcg G418/ml. Cell counts
were made after 14 days after G418 exposure was started.

Adenylate Cyclase Assays

Adenylate cyclase assays were performed according to a modified version of
the Salomon method [118]. *Xenopus* A6 cell cultures were washed twice with serum-
free media and then incubated for 4 hours in 1 ml of the same media containing 1.2
mcCi [^{3}H]adenine. The tritium-containing media was then aspirated and replaced with
serum-free F12 Ham's media containing a phosphodiesterase inhibitor (50 mcM Ro
20-1724). These cultures were incubated at 37° for 40 min in the presence of various
concentrations of forskolin. Incubations were terminated by the addition of 300 mcl of
Stop Solution (2% SDS, 1.3 mM cyclic AMP), followed by addition of 100 mcl

concentrated perchloric acid, and 750 mcl water. [^{14}C]cyclic AMP (5000 CPM in 50 mcl) was added to each plate to correct for recovery. After transferring the contents of culture dishes to 1.5 ml centrifuge tubes, 12 M KOH was added to neutralize the samples. The resulting precipitate was pelleted by centrifuging at 10,000 g for 10 minutes. Cyclic AMP in the supernatants was isolated by sequential chromatography over Bio-Rad AG-50W-X4 cation exchange resin and neutral alumina. Concentrations of [^{3}H]cyclic AMP and [^{14}C]cyclic AMP in eluates were determined simultaneously using a Beckman scintillation counter (^{3}H channels 0 - 250, ^{14}C channels 350 - 670). Counts were corrected for crossover and recovery.

Results

Evaluation of Transfection Methods

Calcium Phosphate-Based Transfection

Using combinations of four HeBS solutions at different pH with six different plasmid DNA concentrations ranging from 1.5 to 0.5 mcg, few GFP expressing cells were observed 48 hours after transfection. This indicated that *Xenopus* A6 cells are, for practical purposes, untransfectable using the calcium phosphate precipitate method.

Electroporation

Electroporation-mediated transfection of *Xenopus* A6 cells was evaluated at four different field strengths using a pulse duration of 3 msec. The effect of field strength on cell survival is presented in Figure 26. Despite an effect on cell survival, few GFP-expressing cells were observed in any of the treatment groups, indicating low transfection efficiency. Based on the low transfection efficiency observed, electroporation was excluded as a viable method for transfection of *Xenopus* A6 cells.
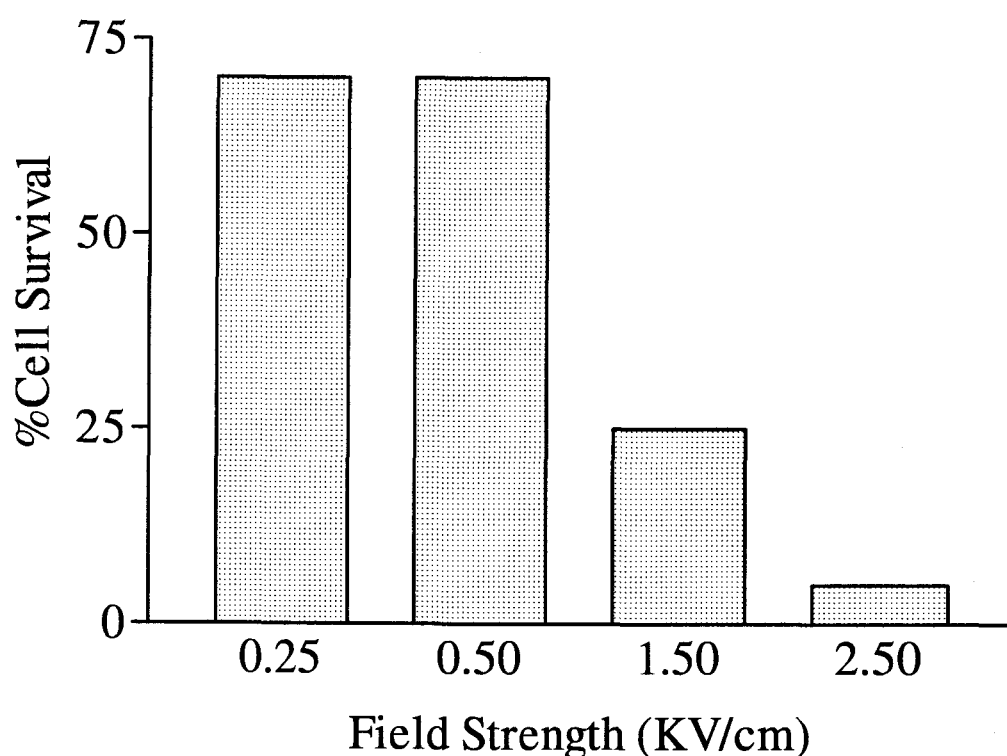
Figure 26: Effect of electroporation field strength on *Xenopus* A6 cell survival. Survival estimates are based on cell counts. Electroporation conditions are described in detail in the text.

Lipid-Mediated Transfection

Six volumes of the four lipid reagents outlined above were evaluated for ability

to mediate transfection of *Xenopus* A6 cells. Each of these lipids produced significant

levels of transfection. Highest levels of expression were produced by the largest

volume of each lipid used (7.5 mcl). Relative transfection efficiency is presented in
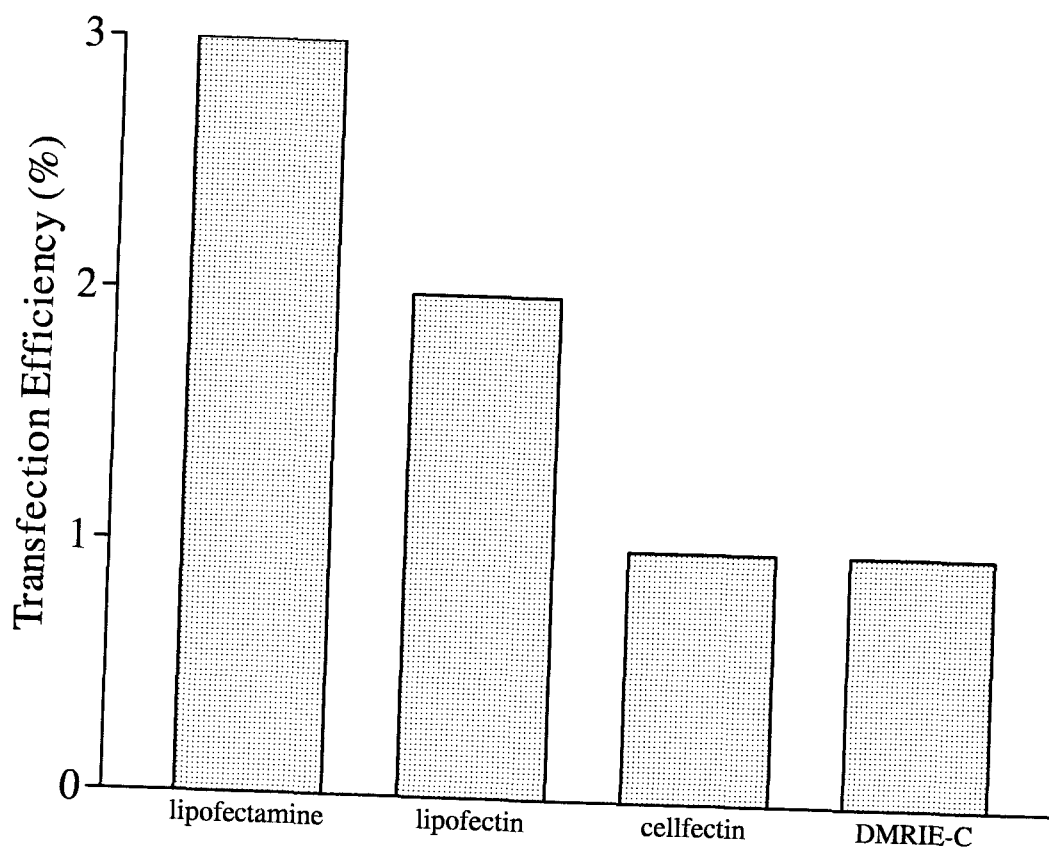
Figure 27.

Figure 27. Efficiency of *Xenopus* A6 cell transfection produced by four lipid reagents. 7.5 mcl of each reagent and 1.5 mcg of DNA (pEGFP-C) were used to transfect cells cultured to about 70% confluence in wells of a 24-well plate. Transfection efficiency was estimated from counts of GFP-expressing cells.

Selection of Stable Cell Lines

Initial attempts to select *Xenopus* A6 cells that had stably integrated the

pEGFP-C plasmid were made using G418 at 750 mcg/ml. At this G418 concentration

no toxicity was seen. This indicated that higher antibiotic concentrations would be

required. To determine an effective G418 concentration, a dose-response experiment

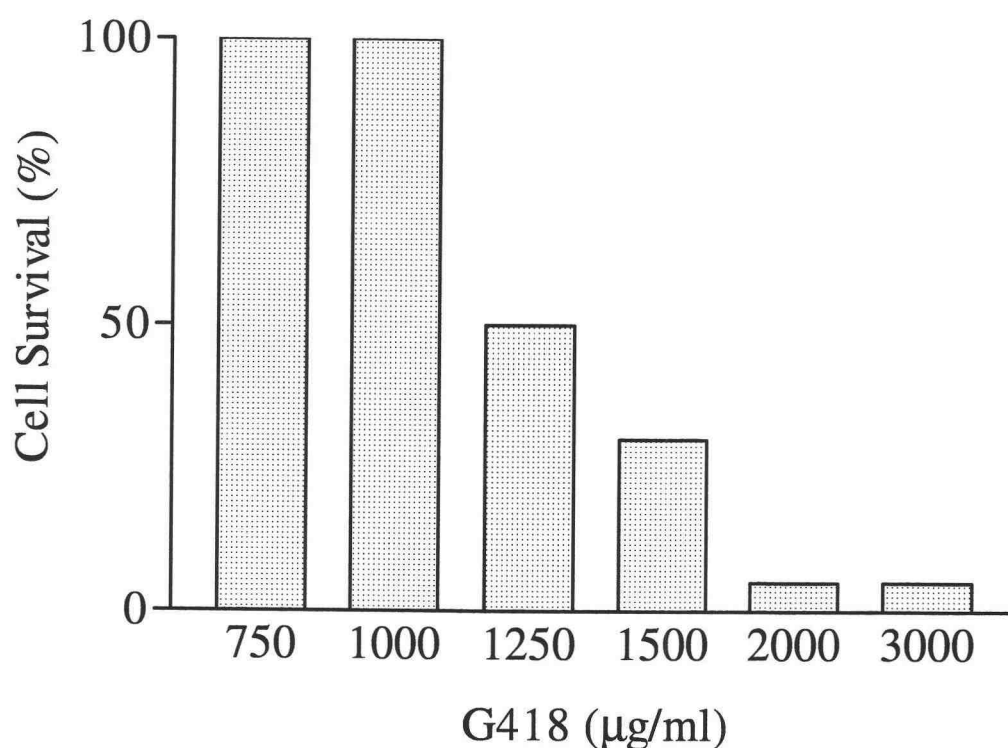was conducted. Results of this experiment are presented in Figure 28.

Figure 28. Effect of G418 concentration on *Xenopus* A6 cell survival. Cells cultured
to confluence in a 6-well plate were split into 100 mm dishes containing media with
G418 at the concentrations shown. Cell counts were made 14 days after selection
began.

Adenylate Cyclase Assays

Results of a forskolin dose-response experiment are presented as Figure 29.

This experiment was done to determine the optimal concentration of forskolin to use

to evaluate the ability of cannabinoids to inhibit adenylate cyclase activity.
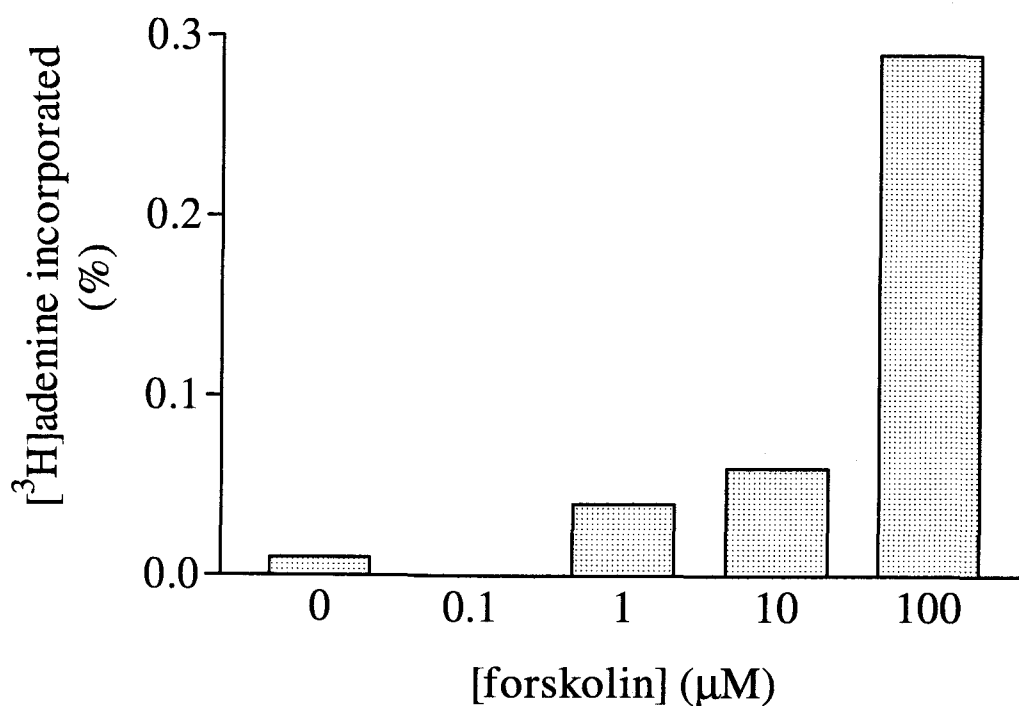

Figure 29. Forskolin stimulation of adenylate cyclase activity in *Xenopus* A6 cells.
Cultures grown in 6-well plates were exposed to the concentrations of forskolin
indicated for 25 min. Tritiated-adenine incorporation to cAMP was quantified using
the modified Salomon method described in the methods section above.

Discussion

Evaluation of calcium phosphate and electroporation-mediated methods of

transfection revealed that they produced low levels of transfection efficiency in

Xenopus A6 cells. Other cell lines have been reported to be untransfectable by the calcium phosphate method [133]. It is interesting that electroporation was effective in producing *Xenopus* cell death without resulting in significant levels of transfection. It may be instructive to optimize electroporation pulse duration with these amphibian cells. It is possible that a more thorough optimization of electroporation conditions will allow this method to be successfully employed with *Xenopus* A6 cells.

All of the lipid reagents used for lipid-mediated transfection of *Xenopus* A6 cells were effective. Of the reagents evaluated, lipofectamine produced the highest level of transfection efficiency and so was selected for further use. For transfection of *Xenopus* A6 cells cultured in 35 mm dishes, 10 mcl of lipofectamine with 3 mcg of plasmid DNA were found to produce from 3-5% transfection efficiency.

One problem with use of the lipid transfection reagents with the *Xenopus* A6 cell line was that significant toxicity was observed over the course of the four hour incubation period. This toxicity was most problematic in transfected cells used for adenylate cyclase assays; the additional manipulation associated with this assay further increased toxicity. Toxicity associated with cyclase assays may have contributed to variance in data produced.

Optimization of G418 concentrations required to kill *Xenopus* A6 cells not expressing a neomycin resistance factor revealed that high concentrations of the antibiotic is required. Full efficacy was observed at 2000 mcg/ml. This is approximately three-fold higher than the highest concentrations generally recommended for use with mammalian cell lines [115]. Even at this concentration, a

small percentage of untransfected cells survived (5 %). This indicates that a second

method of screening for transfectants is required, which was accomplished by

cotransfection of pEGFP-C with pTL1nCB1myc. Using the green fluorescent

protein-encoding plasmid, G418-resistant colonies could also be screened on the basis

of their expression of green fluorescent protein.

In addition to low G418 sensitivity, *Xenopus* A6 cells are also resistant to

stimulation of adenylate cyclase activity by forskolin. The highest concentrations of

forskolin used only produced modest levels of adenylate cyclase stimulation relative to

that produced by lower forskolin concentrations in other cell lines (Table 6).

Table 6: Forskolin concentrations used with various cell lines and cultures

Cell line/culture	[forskolin]	Avg. Stimulation (% Adenine Incorporated to cAMP)
Xenopus A6	100 mcM	0.1 - 0.3
CHO	50 mcM	0.8 - 2.0
CATH.a	10 mcM	0.5
cerebellar granule cell primary	0.5 mcM	0.5

This low-level stimulation by forskolin in *Xenopus* A6 cells reduced the measurable

signal in adenylate cyclase assays. Reduced signal, combined with toxicity problems

related to lipid-mediated transient transfections, rendered these cells difficult to use for

the measurement of alterations of cyclase activity. It is possible that these cells will

represent an adequate system when stably-expressing a protein of interest.